Forschungszentrum Jülich

Cell Culture Models as Alternatives to Animal Experimentation for the Testing of Neuroprotective Compounds in Stroke Research

Practical Handbook of Methods

Edited by
A.J. Carter and H. Kettenmann

Lebenswissenschaften
Life Sciences

Schriften des Forschungszentrums Jülich
Lebenswissenschaften/Life Sciences Band 3

Forschungszentrum Jülich GmbH
Projektträger Biologie, Energie, Umwelt des
Bundesministeriums für Bildung und Forschung

Cell Culture Models as Alternatives to Animal Experimentation for the Testing of Neuroprotective Compounds in Stroke Research

Practical Handbook of Methods

Edited by
Adrian J. Carter and Helmut Kettenmann

Schriften des Forschungszentrums Jülich
Reihe Lebenswissenschaften / Life Sciences Band 3

ISSN 1433-5549 ISBN 3-89336-250-9

Die Deutsche Bibliothek - CIP-Einheitsaufnahme

Cell Culture models as alternatives to animal experimentation for the testing of neuroprotective compounds in stroke research :
practical handbook of methods / Forschungszentrum Jülich.
Hrsg.: Adrian J. Carter, Helmut Kettenmann. - Jülich : Forschungszentrum Jülich, Zentralbibliothek, 1999
(Schriften des Forschungszentrums Jülich Reihe Umwelt ; Band 3)
ISBN 3-89336-250-9

Herausgeber und Vertrieb:	Forschungszentrum Jülich GmbH ZENTRALBIBLIOTHEK D-52425 Jülich Telefon (0 24 61) 61-53 68 · Telefax (0 24 61) 61-61 03 e-mail: zb-publikation@fz-juelich.de Internet: http://www.fz-juelich.de/zb
Umschlaggestaltung:	Grafische Betriebe, Forschungszentrum Jülich GmbH
Druck:	Grafische Betriebe, Forschungszentrum Jülich GmbH
Copyright:	Forschungszentrum Jülich 1999

Schriften des Forschungszentrums Jülich
Reihe Lebenswissenschaften / Life Sciences Band 3

ISSN 1433-5549
ISBN 3-89336-250-9

Die diesem Bericht zurgrundeliegenden Vorhaben wurden mit Mitteln des Bundesministeriums für Bildung und Forschung unter den Förderkennzeichen 0319520B, 0310015B, 0319998B und 0310774 im Rahmen des Förderschwerpunktes „Ersatzmethoden zum Tierversuch" gefördert. Die Verantwortung für den Inhalt dieser Veröffentlichung liegt bei den Autoren.

Contents

An Introduction to cell culture models as alternatives to animal experimentation for the testing of neuroprotective compounds in stroke research

Adrian J. Carter and Helmut Kettenmann

The use of living animals in scientific research can be considered justified if it is likely to produce appreciable benefit to society, if there is no other way to conduct the research in question and if all reasonable steps are taken to keep any distress or suffering to a minimum.

Lord E.D. Adrian FRS

This handbook is the result of a project partly financed by the German Ministry for Education, Research, Science and Technology (BMBF) which ran for three years from 1995 to 1998 and involved several research groups in Germany. The statement of Lord Adrian, famous for his discovery that the frequency of firing in a nerve cell is a measure of the intensity of the stimulus, quoted above is a way of ethically justifying the use of animals in research. It also contains a very important caveat. It requires us to ask ourselves carefully whether there is really *no other way* of conducting the research in question. And this is the aim that we have set ourselves for our joint project. During the course of our work we have developed and refined different cell assay techniques which can be used for investigating the effects of neuroprotective compounds in stroke research. We thought it would be worthwhile to share some of the experimental details from our findings with a wider audience. And we have therefore decided in association with the BMBF to print a handbook which summarizes these methods. But first, why have we chosen human stroke as our research target?

Thromboembolic stroke causes the death of nerve cells by depriving the brain of an adequate supply of oxygenated blood. The process is called cerebral ischaemia and is primarily a vascular event which leads to damage of brain tissue and impaired function. Stroke is the third leading cause of death after coronary heart disease and cancer, and is an important source of adult disability in industrialized nations (Bonita, 1992). Surprisingly, funding of stroke research per death by the National Institutes of Health in the United States falls well behind that of many other of these diseases (NIH, 1998).

The brain depends on arterial blood for a continuous supply of oxygen and glucose. Even if blood flow is interrupted for only a few minutes, certain highly vulnerable neurons will degenerate. If the interruption is sustained, then all types of brain cells will eventually die. Fundamental to our understanding of the process of cerebral ischaemia has been the presumption that brain cells do not simply die because of energy failure. The link between ischaemia and neuronal death is considerably more complicated. Stroke triggers a chain reaction of electrical and chemical activity which is related to ischaemic depolarization, the release of excitatory amino acids and changes in calcium homeostasis (Mattson and Mark, 1996; Tymianski and Tator, 1996). These events act in concert to orchestrate cell death.

The core area of an infarct is probably beyond treatment. This area of the brain is totally deprived of oxygen and glucose and dies within minutes. However, the area at risk surrounding the core, often called the penumbra because it is similar to the partially lit penumbra of a lunar eclipse, does not die immediately. The collateralization or natural redundancy of the brain's blood supply allows this area to continue functioning with a reduced blood flow. It is here that the chain reaction of secondary injury, if not stopped, will cause the brain tissue to eventually succumb to the ischaemia. The penumbra therefore represents an opportunity for intervention (Ginsberg, 1997).

Strategies for the treatment of acute ischaemic stroke are based on three main approaches, the three Rs of stroke research:

- Restoring blood flow as soon as possible
- Rescue brain cells from the deleterious consequencies
- Repair brain cells to regain lost functions

Clinical investigators attempting to treat the consequences of thromboembolic stroke first turned their attention to restoring blood flow by removing the offending blood clot with thromboembolic agents (Önal and Fisher, 1996). Many pharmaceutical companies have also concentrated their activities on designing neuroprotective drugs that interfere with the host of biological processes that are set in motion by the original ischaemic event (Barinaga, 1996; Koroshetz and Moskowitz, 1996; Schehr, 1996). The idea behind this is such agents may slow down the destructive processes to buy more time to administer thrombolytic agents. Finally, many groups are also turning their attention to enhancing the repair mechanisms of the brain as a way of recovering lost function. These approaches assume, however, that we have preclinical models which can be used to investigate the pathological mechanisms involved and predict the efficacy in the clinical.

Although stroke displays considerable diversity in its pathogenesis, manifestations and anatomical sites (Chopp and Zhang, 1995), approximately 80% of all events are caused by ischaemic infarction (Bamford, 1992). Animal models of cerebral ischaemia fall into two categories: global and focal. Global models, as their name implies, produce ischaemia in large areas of the brain and cause selective necrosis within vulnerable brain regions (Ginsberg and Busto, 1989). They are thought to represent damage that occurs after myocardial infarction or coronary artery bypass operations. In contrast, focal models produce infarction in clearly defined regions of the brain (Ginsberg and Busto, 1989; Macrae, 1992). They are considered more relevant to acute ischaemic stroke. Until beneficial effects of a drug have been demonstrated in the clinic, however, the predictive value of all of these models remains uncertain (Hunter et al., 1995; Grotta, 1994). Moreover, all of these animal models require surgery and anaesthesia. For instance, to occlude the middle cerebral artery in the brain to induce focal cerebral ischaemia, the skull has to be exposed by cutting skin and pulling back facial muscles, it has to be opened with a drill and, finally, the artery occluded with an electric coagulating iron. All of these manipulations are not painful when performed under anaesthesia. Nevertheless, the animals exhibit impaired function in the hours and days following the operation due to the infarct in the brain. It has therefore always been the goal of the researchers to reduce the number of animal experiments by applying cell culture techniques as much as possible.

Modern drug discovery methods of high-throughput screening, recombinant cell systems and rational drug design have revolutionized the way in which drug research is performed in the pharmaceutical industry. It has also resulted in a large drop in the number of animal experiments performed. Indeed, Boehringer Ingelheim has for successive years been able to reduce its animal requirements. Nevertheless, it is getting increasingly difficult to reduce this number even further. As with any indication area, the pathological processes associated with human stroke are very complex and difficult to understand. If we want to reduce the number of cerebral ischaemia experiments performed with animals we have to mimick the effects of ischaemia in our *in vitro* systems. Ischaemia is an event which influences not just neurons but a variety of different cell types in the brain, namely vascular endothelium, glial cells and neurons (Figure 1).

Figure 1. Ischaemia influences a variety of different cell types

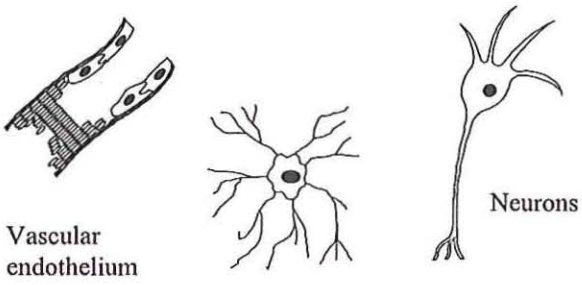

Our research project has involved several groups with different research interests. We have attempted to mimick the effects of ischaemia in a variety of cell systems to investigate the effects of neuroprotective compounds. Christina Bartmann-Lindholm, Thomas Weiser and Adrian Carter at Boehringer Ingelheim Pharma KG have investigated the effects of excitoxicity and oxygen-glucose deprivation in serum-free cultures of primary cortical neurons. Detlev Melzian, Rita Sattler and Thomas Hafner at Mannheim University for Technical Sciences have extended these investigations by studying ion and energy homeostasis in similar neuronal cultures. Katharina Mertsch, Reiner Haselhoff, Matthias Schroeter and Ingolf Blasig at the Institute for Molecular Pharmacology in Berlin have concentrated their efforts on determining the effects of oxygen deprivation and various neuroprotective agents in endothelial cells. Jörg Breder, Clemens Sabelhaus, Ulrich Schröder and Klaus Reymann at the Leibnitz Institute for Neurobiology in Magdeburg have used organotypic hippocampal cell cultures to investigate the effects of various neuroprotective agents. And finally, Susan Lyons and Helmut Kettenmann at the Max Delbrück Centre for Molecular Medicine in Berlin have looked at gial cell vulnerability to oxygen-glucose deprivation. and their selective responses to neuroprotective agents. The results of these studies will appear in scientific journals in the near future, if they have not already been published. However, because of space limitations many of the experimental details may, not

be fully explained. We hope that this handbook can fill this gap by providing a collection of these methods for other researchers.

References

Bamford J (1992) Clinical examination in diagnosis and subclassification of stroke. Lancet 339:400-402.

Barinaga M (1996) Finding new drugs to treat stroke. Science 272:664-666.

Bonita R (1992) Epidemiology of stroke. Lancet 339:342-344.

Chopp M, Zhang RL (1995) Animal modeling for developing stroke therapy. In: Stroke Therapy (Fisher M ed), pp 117-134. Boston: Butterworth-Heinemann.

Ginsberg MD (1997) Injury mechanisms in the ischaemic penumbra - approaches to neuropirtection in acute ischaemic stroke. Cerebrovasc.Dis. 7:7-12.

Ginsberg MD, Busto R (1989) Rodent models of cerebral ischemia. Stroke 20:1627-1642.

Grotta J (1994) The current status of neuronal protective therapy: Why have all neuronal protective drugs worked in animals but none so far in stroke patients. Cerebrovasc.Dis. 4:115-120.

Hunter AJ, Green AR, Cross AJ (1995) Animal models of acute stroke: can they predict clinically successful neuroprotective drugs? Trends Pharmacol.Sci. 16:123-128.

Koroshetz WJ, Moskowitz MA (1996) Emerging treatments for stroke in humans. Trends Pharmacol.Sci. 17:227-233.

Macrae IM (1992) New models of focal cererbal ischaemia. Br.J.Clin.Pharmacol. 34:302-308.

Mattson MP, Mark RJ (1996) Excitotoxicity and excitoprotection in vitro. Adv.Neurol. 71:1-35.

NIH (1998) National Institutes of Health (NIH) research funding per death for HIV/AIDS, diabetes, cancer, heart disease and stroke. Stroke 29:

Önal MZ, Fisher M (1996) Thrombolytic and cytoprotective therapies for acute ischemic stroke: a clinical overview. Drugs of Today 32:573-592.

Schehr RS (1996) New treatments for acute stroke. Nature Biotechnology 14:1549-1554.

Tymianski M, Tator CH (1996) Normal and abnormal calcium homeostasis in neurons: A basis for the pathophysiology of traumatic and ischemic central nervous system injury. Neurosurgery 38:1176-1195.

Pharmacological Characterization of Potential Neuroprotective Compounds with Serum-free, Primary Cortical Cell Cultures Derived from Rats

Christina Bartmann-Lindholm and Adrian J. Carter

Department of Central Nervous System Research

Boehringer Ingelheim Pharma KG

55216 Ingelheim am Rhein

Summary

Primary neuronal cell cultures have been used in the past to investigate the mechanisms of ischaemic damage and to determine the effects of potential neuroprotective compounds. However, many of these systems have relied on the addition of animal serum to encourage differentiation and survival of the neurons. Serum protects neurons from the toxic effects of excitatory amino acids. We therefore adapted a method of culturing rat cortical neurons in a serum-free environment as the basis for establishing a model of neurotoxicity which could be applied to test potential neuroprotective compounds in the pharmaceutical industry. Serum-free primary cultures of cortical neurons were prepared from embryonic rat brains and cultured in B27/Neurobasal® medium which had been previously conditioned by incubating with confluent cultures of astrocyctes derived from newborn rat brains. The neurons exhibited characteristic morphology of differentiated neurons and could be stained with the neuronal specific markers for axons, neurofilament 200, and for dendrites, microtubule-associated protein-2. The neurons remained viable for up to 3 - 4 weeks in culture. Neurotoxicity was induced either by the addition of different excitotoxins or exposing the neurons to hypoxia/hypoglycaemia. The number of living cells was quantified with an assay based on 3-(4,5-dimethylthiazol-2-yl) tetrazolium bromide (MTT). The concentration of glutamate in the medium was measured with high-performance liquid chromatography in association with fluorimetric detection. The results of this study showed that there was an excellent correlation between the number of living cells and the absorbance measurements of MTT dye. The addition of glutamate, N-methyl-D-aspartate, kainate or veratridine induced a conentration-dependent neurotoxicity. The results obtained with glutamate in the MTT assay agreed well with those obtained in an alternative assay for cell death based on the measurement of lactate dehydrogenase. Subjecting the neurons to hypoxia/hypoglycaemia caused neuronal death and glutamate release. The extent of neurotoxicity and the amount of glutamate released depended on the length of hypoxia/hypoglycaemia. In summary, the results of this study show that we have developed a sensitive assay based on serum-free cultures of cortical neurons from rats which can now be applied to determine the neuroprotective effects of different compounds in stroke research.

Introduction

Cerebral ischaemia triggers a chain reaction of electrical and chemical activity which includes ischaemia depolarization, excessive release of excitatory amino acids and increases in intracellular Ca^{2+} (Zivin and Choi, 1991). These events acts in concert to orchestrate cell death. Many pharmaceutical companies and clinicians have concentrated their activities on designing neuroprotective drugs that interfere with the host of biological processes that are set in motion by the original ischaemia event (Schehr, 1996; Barinaga, 1996; Koroshetz and Moskowitz, 1996). The idea behind this is that such agents may slow down the destructive processes to buy more time to administer agents which restore blood flow. Drug industry therefore needs models which can be used to screen for such compounds.

Primary neuronal cell cultures can be used to determine the effects of neuroprotective compounds before testing in animal models. Indeed, many of the original experiments which contribute to our understanding of the pathological mechanisms of cerebral ischaemia were performed with such systems. For instance, experiments with hippocampal cell cultures prompted the proposal that enhanced synaptic activity and release of excitatory amino acids causes the death of neurons that have been deprived of oxygen (Rothman, 1983; Rothman, 1984) Subsequently, work by Goldberg and Choi and others with neuronal cell cultures expanded on this theory by focussing on the importance of one particular subtype of excitatory amino acid receptor, the N-methyl-D-aspartate (NMDA) receptor-channel complex (Goldberg et al., 1988; Choi et al., 1988; Choi et al., 1987).

Neurotoxicity can be induced by adding various excitotoxins such as glutamate to cortical cell cultures (Choi et al., 1987). However, inhibition of energy metabolism is perhaps a more realistic way of mimicking cerebral ischaemia *in vitro*. This has been achieved in number of ways in neuronal cell cultures. Energy metabolism can be inhibited by removing oxygen and/or glucose from the medium (Goldberg et al., 1988; Goldberg et al., 1987) or by inhibiting oxidative phosphorylation and glycolysis with metabolic poisons such as cyanide and 2-deoxyglucose (Peruche et al., 1990; Vornov et al., 1996). Although none of these approaches equate directly to ischaemia, removing oxygen and glucose remains probably the most realistic, albeit also most difficult.

Many of the aforementioned studies with dissociated neuronal cell cultures suffer from one major drawback. The neuronal cells were cultured in media containing serum. Serum protects rat cortical neurons from glutamate-induced neurotoxicity (Dux et al., 1992; Uto et al., 1994; Dux et al., 1996) probably because it contains a variety of different growth factors such as basic fibroblast growth factor (bFGF) and nerve growth factor (NGF). NGF and bFGF attenuate hypoglycaemic damage and glutamate-induced neurotoxicity (Cheng and Mattson, 1991; Mattson et al., 1993a; Mattson et al., 1995) probably because they can differentially regulate the expression of various glutamate receptors (Mattson et al., 1993b; Cheng et al., 1995). Consequently, the presence of serum in any given medium may influence the sensitivity of neurotoxicity and glutamate-receptor expression in neuronal cell cultures.

We therefore adapted a previously described method of culturing rat cortical neurons in a serum-free environment (Banker and Cowan, 1977; Stichel and Müller, 1991) as the basis for establishing a model of neurotoxicity which could be applied to test potential neuroprotective compounds. We have induced neurotoxicity in these cell cultures by adding different excitotoxins or subjecting them to hypoxia/hypoglycaemia. We have quantitated the number of living cells with an assay based on a formazan dye and measured the release of glutamate

with high-performance liquid chromatography (HPLC). And this has all been performed in 96-well plates suitable for drug screening.

Materials and Methods

Reagents. Dulbecco's modified essential medium (DMEM), B27 and Neurobasal® medium were purchased from Gibco (Eggenstein, Germany), foetal calf serum (FCS) and trypsin/EDTA from Boehringer Mannheim (Germany), cytosine ß-D-arabinofuranoside and o-phthalaldehyde (OPA) from Sigma (Deisenhofen, Germany), and Dulbeccos's phosphate buffered salt solution (DPBS) from BioWhittaker (Verviers, Belgium). DPBS had the following composition NaCl (137 mmol/L), KCl (2.7 mmol/L), $CaCl_2$ (0.9 mmol/L), $Na_2HPO_4{\cdot}2H_2O$ (5.6 mmol/L), $Na_2HPO_4{\cdot}H_2O$ (0.9 mmol/L), $MgSO_4{\cdot}7H_2O$ (0.8 mmol/L) and KH_2PO_4 (1.5 mmol/L), and modified Ringer buffer the following composition NaCl 124 mmol/L, KCl 4.9 mmol/L, $MgSO_4.7H_2O$ 1.3 mmol/L, $CaCl_2.2H_2O$ 2.0 mmol/L, KH_2PO_4 1.2 mmol/L and $NaHCO_3$ 25.6 mmol/L, pH 7.4. L-Glutamate and 2-mercaptoethanol were purchased from Serva (Heidelberg, Germany), kainate and quisqualate from Tocris (Bristol, England) and N-methyl-D-aspartate (NMDA) was synthesized in the Department of Medicinal Chemistry at Boehringer Ingelheim (Ingelheim, Germany). Stock solutions were diluted in medium and filtered sterile. Disposable plastic materials for cell culture were obtained from Falcon (Heidelberg, Germany), Greiner (Frickenhausen, Germany) or Sarstedt (Nümbrecht, Germany). All other chemicals were at least of analytical reagent grade and purchased from E. Merck (Darmstadt, Germany).

Astrocyte-conditioned medium (ACM). Astrocytes were prepared from newborn Wistar rats (P1-2) by modifying a previously described method (Stichel, Müller, 1991). The cortices were collected in DMEM and trituated in 4 mL DMEM. The single cell suspension was washed with DMEM by filling up to 50 mL medium and centrifuging at 350 x g for 5 min at room temperature. Cells from one cortex were cultured in one 75 cm^2 flask with 20 mL DMEM/10% FCS in a humid atmosphere supplemented with 10% CO_2. The medium was changed twice a week. After two weeks, when the cell layer was confluent, the cells were shaken vigorously at 120 rpm overnight at 37°C in a Braun rotary shaker (Schöffengrund, Germany) to remove any residual neurons. The cells were then washed three times with DPBS and 30 mL of the B27/Neurobasal® medium was added and incubated at 37°C in a humid atmosphere supplemented with 10% CO_2 to allow the astrocytes to condition the medium. B27/Neurobasal® medium is a serum-free, defined synthetic medium supplemented with insulin, transferrin, progesterone, selenium, biotin, triiodothyronine, vitamin E, linoleic acid and putrescine(Brewer et al., 1993; Brewer, 1995). The ACM was decanted, shock frozen in liquid N_2 and stored at -80°C. A second batch of medium was conditoned by adding another 30 mL of B27/Neurobasal® medium to the same astrocytes and incubating for a further three days.

Coating of 96-well plates. Primaria® 96-well plates (Falcon, Heidelberg, Germany) were coated by adding poly-L-lysin 30 µg/cm^2 (50 µL per well from a 0.2 mg/mL stock solution in DBPS) and incubating for 15 min at room temperature. The plates were then washed three times with purified water (Milli Q, Millipore, Eschborn, Germany), dried for 1 hour in a sterile flow bank and stored overnight at 4°C. Subsequently, the 96-well plates were incubated with laminin 0.3 µg/cm^2 (50 µL per well from a 2 µg/mL stock solution in DPBS) for 1 hour at 37°C. The laminin-coated plates were washed twice with DMEM and an aliquot of 60 µL ACM was added to the poly-L-lysin/laminin-coated well to prevent it from drying out.

Primary cortical cell cultures. Serum-free primary cultures of cortical neurons were prepared from rat brains by modifying previously described methods (Banker, Cowan, 1977) (Stichel, Müller, 1991). The cortical hemispheres were dissected from embryonic Wistar rats (E18-19), collected in DMEM and centrifuged at 350 x g for 5 minutes at room temperature before removing the supernatant. The cells were dissociated by incubating with trypsin/EDTA (0.05%/0.02%) for 8 minutes at 37°C. The reaction was stopped by adding DMEM with 10% FCS and centrifuging at 350 x g for 5 min at room temperature. The pellet FCS was subsequently washed twice with DMEM. The cell pellet was resuspended in serum-free B27/Neurobasal® medium and the neurons were triturated with fire-polished pasteur pipettes. The neurons were counted, diluted and an aliquot containing 50,000 cells in 60 µL B27/Neurobasal® medium was added to each coated well such that the final volume was 120 µL per well. One day later, we added cytosine ß-D-arabinofuranoside to give a final concentration of 5 µmol/L (13 µL per well from a 50 µmol/L stock solution) to inhibit proliferation of dividing non-neuronal cells. Two thirds of the medium was changed twice a week. All cultures were maintained in a humid atmosphere of air with 10% CO_2 at 37°C in a Cytoperm® incubator from Heraeus (Hanau, Germany).

Assessment of neurotoxicity. The sensitivity of the primary cultures of cortical neurons to a variety of different excitoxins or to hypoxia/hypoglycaemia was quantified by means of a cell titer 96® kit from Promega (Heidelberg, Germany). Previous experiments have demonstrated that the cell cultures develop an adequate response to various glutamate agonists after 11-13 days in culture. We therefore waited until the cultures described here had also attained this age before performing experiments with them. The cells were exposed to various glutamate agonists for 24 hours at 37°C and the number of living cells measured with the colourimetric assay. The assay is based on the principle that living cells convert a tetrazolium to a blue formazan derivative (Mosmann, 1983). After incubating for 4 h a detergent was added to the cells to solubilize them and the crystals to allow measurement of the absorbance with a plate reader from MWG-Biotech (Ebersberg, Germany) at 570 nm. To validate the MTT assay, we compared the effects of adding glutamate with an assay for lactate dehydrogenase (LDH). LDH is released by dead cells into the surrounding medium and can be quantified by measuring the reduction of the terazolium dye INT with a plate reader at 490 nm (Nachlass et al., 1960; Decker and Lohmann-Matthes, 1988). Further experiments were also performed in which the sodium channel opener veratridine was added at different concentrations for 20 minutes. The medium containing veratridine was subsequently replaced with normal medium and the cell number quantified 24 h later.

Oxygen measurements. The oxygen concentration in the cell culture medium as well as in the atmosphere of the gas-impermeable chamber was measured by an oxygen-sensitive electrode Oxi 325-B from WTW (Melsungen, Germany). The oxygen-sensitive electrode was inserted into the chamber via a gas impermeable valve mounted by the workshop at Boehringer Ingelheim. Various measurements were made to ensure that the oxygen concentration could be reproducibly reduced to 0.2 - 0.3 % in the atmosphere of the chamber. This concentration was reached within 2-3 minutes after exchanging the atmosphere and maintained until the end of the hypoxic treatment.

Analysis of glutamate. The concentration of glutamate in the cell culture medium was measured by high performance liquid chromatography (HPLC). The system consisted of an L-6200A intelligent pump from Merck-Hitachi (Darmstadt, Germany), a Gilson 231 autosampler with a 401 diluter and cooling block from Abimed (Düsseldorf, Germany), a CMA/280 fluorescence detector from CMA Microdialysis (Stockholm Sweden), and a DG-

1200 on-line degasser from VDA Optilab (Berlin, Germany) to ensure that the mobile phase was free from air. A nucleosil 100 C18 (60 x 4 mm i.d.) column filled with material of pore size 5 µm was used in association with a guard column of same material (10 x 4 mm i.d.). The mobile phase consisted of two parts: methanol and 0.1 mol/L sodium acetate adjusted to a pH of 6.94 with glacial acetic acid combined with 3.75% methanol and 1.5% Lichrosolv® quality tetrohydrofurane (THF). The sodium acetate-methanol-THF mixture was pumped at a flow rate of 1.2 mL/min for 6 min to separate glutamate and aspartate. The column was subsequently perfused with methanol at a flow rate of 1.2 mL/min for 2 min to wash the remaining amino acids out before allowing the column to equilibrate again with the sodium acetate-methanol-THF mixture for a further 2 min ready for the next injection. Glutamate was derivatized for 1 minute with OPA in an aqueous solution of boric acid buffer and 2-mercaptoethanol. The boric acid buffer was made by dissolving 2.47g boric acid in approximately 90 mL distilled water, adjusting the pH to 10.4 with NaOH (32%) and making up to 1000 mL with distilled water. The OPA working reagent was made by dissolving 27 mg OPA in 0.5 mL ethanol, adding 20 µL 2-mercaptoethanol and making up to 5 mL with boric acid buffer. This reagent was always allowed to stand for 24 h before use and was made freshly every 2 weeks during which time 5 µL 2-mercaptoethanol was added every 3 days. The derivatisation procedure was performed with a Gilson autosampler. Equally sized aliquots (15 µL) OPA reagent and sample to be measured were pipetted into an empty tube and mixed. One minute later 15 µL of this mixture was injected onto the HPLC column. Peak identification was performed with external standards and concentrations were calculated on the basis of peak height. HPLC data were collected with a Ziatech IEEE-488 card and Nelson analytical series 900 interface from ESWE Analytik (Sinsheim, Germany). Peak integration was carried out with Turbochrom® 4.03 software from Axel Semrau (Sprockhövel, Germany) running on a Dell Pentium® personal computer.

Hypoxia/hypoglycaemia. The cells were maintained in Neurobasal® without glucose or in a modified Ringer buffer whilst subjecting them to hypoxia/hypoglycaemia by bubbling an aliquot of 30 mL of glucose-free medium or buffer with 95% N_2/5% CO_2 for 10 minutes at 37°C. Each of the 96 wells received 50 µL of this buffer. Only one plate was treated at a time to prevent the oxygen from diffusing back into the medium. The 96-well plate was placed in a gas-impermeable chamber from Billups-Rothenberg (Del Mar, California) and incubated at 37°C in an oxygen-free atmosphere. The duration of the hypoxia/hypoglycaemia treatment varied from 60 to 120 minutes after which time the medium or buffer was replaced with Neurobasal® medium containing glucose and the number of living neurons quantified 24 h later with the MTT test.

Immuncytochemistry. Cells were cultured on coverslips coated with poly-L-lysin and laminin as described above and fixed with ethanol/glacial acetic acid (95:5; v/v) at -20°C for 10 minutes. The coverslips were subsequently washed 0.2% FCS in DPBS three times for 5 min. Primary monoclonal antibodies raised against neurofilament 200 (Boehringer Mannheim, 814342, Mannheim, Germany) or MAP2 (Boehringer Mannheim, 1284959, Mannheim, Germany) were diluted in antibody buffer (10% FCS and 0.1% NaN_3 in DPBS) and incubated for 30 minutes at room temperature. After washing three times for 5 minutes with washing buffer, the secondary antibody, fluorescine isothiocyanate (FITC)-conjugated anti-mouse IgG (Boehringer Mannheim, 821462, Mannheim, Germany) was diluted 1:50 and incubated for 30 minutes. The cells were then washed as previosly described, mounted in glycerin (9 parts glycerine, 2.5% potassium iodide and 1 part PB containing 14.5 g $Na_2HPO_4xH_2O$ and 2.6 g $NaH_2PO_4xH_2O$ in 1 L distilled water) and sealed with nail varnish.

The cells were viewed using phase contrast optics with an Olympus inverted microscope with a fluorescence filter at 375-495 nm.

Results

Stable, serum-free primary cultures of cortical neurons could be obtained from embryonic rat brains in B27/Neurobasal® medium which had been previously conditioned by incubating with confluent cultures of astrocytes derived from newborn rat brains. The neurons could be cultured either on small glass coverslips for immunofluorescence studies or in 96-well plates. The neurons exhibited classical neuronal morphology within a few days of preparation characterized by the formation of a dense network of connections (Fig. 1). The neurons were also fixed after 13 days in culture and stained positively with monoclonal antibodies for MAP-2 to show the dendritic network and neurofilament 200 to show the axonal network.

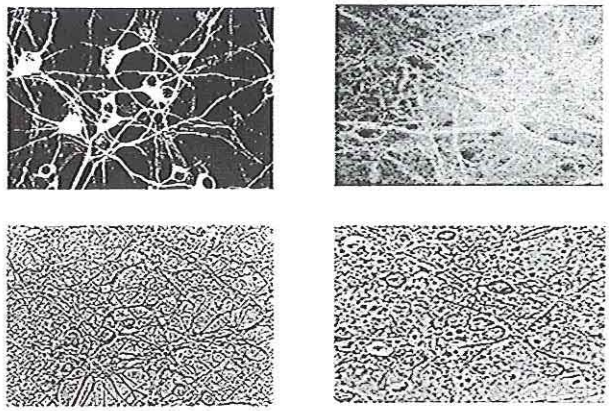

Fig. 1. Photomicrographs of primary, serum-free cultures of cortical neurons from the brain of rat embryos (E17-18): (Upper left) neurons stained with a monoclonal antibody against MAP-2; (Lower left) accompanying phase-contrast picture of the dense dendritic network of 13-day old neurons; (Upper right) neurons stained with a monoclonal antibody against neurofilament 200 (Lower right) accompaying phase-contrast picture of the dense axonal network. The binding of the monoclonal antibodies was visualized by a second anti-mouse antibody coupled to fluorescine isothiocyanate and fluorescence microscopy.

We performed experiments in which the cortical neurons were counted and seeded at different densities. Several days later the neurons were quantified with the MTT assay (Celltiter 96®) from Promega (Heidelberg, Germany) and the relative absorbance was compared with the number of original cells. There was an excellent linear relationship ($r = 0.95$) between the absorbance of the formazan derivative and the number of cells over the range of 1 000 to 500 000 cells (Fig. 2).

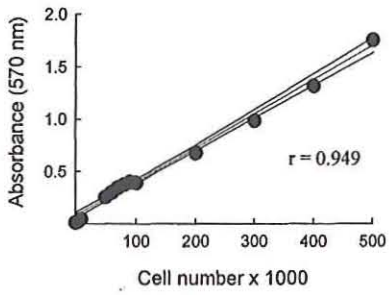

Fig. 2. Correlation between the number of cortical neurons seeded into one well of a 96-well plate and the relative absorbance of MTT measured. The assay is based on the principle that living cells convert MTT to a blue formazan derivative. After incubating for 4 h a detergent was added to the cells to solubilize the crystals and the absorbance was measured with a plate reader from MWG-Biotech (Ebersberg, Germany) at 570 nm. Results are expressed as the mean of at least four different preparartions.

We determined effects adding different concentrations of glutamate on cell viability with the MTT test. In a parallel series of experiments we also determined the effects of glutamate on cell death as measured by the release of lactate dehygrogenase (LDH) into the medium. There was a very good agreement between the two types of test: The concentration of glutamate required to reduce the number of living cells by 50% (EC_{50}) as measured with the MTT assay was 5 µmol/L and the concentration required to cause 50% cell death with the LDH test was 4 µmol/L (Fig. 3).

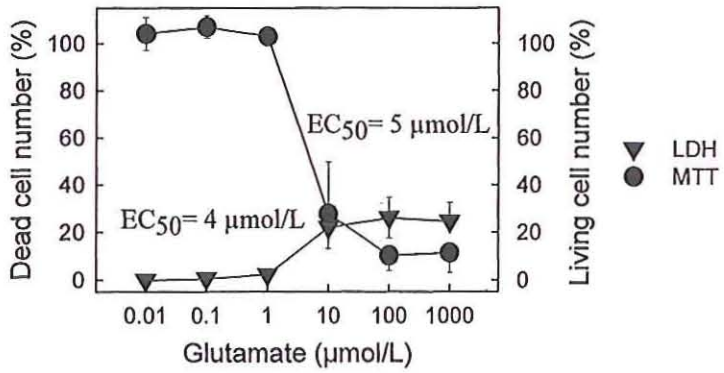

Fig. 3. A comparison of the ability of the addition of different concentrations of glutamte to influence cell viability as measured with the MTT assay and to influence cell death as measured with the LDH test. Glutamate was added to the medium and cell viability/death was measure on the following day. All results are the mean ± SEM of four separate preparations and are normalized as a function of the untreated cell group.

We compared the ability of the excitotoxins glutamate, NMDA, kainate as well as the Na^+ channel opener veratridine to influence cell viability in the cultured cortical neurons. All agents were added to the the 96-well plates which were then incubated overnight before determining the number of living cells with the MTT assay. All four agents caused reductions in the number of living cells. The table shows the conentrations required to inhibit cell viability by 50% (EC_{50}). Results are the mean of at least four different preparations.

Neurotoxin	EC_{50} (µmol/L)	95% Confidence intervals
glutamate	1.25	0.67 - 1.83
NMDA	10.90	6.97 - 14.84
kainate	21.07	12.15 - 29.98
veratridine	1.47	0.36 - 2.59

We determined the effects of subjecting primary cultures of cortical neurons to hypoxia/hypoglycaemia on cell viability as measured by the MTT assay and glutamate release as measured by HPLC. Fig. 4 shows a typical HPLC separation of glutamate and aspartate.

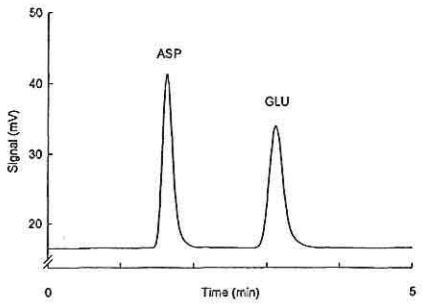

Fig. 4. Typical separation of a standard mixture of aspartate and glutamate. A nucleosil 100 C18 (60 x 4 mm i.d.) column filled with material of pore size 5 µm was used in association with a guard column of same material (10 x 4 mm i.d.). The mobile phase consisted of two parts: methanol and 0.1 mol/L sodium acetate adjusted to a pH of 6.94 with glacial acetic acid combined with 3.75% methanol and 1.5% Lichrosolv® quality tetrohydrofurane (THF). The sodium acetate-methanol-THF mixture was pumped at a flow rate of 1.2 mL/min for 6 min to separate glutamate and aspartate. The column was subsequently perfused with methanol at a flow rate of 1.2 mL/min for 2 min to wash the remaining amino acids out before allowing the column to equilibrate again with the sodium acetate-methanol-THF mixture for a further 2 min ready for the next injection. Glutamate was derivatized for 1 minute with OPA in an aqueous solution of boric acid buffer and 2-mercaptoethanol.

Subjecting the neurons to hypoxia/hypoglycaemia caused neuronal death and glutamate release. The extent of neurotoxicity and the amount of glutamate released depended on the length of hypoxia/hypoglycaemia (Fig. 5). However, extensive toxicity appeared to occur before large amounts of glutamate had been released.

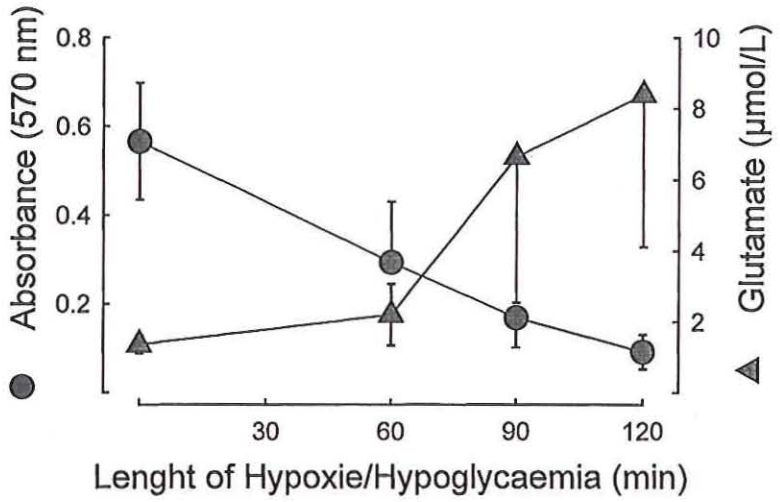

Fig. 5. The effects subjecting cortical cell cultures to different durations of hypoglycaemia/hypoxia on cell viability and glutamate release. The cells were maintained in DPBS whilst subjecting them to hypoxia/hypoglycaemia by bubbling an aliquot of 30 mL of glucose-free DPBS with 95% N_2/5% CO_2 for 10 minutes at 37°C. Each of the 96 wells received 50 µL of this buffer. The 96-well plate was placed in a gas-impermeable chamber from Billups-Rothenberg (Del Mar, California) and incubated at 37°C in an oxygen-free atmosphere. The duration of the hypoxia/hypoglycaemia treatment varied from 30 to 120 minutes after which time the buffer was replaced with Neurobasal® medium and the number of living neurons quantified 24 h later with an MTT test.

Discussion

Cultures of primary cortical neurons were prepared from embryonic rat brains and cultured in B27/Neurobasal® medium which had been previously conditioned by incubating with confluent cultures of astrocytes derived from newborn rat brains. The neurons remained viable for up to 3- 4 weeks in culture. Originally methods were devloped for culturing primary neurons in serum-containing medium for up to 3 weeks (Banker and Cowan, 1977; Banker and Cowan, 1979). Later, these techniques were refined by replacing serum either with a defined synthetic supplement (Bottenstein and Sato, 1979) or with a medium conditioned by confluent cultures of astrocytes (Stichel and Müller, 1991). However in our hands, such preparations were not reproducible enough to test the effects of neuroprotective compounds. We therefore tried using other defined artificial supplements such as B27/Neurbasal®, but found them also to inadequate on their own. We achieved the most stable and reliable cortical cell cultures when we combined both B27/Neurobasal® and astrocyte conditioning. Indeed, we strongly recommend this method for culturing primary cortical neurons.

We have applied a method usually used to measure cell proliferation for assessing neuron viability in culture. This method uses a tetrazolium salt and is based on the principle that a membrane permeable pale yellow dye is converted to a blue insoluble salt by the action of

lactate dehydrogenase enzymes in living cells (Mosmann, 1983). We were able to show that the number of living neurons correlated directly with the signal over a broad range. Moreover, we were also able to demonstrate that the results obtained with the tetrazolium assay agreed well with the results obtained with another method of measuring cell death, namely the measurement of lactate dehydrogenase released extracellularly (Nachlas et al., 1960). We prefer to use the terazolium assay because it less time consuming and more reproducible.

We investigated the effects of three different excitaory amino acids and an agent which opens voltage-dependent Na^+ channels. All of these agent induced rapid cell death in our hands. Interestingly, the EC_{50} values determined for these agents were considerably lower than values obtained by other groups using mixed glia-cortical neurons cultures. For example, Choi et al. (1987) reported an EC_{50} value for glutamate between 50 – 100 µmol/L , whereas we obtained an EC_{50} value of 1.25 µmol/L. This difference may be caused by an increased sensitivity of neurons to glutamate when grown in the absence of direct contact with glial cells, or perhaps because glial cells in mixed cultures are able to take up glutamate before it becomes toxic for the neurons.

We also applied a sensitive HPLC method for measuring the concentration of glutamate in the medium. Using this method we were able to show that subjecting our neuronal cultures to oxygen-glucose deprivation for different lengths of time caused glutamate release into the medium. This was associated with a parallel increase in cell death which was also dependent on the length of oxygen-glucose deprivation. The effects of hypoxia or oxygen-glucose deprivation have been previously studied in mixed neuronal-glial cultures (Goldberg et al., 1987; Goldberg and Choi, 1993; Kaku et al, 1991). This is the first time that this method has been applied to studying such effects in pure serum-free cultures of cortical cultures. Interestingly, the time required to cause maximum cell death in the mixed neuronal-glia cultures was about 60 min (Goldberg and Choi, 1993; Kaku et al.,1991), whereas we needed almost 120 min to cause maximum cell death in our pure serum-free cortical cultures. The reason for this discrepancy is not clear.

In summary, the results of this study show that we have developed a sensitive assay based on serum-free cultures of cortical neurons from rats which can now be applied to determining the neuroprotective effects of different compounds in stroke research.

References

Banker GA, Cowan WM (1977) Rat hippocampal neurons in dispersed cell culture. Brain Res. 126:397-425.

Banker GA, Cowan WM (1979) Further observations on hippocampal neurons in dispersed culture. J.Comp.Neurol. 187:469-494.

Barinaga M (1996) Finding new drugs to treat stroke. Science 272:664-666.

Bottenstein JE, Sato GH (1979) Growth of a rat neuroblastoma cell line in serum-free supplemented medium. Proc.Natl.Acad.Sci.USA 76:514-517.

Brewer GJ (1995) Serum-free B27/neurobasal medium supports differentiated growth of neurons from the striatum, substantia nigra, septum, cerebral cortex, cerebellum, and dentate gyrus. J.Neurosci.Res. 42:674-683.

Brewer GJ, Torricelli JR, Evege EK, Price PJ (1993) Optimized survival of hippocampal neurons in B27-supplemented neurobasal™, a new serum-free medium combination. J.Neurosci.Res. 35:567-576.

Cheng B, Furukawa K, O'Keefe JA, Goodman Y, Kihiko M, Fabian T, Mattson MP (1995) Basic fibroblast growth factor selectively increases AMPA- receptor subunit GluR1 protein level and differentially modulates Ca^{2+} responses to AMPA and NMDA in hippocampal neurons. J.Neurochem. 65:2525-2536.

Cheng B, Mattson MP (1991) NGF and bFGF protect rat hippocampal and human cortical neurons against hypoglycemic damage by stabilizing calcium homeostasis. Neuron 7:1031-1041.

Choi DW, Koh J-Y, Peters S (1988) Pharmacology of glutamate neurotoxicity in cortical cell culture: attenuation by NMDA antagonists. J.Neurosci. 8:185-196.

Choi DW, Maulucci-Gadde M, Kriegstein AR (1987) Glutamate neurotoxity in cortical cell culture. J.Neurosci. 7:357-368.

Decker T, Lohmann-Matthes M-L (1988) A quick and simple method for the quantitation of lactate dehyrogenase release in measurements of cellular cytotoxicity and tumor necrosis factor (TNF) activity. J.Immunol.Meth. 15:61-69.

Dux E, Oschlies U, Uto A, Kusumoto M, Siklos L, Joo F, Hossmann KA (1996) Serum prevents glutamate-induced mitochondrial calcium accumulation in primary neuronal cultures. Acta Neuropathol.(Berl) 92:264-272.

Dux E, Wiessner C, Hossmann K-A (1992) Glutamate-induced ribosomal disaggregation and ultrastructural changes in rat cortical neuronal culture: protective effect of horse serum. Neurosci.Lett. 141:173-176.

Goldberg MP, Choi DW (1993) Combined oxygen and glucose deprivation in cortical cell culture: Calcium-dependent and calcium-independent mechanisms of neuronal injury. J.Neurosci. 13:3510-3524.

Goldberg MP, Viseskul V, Choi DW (1988) Phencyclidine receptor ligands attenuate cortical neuronal injury after N-methyl-D-aspartate exposure or hypoxia. J.Pharmacol.Exp.Ther. 245:1081-1087.

Goldberg MP, Weiss JH, Pham PC, Choi DW (1987) N-methyl-D-aspartate receptors mediate hypoxic neuronal injury in cortical culture. J.Pharmacol.Exp.Ther. 243:784-791.

Kaku DA, Goldberg MP, Choi DW (1991) Antagonism of non-NMDA receptors augments the neuroprotective effect of NMDA receptor blockade in cortical cultures subjected to prolonged deprivation of oxygen and glucose. Brain Res. 554:344-347.

Koroshetz WJ, Moskowitz MA (1996) Emerging treatments for stroke in humans. Trends Pharmacol.Sci. 17:227-233.

Mattson MP, Kumar KN, Wang H, Cheng B, Michaelis EK (1993b) Basic FGF regulates the expression of a functional 71 kDa NMDA receptor protein that mediates calcium influx and neurotoxicity in hippocampal neurons. J.Neurosci. 13:4575-4588.

Mattson MP, Lovell MA, Furukawa K, Markesbery WR (1995) Neurotrophic factors attenuate glutamate-induced accumulation of peroxides, elevation of intracellular Ca^{2+} concentration, and neurotoxicity and increase antioxidant enzyme activities in hippocampal neurons. J.Neurochem. 65:1740-1751.

Mattson MP, Zhang Y, Bose S (1993a) Growth factors prevent mitochondrial dysfunction, loss of calcium homeostasis, and cell injury, but not ATP depletion in hippocampal neurons deprived of glucose. Exp.Neurol. 121:1-13.

Mosmann T (1983) Rapid colorimetric assay for cellular growth and survival: application to proliferation and cytotoxicity assays. J.Immunol.Meth. 65:55-63.

Nachlas MM, Margulies SI, Goldberg JD, Seligman AM (1960) The determination of lactic dehydrogenase with a tetrazolium salt. Anal.Biochem. 1:317-326.

Peruche B, Ahlmeyer B, Brungs H, Krieglstein J (1990) Cultured neurons for testing antihypoxic drug effects. J.Pharmacol.Meth. 23:63-770.

Rothman SM (1983) Synaptic activity mediates death of hypoxic neurons. Science 220:536-537.

Rothman SM (1984) Synaptic release of excitatory amino acid neurotransmitter mediates anoxic neuronal death. J.Neurosci. 4:1884-1891.

Schehr RS (1996) New treatments for acute stroke. Nature Biotechnology 14:1549-1554.

Stichel CC, Müller HW (1991) Dissociated cell culture of rat cerebral cortical neurons in serum-free, conditioned media: GABA-immunopositive neurons. Developmental Brain Research 64:145-154.

Uto A, Dux E, Hossmann K-A (1994) Effect of serum on intracellular calcium homeostasis and survival of primary cortical and hippocampal CA1 neurons following brief glutamate treatment. Metabolic Brain Disease 9:333-345.

Vornov JJ, Thomas AG, Jo D (1996) Protective effects of extracellular acidosis and blockade of sodium/hydrogen ion exchange during recovery from metabolic inhibition in neuronal tissue culture. J.Neurochem. 67:2379-2389.

Zivin JA, Choi DW (1991) Stroke Therapy. Scientific American 7:35-43.

Advanced Cell Culture Based Techniques for the Investigation of Neuroprotective Compounds: Electrophysiological Investigations of the Effects of Excitotoxic Challenges, As well as Cryopreservation of Primary Cultured Cortical Neurons Help to Reduce the Number of Animals as Tissue Donors

Thomas Weiser, Dept. of CNS Research, Boehringer Ingelheim, Germany

Ischaemic stroke of the brain is one of the main causes of death and disability in the industrialized countries. The development of compounds which reduce the damages after ischaemic insults is therefore a research target of many pharmaceutical companies, as well as academic institutions.

Stroke is in most of the cases induced by the occlusion of a cerebral blood vessel, leading to the death of neurons in a limited part of the brain. In an avalanche-like process, the damage spreads from this focus into neighboured brain regions. Glutamate and other excitatory amino acids play a crucial role for the progression of the injury. The investigation of the effects of excitatory amino acids *in vivo* has yielded important results about ischaemic disorders (for review: Meldrum and Garthwaite, 1990). On the other hand, such experimental techniques put severe stress on the animals. To circumvent this problem, and to investigate the mechanism of excitotoxicity in a better defined environment, cell culture based models have been developed (e. g. Choi et al., 1987). These assays can be used for the screening and characterization of putative neuroprotective compounds. There is no doubt that such *in vitro* models can be extremely useful for mechanistic investigations, and that many animal experiments can be avoided by the employment of sophisticated cell culture models. The effectivity of e. g.

antagonists of glutamate receptors of the N-methyl-D-aspartate (NMDA) subtype in reducing damages in neuronal cultures after excitotoxic challenges are highly predictive for their effects *in vivo* (for example in animal models of focal ischemia, Gill et al., 1991).

On the other hand, even for these *in vitro* models animals have to be sacrificed, since neurons are post-mitotic and therefore only primary neuronal cell cultures can be used. Other cell lines like e.g. P19 cells, gave inconsisting results concerning their responses to excitotoxic challenges and cannot be applied for the testing of putative neuroprotective principles. Thus, up to now primary cultured neuronal cultures cannot be replaced by other cell culture models. My aim within this joint project was to further reduce the number of animals which have to be sacrificed for cell culture based assays. For this purpose, I developed a method for the testing of anti-excitotoxic compounds which needs only a very small number of neurons to be studied. In a second approach I increased the effectivity of the cell culture by cryopreservation of unused neuronal cells. Both approaches are now standard procedures in my laboratory and helped to reduce the number of animals which have to be sacrificed for the investigation of neuroprotective compounds.

1. Functional Investigations of the Effects of Excitotoxic Challenges on Electrophysiological Properties of Primary Cultured Rat Cortical Neurons

The first approach to reduce the number of animals used for the preparation of neuronal cultures is the development of functional assays, which consume only a very small number of neurons to test the effects of putative neuroprotective compounds. Here, I made use of certain specific changes in the electrophysiological properties of cortical cell cultures after excitotoxic challenges.

1.1 Material and Methods

A neuron-glia cell suspension was established from dissociated embryonic rat cortical cells. Cortex tissue was isolated from the brains of Wistar rat fetuses (18d gestation). Cortices were collected in 50 ml of Dulbecco's modified eagles medium with 4.5 g/ml glucose (DMEM) and centrifuged for 5 min (440 g). The DMEM was decanted and 5 ml trypsin-EDTA solution (0.05%, Boehringer Mannheim, Germany) were added. After 7 min incubation at 37°C the trypsin solution was carefully removed and 15 ml DMEM with 10% fetal calf serum (FCS, Boehringer Mannheim, Germany) were added to stop the enzyme digestion. Cortices were

carefully shaken, and again centrifuged (5 min, 440 g). The supernatant was discarded, and the cortices were resuspended in 2-3 ml DMEM. The tissue was homogenised with a series of 4 Pasteur pipettes with increasingly smaller tip diameters (4-10 strokes per trituration steps). Cells were counted and brought to a density of $2x10^7$ cells/ml with serum-based medium or DMEM. Cells were now seeded on glass cover slips which had previously been coated with poly-L-lysin/laminin at a density of $1.3x10^5$ cells/cm^2 in 24-well cell culture plates. The feeding medium (2 ml/well) was changed twice weekly. After 3 days *in vitro*, 5 µM of the mitosis inhibitor cytosine-arabinofuranoside (SIGMA, Deisenhofen, Germany) was added for four days to suppress the growth of non-neuronal cells. Cells were cultured in astrocyte-conditioned medium (ACM; see contribution by Bartmann-Lindholm and Carter).

Embryonic rat cortical neurons were exposed to 100 µM glutamate, or 100 µM glutamate and a given test compound for 20 h. After this treatment, cultures were kept in standard cell culture medium and electrophysiologically investigated 24 h after the onset of the treatment.

Electrophysiology

Recordings were made in the whole-cell configuration according to standard patch-clamp techniques (Hamill et al., 1981) with EPC7 or EPC9 amplifiers (HEKA, Lambrecht, Germany). The recording pipettes were made from borosilicate glass (Hilgenberg, Malsfeld, Germany) and had resistances of 3 to 5 MOhm. The pipette solution ("KF1") consisted of (mM): KF 110, KCl 40, $MgCl_2$ 1, BAPTA 0.1, HEPES 10, ATP 1, pH 7.2. In some experiments, potassium was replaced by cesium and tetraethyl-ammonium to suppress voltage-dependent potassium currents (medium: "CsF1"). The extracellular medium ("R2") consisted of (mM): NaCl 140, KCL 5.3, $CaCl_2$ 1.8, $MgCl_2$ 0.8, glucose 21.5, HEPES 10, pH 7.4.

Cells were clamped to a holding potential of -60 or -80 mV, and a voltage step protocol (nine depolarizing voltage jumps, 10 mV increment, 50 ms duration) was applied. For the measurement of the cell capacity the read-out of the compensatory circuitry of the patch-clamp amplifier was used. The steady-state potassium outward current and the peak sodium inward current at the ninth voltage jump was analyzed.

Fig. 1

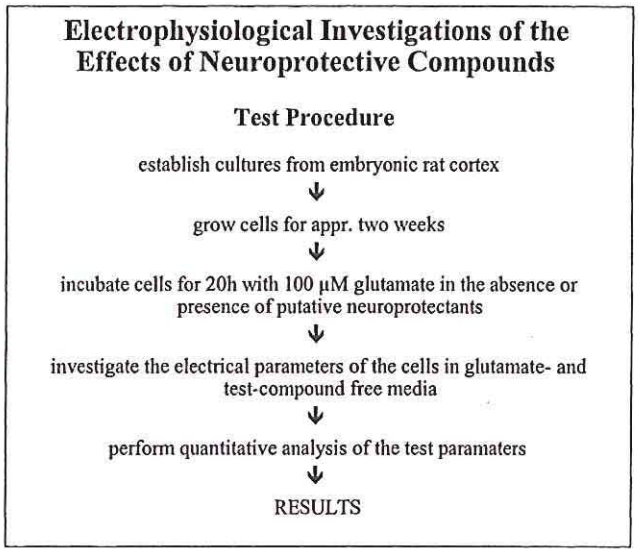

Scheme of the test procedure for the investigation of the effects of excitotoxic challenges on electrical parameters of cultured rat cortical neurons. Details are described in the text.

1. 2 Results

In previous investigations it had turned out that the exposure of cortical cell cultures to glutamatergic agonists for 20 h selectively reduced the amplitude of voltage-activated sodium currents, as well as the membrane capacity, in primary cultured cortical neurons. No significant effects on potassium outward currents or the resting membrane potential could be observed. I now tested whether putative neuroprotective compounds were able to counteract these effects. The compounds tested were e. g. two non-competitive NMDA antagonists (MK 801, BIII 277), a competitive antagonist of (S)-a-amino-3-hydroxy-5-methyl-4-isoxazolepropionic acid (AMPA)-type glutamate receptors (2,3-dihydro-6-nitro-7-sulfamoyl-benz(F)quinoxaline, NBQX), a blocker of voltage-activated sodium channels (TTX), and a broad-spectrum inhibitor of voltage-activated calcium channels (methoxy-verapamil=D600). All of these principles have been discussed to be neuroprotective *in vivo*. The results were as follows: MK 801 and BIII 277 (at 1 µM) completely prevented the glutamate-induced reduction of voltage-activated sodium currents. The same was the case for D600 (at 100 µM), whereas NBQX and TTX (at 1 µM each) could not prevent the attenuation of sodium currents. These results are in line with those obtained with other cell culture-based assays (see

e. g. the contribution by Bartmann-Lindholm and Carter). However, the cell numbers used for the experiments were rather small, compared to those needed for biochemical assays. For statistically significant determinations, about 15 to 30 cells per treatment group (control, 100 µM glutamate, 100 µM glutamate plus test compound) had to be investigated. Therefore, this method uses neuronal cell cultures very economically.

Fig. 2

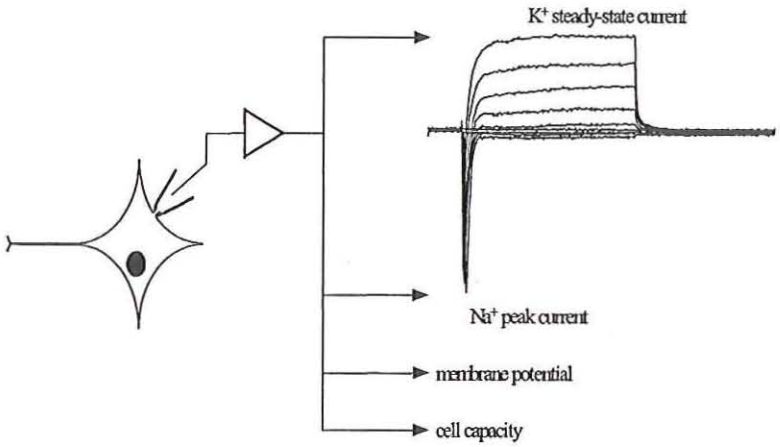

Electrophysiological parameters investigated after incubation of primary cultured cortical neurons in solutions containing 100 µM glutamate with or without a given test compound. Cells were voltage-clamped to a membrane potential of -60 or -80 mV, and 9 depolarizing voltage steps (50 ms duration, 10 mV increment) were applied to investigate the effects of the treatment on sodium inward and potassium outward currents. In addition, the cell's resting membrane potential and cell capacity were determined.

Fig. 3

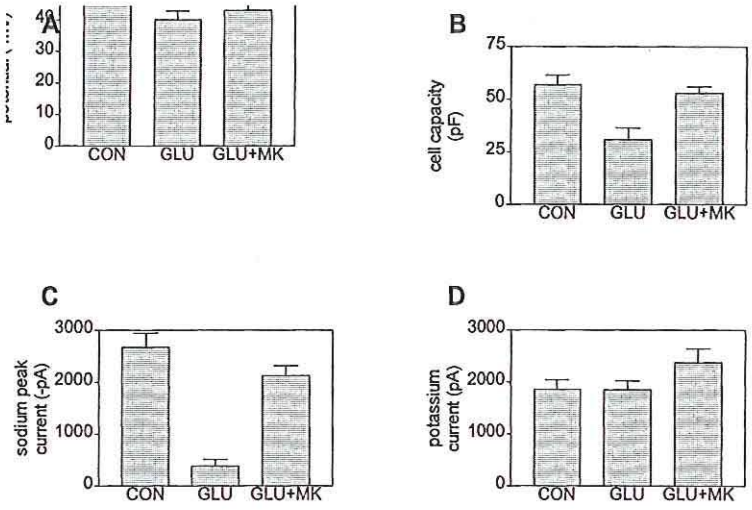

Results from a typical experiment performed according to figures 1 and 2. Cells were treated with either 100 µM glutamate (GLU), or 100 µM glutamate plus 1 µM MK801 (GLU+M) for 20 h and compared to untreated controls (CON). The glutamate treatment reduced the membrane capacity (B), as well as the sodium peak current (C), whereas resting membrane potential (A) and potassium outward currents (D) were only insignificantly affected. Coapplication of the non-competitive NMDA antagonist MK801 counteracted the effects of the glutamate treatment. N=15-23 per group, data are given ± SEM.

2. Cryopreservation of Primary Cultured Rat Cortical Neurons

Primary rat cortical cell cultures are normaly prepared from embryonic tissue. A pregnant rat bears about 10-14 embryos, and well-trained cell culture personnel can prepare high numbers of cortical neurons from this high number of organ donors. For my electrophysiological investigations neurons are cultured on glass coverslips at a density of 130000 cells/cm^2. Given a number of 10^7 neurons per embryonal cortex, theoretically appr. 40 coverslips can be prepared from one embryo (therefore appr. 500 from one pregnant rat). These cells have only a limited lifetime and can be used from day 11 to day 28 *in vitro*. Thus, normally much more cells are prepared than a small laboratory with a few electrophysiological setups can use up. The consequence is that a high fraction of the cells are wasted. It would be therefore

useful to have a method available which allows to store the cell cultures for later use. I followed this approach and developed a cryopreservation method which allows to store neuronal cell suspensions in liquid nitrogen for a theoretically unlimited time, and to take them in culture with a high yield of surviving neurons. Many parameters were optimized for the method which is described in the following section. Thorough functional tests demonstrated that these cryopreserved neurons have highly comparable properties, compared to their unpreserved counterparts.

2.1 Material and Methods:

Cell Culture

The culture of embryonic rat cortical neurons was done as described above. Various feeding media were used, namely: serum-based medium (DMEM with 10% FCS, 10% horse serum, 2 mM glutamine), astrocyte-conditioned medium (ACM; see contribution by Bartmann-Lindholm and Carter), or ACM supplemented with 2% B27 (Gibco, Eggenstein, Germany).

Cryopreservation Procedure

For preserving the cortical cell suspensions, the following changes to the standard cell culture procedure were introduced: Five ml of the cell suspension (density: $2x10^7$ cells/ml) were added to a mixture of 1 ml FCS, 0.8 ml DMSO, and 3.2 ml methyl-cellulose (Sigma, Deisenhofen, Germany; 4000 centipoise; 0.3% w/v) in DMEM. Thus, the final concentrations were $1x10^7$ cells in 10% (v/v) FCS, 8% (v/v) DMSO, and 0.1% (w/v) methyl-cellulose. One ml aliquots of the suspensions were filled into cryovials, put into a cryocontainer (Nalgene, Wiesbaden, Germany), frozen down overnight at -80°C, and stored in liquid nitrogen.

After periods of up to 12 months, frozen cell suspensions were plazed into a 37°C waterbath and removed immediately upon thawing. Cells were diluted in feeding medium to get a final density of $1.3x10^5$ cells/cm^2 and seeded on glass coverslips in 24-well cell culture plates. In some cases, cells were first centrifuged in 50 ml feeding medium and resuspended to remove the cryoprotectants (DMSO and methyl-cellulose). Various feeding media were used (serum-based, ACM, ACM+B27; see above).

Quantification of Cell Yields

For estimating the number of surviving neurons with and without different cryopreservation protocols, microphotographs of arbitrarily chosen regions (0.345 mm^2 each) of the culture dishes were taken after four days *in vitro*. The number of neurons per photograph was counted in a blinded manner. At least eight photographs per treatment group were analysed.

Electrophysiology

Recordings were made in the whole-cell configuration according to standard patch-clamp techniques (Hamill et al., 1981) with EPC7 or EPC9 amplifiers (HEKA, Lambrecht, Germany) as described above. The pipette solution "KF1" or "CsF1" were used. The extracellular medium ("R2") consisted of (mM): NaCl 140, KCL 5.3, $CaCl_2$ 1.8, $MgCl_2$ 0.8, glucose 21.5, HEPES 10, pH 7.4.

Ligands of transmitter-activated ion channels were applied using the following concentrations: N-methyl-D-aspartate (NMDA): 300 µM, kainic acid: 300 µM, gamma-amino-butyric acid (GABA): 30 µM. Media for the investigation of ligand-activated ion channels contained 300 nM tetrodotoxin (TTX) to suppress voltage-activated sodium channels. When NMDA was applied, 5 µM glycine were added to the extracellular medium, calcium was reduced to 0.1 mM, and magnesium was omitted. Drug solutions were applied using a gravity-driven application system, which allowed to change the extracellular medium surrounding the cell under study within 20-30 ms (Weiser and Wienrich, 1996).

If not otherwise stated, data are given as means$\pm$SEM.

2.2 Results

Cell Yield

One crucial issue concerning the cryopreservation of post-mitotic cells is the cell yield after the preservation process. In the course of the optimization of this method, the influences of many parameters on the survival rate of neurons were tested (e. g. amount of DMSO, glucose, or methyl-cellulose in the freezing medium; use of tissue blocks versus cell suspensions; different freezing protocols; different thawing media, etc.). In unfrozen controls (cultured in ACM+B27) the neuronal density was 58870$\pm$2842 neurons/cm^2; compared to the seeding density of $1.3x10^5$ cells/cm^2 this amounts to 45$\pm$2.2 %. This comes close to the maximum yield of neurons in a cell culture preparation (McManus and Brewer, 1997). No attempts were

made to discriminate between neuronal and non-neuronal cells during the cell culture process, thus one can estimate a relativelly high percentage of non-neuronal cells in the preparation.

In previous experiments the freezing medium was optimized (see materials and methods). I now investigated whether the media for thawing and subsequent feeding had an effect on the number of surviving neurons.

The highest yield was obtained with ACM+B27 (48.3±1.5%), compared to the unfrozen controls. In serum-based medium only 19.7±4.6 of the neurons survived. Thus, ACM+B27 is now used as standard thawing and feeding medium for the cryopreserved neurons. What is the reason for these improved properties of ACM+B27? In my observations it turned out that glial cells are relativelly sensitive for the cryopreservation procedure. On the other hand, in serum-fed cultures neuronal survivial is critically dependent on the presence of vital astrocytes. Possibly, the low yield of cryopreserved neurons in serum-based medium is due to the fact that only a small number of glial cells survive the treatment, leading to increased mortality in the neuronal population. In contrast, ACM+B27 suppresses the growth of glial cells, but on the other hand provides all the glial factor which are neccessary for promoting neuronal survival.

Table 1

Effects of different combinations of freezing/thawing media on the survival of cryopreservered cell suspensions prepared from embryonic rat cortex.

Freezing Medium	**Thawing Medium**	**Cells/cm^2**	**% of control**
Unpreserved controls	--	58809±2840	100
DMEM, 10% FCS, 8% DMSO	serum-based	11014±2318	19±3.9
DMEM, 10% FCS, 8% DMSO	ACM/B27	28405±869	48±1.5
DMEM, 10% FCS, 8% DMSO, 0.1% methyl-cellulose	serum-based	7246±860	12±1.4
DMEM, 10% FCS,	ACM/B27	11594±2724	20±4.6

8% DMSO 0.1% methyl-cellulose

Electrophysiological Characterization

Cryopreserved neurons and their sister cultures of comparable ages *in vitro* were investigated concerning the following parameters: Resting membrane potential, cell capacity, maximum sodium inward current, maximum potassium outward current, neurotransmitter-activated currents (in response to pulse applications of kainic acid, NMDA, and GABA). None of these parameters was statistically different between unpreserved neurons and neuronal preparations, which had been cryopreserved for up to one year. Thus, cryopreserved neurons can be postulated to behave comparable to unfrozen cultures in electrophysiological test assays.

3. Discussion and Conclusions

In vitro methods for testing the effects of putative neuroprotective compounds have been shown to be very useful surrogates for *in vivo* experiments. The aim of my contribution was to further reduce the number of animals which have to be sacrificed for the preparation of neuronal cell cultures.

My first approach to reduce the number of animals for the tissue culture was to develop techniques which need only small numbers of cells for a given experiment. This approach is described in the second part of this chapter. The down-regulation of neuronal sodium channels in response to excitotoxic challenges turned out to be a sensitive read-out for the effects of putative neuroprotective compounds. The question remains, which effects on the cellular level underlie the down-regulation of neuronal sodium channels by excitotoxic challenges. Li et al. (1993) have shown that the amplitudes of currents flowing through voltage-activated sodium channels are reduced by activating protein kinase C (PKC). O'Reilly et al. (1997) reported that oxygen deprivation can reduce sodium currents in hippocampal neurons via this mechanism. On the other hand, Hara et al. (1997) report a down-regulation of PKC in the

brains of mice after transient occlusion of the medial artery. Thus, more experiments are neccessary to clarify these findings.

Another possible explanation might be that sodium channels are internalized by neurons in response to the increase of intracellular sodium concentrations (Dargent and Couroud, 1990; Paillar et al., 1996). Sodium concentrations have been reported to increase in response to glutamate challenges (up to 60 mM; Kiedrowski et al., 1994). Thus, the active internalization of sodium channels might be the reason for the effects reported in this study.

Irrespective of the underlying mechanism, this method efficently saves neuronal tissue for the investigations. Given a number of 100 cells per experiment, I leave the calculation to the reader how many experiments theoretically could be performed from the 10^7 neurons of an embryo's cortex. Thus, this method and cryopreservation techniques of embryonic neurons give a powerfull combination of methods to reduce the number of animals to be sacrificed for *in vitro* investigations of neuroprotective compounds.

The other approach followed the idea to increase the useful number of cultured neurons by the application of cryopreservation techniques. Some researchers reported findings about the cryopreservation of neuronal tissue for cell cultures (e. g. Sucher et al., 1991; Petite and Calvet, 1995, 1997;) or grafts for transplantation (Sautter et al., 1996; Yoshimoto et al., 1993). Nevertheless, figures describing the cell yield are sparse. Here, I described a method for the effective cryopreservation of embryonic cortical neurons. The cell yield is high (about 50% of the neurons survive the treatment), and in the applied functional assays these cells were indistinguishable from their unfrozen counterparts. This method is now established as a standard technique in my cell culture laboratory: Cells, which are not used for "fresh" neuronal cultures and which normally would be discarded are now preserved for future use. Thus, no embryonic brain tissue is wasted. In the long run, this method can be calculated to reduce the number of animals to be sacrificed as tissue donors by 50 to 75%.

Acknowledgements

The skillful technical assistance of W. Berger, K. Kappertz, D. Linn, B. Reich, M. Vogt and H. Wölfel is gratefully acknowledged. Some of the ACM samples were provided by C. Bartmann-Lindholm.

References

Choi, D. W., Maulucci-Gadde, M. and Krieglstein, A. R. (1987)
Glutamate neurotoxicity in cortical cell culture
J. Neurosci. **7**, 357-368

Dargent, B. and Couraud, F.(1990)
Down-regulation of voltage-dependent sodium channels initiated by sodium influx in developing neurons
Proc. Natl. Acad. Sci. USA **87**, 5907-5911

Gill, R., Brazell, G. N., Woodruff, G. N. and Kemp, J. A. (1991)
The neuroprotective action of dizocilpine (MK-801) in the rat middle cerebral artery occlusion of focal ischaemia
Br. J. Pharmacol. **103**, 2030-2036

Hamill, O. P., Marty, E., Neher, E., Sakmann, B. and Sigworth F. J.(1981)
Improved patch-clamp techniques for high-resolution current recording from cells and cell-free membrane patches
Pflügers Arch. **391**, 85-100

Hara, H., Ayata, G., Huang, P. L. and Moskowitz, M. A.(1997)
Alteration of protein kinase C activity after transient focal cerebral ischemia in mice using *in vitro* [^{3}H]phorbol-12,13-dibutyrate binding autoradiography
Brain Res. **774**, 69-76

Kiedrowski, L., Wroblewski, J. T. and Costa, E.(1994)
Intracellular sodium concentration in cultured cerebellar granule cells challenged with glutamate
Mol. Pharm. **45**, 1050-1054

Li, M., West, J. W., Numann, R., Murphy, B. J., Scheuer, T. and Catterall, W. A.(1993)
Convergent regulation of sodium channels by protein kinase C and cAMP-dependent protein kinase
Science **261**, 1439-1442

McManus, D. Q. and Brewer, G. J.(1997)
Culture of neurons from postmortem brain
Neuroscience Lett. **224**,193-196

Meldrum, B. and Garthwaite, J.(1990)
Excitatory amino acid neurotoxicity and neurodegenerative disease
In: Lodge, D. and Collingridge, G. (eds.)TIPS Special Report: The Pharmacology of Exciatory Amino Acids, Elsevier, 54-62

O'Reilly, J. P., Cummins, T. R. and Haddad, G. G.(1997)
Oxygen deprivation inhibits Na^+ current in rat hippocampal neurones via protein kinase C
J. Physiol. **503.3**, 479-488

Paillart, C. P., Boudier, J.-L., Boudier, J.-A., Rochat, h., Couraud, F. and Dargent, B.(1996)
Activity-induced internalization and rapid degradation of sodium channels in cultured fetal neurons
J. of Cell Biology **134(2)**, 499-509

Petite, D. and Calvet, M.-C.(1995)
Cryopreserved neuronal cells in long-term cultures of dissociated rat cerebral cortex: survival and morphometric characteristics as revealed by immunocytochemistry
Brain Res. **669**, 263-274

Petite D. and Calvet, M.-C.(1997)
Morphometric characteristics of cryopreserved mesencephalic dopamine neurons in culture
Brain Res. **769**, 1-12

Sucher, N. J., Cheng, O. P. and Lipton, S. A.(1991)
Crypreservation of postnatal rat retinal ganglion cells: persistance of voltage- and ligand-gated ion currents
Neuroscience **43(1)**, 135-150

Weiser, T. and Wienrich, M.(1996)
The effects of copper ion on glutamate receptors in cultured rat cortical neurons
Brain Res. **742**, 211-218

Yoshimoto, Y., Date, I. and Ohmoto, T.(1993)
Improved cryopreservative medium suitable for the freeze-storage and transplantation of fetal neural tissues
Restorative Neurology and Neurosciences **6**, 73-81

Fluorimetric Methods For The Assessment Of Neuronal Cell Death As Well As Ion- And Energy Homeostasis Using *In Vitro* Models of Excitotoxicity and Ischemia

Detlev Melzian, Rita Sattler and Mathias Hafner
Department of Molecular Biology and Cell Culture Technology
Mannheim University of Applied Sciences
Windeckstr. 98
D-68163 Mannheim

Summary

Over the past ten years experimental evidences have been made to clarify the understanding of the basic pathophysiological mechanism in excitotoxic and hypoxic-ischemic evoked neuronal cell injury. The neurotransmitter glutamate is becoming accepted as an important mediator of hypoxic/ischemic brain damage. Little information is available on the role of proton and sodium ion balance and the direct disturbance of the energy metabolism in excitotoxic brain injury. Specific glutamate receptor antagonists are one of the recent pharmcologic strategies for reducing hypoxic/ischemic neuronal damage. However, the established methods to demonstrate the neuroprotective potency of drugs still use *in vivo* animal tests (e.g. MCAO-model). The objective of the present study, therefore, was to develop *in vitro* screening systems based on neuronal cell cultures, to reduce animal tests in preclinical drug screening to a minimum. The *in vitro* tests focused on i) an excitotoxicity assay with high throughput screening capacity based on a fluorescence multiwell reader and ii) digitized fluorescent imaging of individual neurons, with respect to their intracellular ion dynamics and changes in mitochondrial membrane potential as predictive markers of neurotoxicity. Neurotoxic concentrations of glutamic acid induced a rapid and irreversible increase of the intracellular calcium concentration which was accompanied by a transient acidic shift of the intracellular pH, and followed by an intracellular alkalinisation in cultured murine cortical neurons. In addition, glutamate triggered a continuous increase in intracellular sodium and destroyed mitochondrial membrane potential. The loss of rhodamine-123 fluorescence highly correlated with the ongoing neuronal cell death and was shown to be a suitable parameter to determine the neuroprotective action of pharmaceutical compounds. However, among the pharmacological compounds tested only the non-competetive NMDA-receptor antagonist

MK-801 was found to preserve neuronal viability by improving mitochondrial membrane potential and normalizing intracellular ion homeostasis. We also developed a new assay system, which allows the multiparametric monitoring of intracellular and extracellular parameters associated with stroke in a refined model of "*in vitro* ischemia". This model makes use of a sealed temperature controlled chamber placed on a microscope stage to mimic defined anaerobic/ischemic conditions. The following modifications have been made to the chamber to facilitate routine ischemia experiments: oxygen and pH sensors are used to monitor oxygen concentration and extracellular pH value in the chamber solution. The electrodes are mounted on top of the chamber and placed directly above the cells. An optical window allows the video control of cells with phase contrast and fluorescence optics during the entire experiment. The following parameters were used to asses neuronal cell death: i) microscopic observation by phase contrast microscopy, ii) vital dye exclusion/-uptake with trypan blue or propidium iodate, iii) intracellular changes of calcium, proton or sodium concentrations, iv) changes of mitochondrial membrane potential. We anticipate that the described *in vitro* assays can be used to predict neuronal death during hypoxia/ischemia related insults and to further characterize the neuroprotective effect of drugs as a supplement for currently used animal tests and hence reduce the number of laboratory animals.

Abbreviations

1S,3R-ACPD: 1S,3R-aminocyclopentane-1,3-dicarboxylic acid; **AMPA**: (-amino-3-hydroxy-5-methyl-4-isoxazole propionic acid; **BCECF**: 2´,7´-bis-(Carboxyethyl)-3(6´)-carboxyfluorescein; **BSA**: bovine serum albumine; **CNQX**: 6-cyano-7-nitroquinoxaline-2,3-dione; **DABCO**: diazobicyclooctane **DAPI**: 4´,5-diamidino-2-phenylindole-dihydrochlorid; **DIV**: day in vitro; **DMSO**: dimethyl suflfoxide; **FITC**: fluorescein Isothiocyanate; **HBSS**: Hepes buffered salt solution; **HEPES**: N-(2-hydroxyethyl)piperazine-N´(2-ethanesulfonic acid); **MEM**: Minimal essential medium; **LDH:** lactate dehydrogenase, **L-NAME**: N(G)-nitro-L-arginine methyl ester; **MK-801**: (5R,10S)-(+)-5methyl-10,11-dihydro-5H-dibenzo[a,d]cyclohepten-5,10-imine; **NBQX**: 6-Nitro-7-sulphamyl-benzo[f]quinoxaline-2,4.dione; **NMDA**: N-methyl-D-aspartate; **PBS**: phosphate buffered saline; **PI**: propidium iodide; **rhd-123**: rhodamine-123; **RT**: room temperature; **Tris**: *tris*(hydroxymethyl)aminomethane; **TTX**: tetrodotoxin; **U-83836E**: (-)2-((2,6-di-1-pyrrolidinyl-4-pyrimidyl)-1-piperazinyl)methyl)-3,4-dihydro-2,5,7,8-tetramethyl-2H-1-benzopyran-6-ol-dihydrochloride

Introduction

Currently used animal tests for stroke. Substantial efforts are being made by pharmaceutical industries to develop drugs which will protect the brain from neurodegeneration that follows a variety of diseases. Stroke is the third leading cause of mortality and a major cause of long-lasting physical disability. Because neither stroke nor other severe neuropathological conditions can presently be treated effectively, causative therapies to reduce mortality and to improve neurological outcome are eagerly needed to ameliorate the medical, social and economical consequences of stroke. These efforts now concentrate on the development of drugs which are neuroprotective, that is drugs which can be given to minimize the neuronal damage or increase the neuronal outcome in patients after stroke.

Experiments in pharmacology are usually dependent on the use of animals, which is accompanied by ethical problems and little public acceptance. A key factor in this process has been the development of various animal tests that mimic the neuropathological consequences of stroke. The occlusion of an intracranial artery, usually the proximal middle cerebral artery (MCAO-test), is widely used to produce focal ischemia in animals, mainly rodents (McAuley, 1995). Beside causing substantial stress, pain and anxiety to the animals these *in vivo* bioassays suffer from several problems mostly arising from their inter- and intra-assay variability. Almost sixty rats are needed to test the effect of one drug with the appropriate certainty after statistical evaluation, making the *in vivo* assay labor-intensive and expensive. However, although one of the major advances of stroke research has been the development of reproducible techniques for the induction of focal or global ischemia in animals, the fact remains that there is a substantial number of variants of those *in vivo* bioassays (Fox et al., 1993). The drug screening pharmacologist is therefore faced with a variety of test systems, none of which is known to be of predictive value. The reason for this is that, at present, no drug has been shown to have any neuroprotective effect following stroke in humans. Therefore, at present, there is no way of knowing if activity in any animal tests predicts efficacy. Thus, the development of experimental strategies that improves the specificity of the assay and saves animal is a challenge. A probable solution to these problems can be an *in vitro* neuronal cell culture system, which allows the monitoring of pharmaceutical effects in an animal-saving and organ-specific manner (Oberpichler-Schwenk and Krieglstein, 1994). Another advantage of the *in vitro* test, beside saving of time, costs and the number of animals used is the ability to control and to determine the experimental parameters in a wider range than in the whole animal. Furthermore, one can argue, that, on the basis of our improved understanding of the pathocellular mechanisms of neuronal cell death, the indication of this

potential may be obtained equally well in animal or in *in vitro* tests, and, in these cases, the use of animals cannot be justified in an early state of drug development.

Calcium and neuronal cell death. There is a growing body of evidence that the calcium ion can play a critical role in cell killing. Since free intracellular calcium is arguably the most important ion regulating numerous cellular functions, it is not surprising that disruption of intracellular calcium homeostasis is frequently associated with early cell injury. This led to the formulation of the „calcium hypothesis" of cell death, proposing that imbalances in calcium regulation and perturbation of calcium homeostasis may be a final common step in the development of cytotoxicity (Orrenius and Nicotera, 1994). The key role of calcium in cell death is particularly evident in the central nervous system. In neurons principle routes of calcium entry are the voltage sensitive (VSCC) and excitatory amino acid (EAA)-linked receptor operated (ROCC) calcium channels (Meyer, 1989). Glutamate is the most abundant of several endogenous EAA´s and now has become widely accepted as the principal neurotransmitter in the brain. Its interaction with specific membrane receptors is responsible for many neurologic functions including cognition, memory, synaptic plasticity and movement. Systemic administration of glutamate to animals of various species caused acute degeneration of neurons (Olney, 1969). From this and related observations the excitotoxicity concept was proposed by Olney (Olney, 1974; Rothman and Olney, 1986). EAA-mediated toxicity is specific in its characteristic that neuronal cell bodies and dendrites are predominantly affected whereas axons are spared, and that distinct neuronal population differ in their vulnerability. Activation of these receptors leads to the opening of their associated ion channels, which are typified by their different permeability's to Na^+, K^+, and Ca^{2+}. What do we know about the pattern of injury mediated by excessive exposure to glutamate? Briefly, it can be subdivided into an acute swelling and delayed cell degeneration. The first component of glutamate receptor-mediated toxicity includes neuronal swelling caused by Na^+ influx through ligand- and voltage-gated ion channels accompanied by passive Cl^- and water influx (Rothman and Olney, 1986; Melzian et al, 1995). However, delayed cell degeneration, the second and dominant component of glutamate-mediated neurotoxicity leading to cell death, is highly dependent on the presence of extracellular Ca^{2+} and calcium influx through NMDA receptors. Although excessive intracellular calcium concentration may contribute to a series of cytodestructive processes, calcium alone may not be sufficient to trigger these neurotoxic events. NMDA receptor antagonists and the absence of extracellular calcium have been shown to protect neurons in various cell culture models. Furthermore, intracellular calcium chelating agents like BAPTA and related compounds are neuroprotective in models of ischemia *in vivo*

and *in vitro* (Tymianski et al, 1993c). Much less is known, however, about the biochemical processes by which the calcium overload causes neuronal cell death. An increase in intracellular calcium can activate degradative enzymes, such as proteases, endonucleases, phospholipases or other enzymes like nitric oxid synthase, thereby contributing to the excitotoxic process. Available evidence would further suggest that calcium mediated dysfunction of mitochondria and perturbation of cytosceletal components may be of particular importance.

In the past decade, there is a growing body of evidence that protection of mitochondria against calcium mediated damage is a useful way to protect neurons against excitotoxic/ischemic insults. Recent data (White & Reynolds, 1996) indicate, that massive calcium uptake by mitochondria is an important step in buffering cytosolic calcium after physiological stimulation as well as an excitotoxic challenge (White and Reynolds, 1997).

One link between excessive intracellular calcium increase and loss of neuronal function may be the disruption of the mitochondrial membrane potential and ATP production as a result of a massive intra-mitochondrial calcium accumulation. It is known, that mitochondria take up calcium via an uniporter which uses the electrochemical gradient across the inner mitochondrial membrane as a driving force. Therefore, calcium uptake into mitochondria reduces the amount of ATP produced (McCormack and Denton, 1993) under conditions where there is an increased energy demand to maintain cellular ion homeostasis.

Recently, several investigators have shown that mitochondrial calcium transport inhibitors protected mitochondria against glutamate induced calcium accumulation. Dux et al. (1996) have demonstrated, that the protective effect of serum proteins against excitotoxic stimulation is related to their ability to maintain normal intramitochondrial calcium concentrations. Furthermore, a large increase of the mitochondrial matrix calcium concentration induces the opening of the so-called permeability transition pore located in the inner mitochondrial membrane. Uncontrolled opening of the pore resulted in an efflux of solutes and small proteins $\leq$ 1,5 kDa out of matrix inducing mitochondrial swelling and disruption of the membrane potential (Petronilli et al., 1994). The pore is thought to be normally responsible for the osmotic balance between the mitochondrial matrix and the intermembrane space. One consequence of uncontrolled pore opening may be uncoupling of the oxidative phosphorylation and the generation of free radicals by the uncoupled respiratory chain, mainly reactive oxygen species (e.g. superoxide anions). The resulting enhanced oxidative stress could be a contributing factor to glutamate mediated neuronal cell death (Dugan et al. 1995) which was confirmed by the neuroprotective action of several antioxidants and radical scavengers.

Digital imaging of free intracellular ions in cortical neurons. The new understanding of ion-deregulation during neuronal injury is principally the result of new techniques that permit the measurement of transient changes in the free intracellular ion concentration. Perhaps the most fruitful among these methods has been the application of „vital" fluorescent probes (i.e. fluorophores that do not adversely affect cell viability) in combination with video technologies and computer-based image processing. Many factors that complicate quantification of fluorescence in cells can be circumvented by using ratio dyes (i.e. analyzing fluorescence ratios derived from pairs of fluorescence images). This approach has been most commonly applied to characterizing intracellular ion concentrations (Tymianski 1993 a, b). In addition only small numbers of cells are required and quantitative information can be obtained from individual living cells as they undergo changes, without harming them. When applied *in vitro* it is especially useful in those circumstances where there are few cells in primary culture or cells that are hard to grow like murine cortical neurons.

The major objective of the present study, therefore, was to develop *in vitro* assays using digitized fluorescent imaging in which neurons can be studied with respect to their intracellular ion dynamics and changes in the mitochondrial membrane potential as predictive markers of neurotoxicity. This was used in combination with a newly developed high throughput assay system to monitor neuronal cell death in multiwell plates using a modified fluorescence scanner (Sattler et al., 1997). The latter approach was intended to asses potential neuroprotective agents based on the experimental endpoints survival or death of neurons within 24 h. That allows a sufficient period of observation to distinguish between cells destined to survive or die and the automated prescreening of a large number of potential neuroprotective compounds. Compounds identified as neuroprotective agents may than be further studied at the resolution of the single cell level with digital imaging techniques. That approach permits the assessment of cell function and drug action during the course of ischemia by measuring a variety of biochemical parameters in real time under defined conditions.

Materials and Methods

Neuronal cell culture. Cortical cell cultures were prepared from embryonic (E15) NMRI mices (Charles River, Sulzfeld, D). Female mices were killed by cervical dislocation and the embryos were placed in PBS w/o calcium and magnesium. Cortical hemispheres were dissected away from the rest of the brain, the meninges were removed and the resulting tissue placed in PBS at room temperature. Cortices were dissociated by incubation in 0.05 % Trypsin (Fluka, Deisenhofen, D) in calcium and magnesium free PBS supplemented with 0.02 % EDTA for 15 min at 37 °C. Trypsin was inactivated by adding serum containing maintenance media consisting of Eagle´s minimal essential media (MEM, Earle´s salts, Gibco, Eggenstein, D) supplemented with 10 % heat inactivated horse serum (ICN, Eschwege, D) 2 mM glutamine, 25 mM glucose and 26 mM $NaHCO_3$. The tissue was then triturated 10 times using fire polished pasteur pipettes in maintenance medium followed by an additional trituration with a fire polished pipette with reduced tip diameter for 3 times. After centrifugation (10 min, 1000 x g) cells were resuspended in maintenance medium and viability determined by phase contrast microscopy or by staining a small aliquot with fluorescein diacetate, a vital dye, to adjust viable cell density by counting stained cells under fluorescence optics using a hemocytometer (Neubauer).

Plating on glass coverslips. The cell suspension was diluted to 860,000 cells/ml and 5 ml of the resulting cell suspension was plated onto poly-L-ornithine precoated (15 µg/ml, dissolved in 10 mM sodium tetraborate solution, adjusted to pH 8,4 with HCL, 6-12 h) rectangular 40 x 24 mm or 37,5 x 22 mm glass-coverslips (Menzel, D) which were housed in Petri dishes (60 mm diameter). Prior to plating, the coated glass cover slips were washed three times with steril water and incubated at 37° C in plating media (maintenance media supplemented with 10% fetal bovine serum (HighClone, Frickenhausen, D) for 1-2 hours. Normaly, the dissection of one pregnant mouse with 13-15 embryos resulted in 20-25 plated coverslips. Cultures were maintained in a humidified 5 % CO_2, 95 % air atmosphere at 37 °C. After 7 days in vitro (DIV), non neuronal cell division was inhibited by treating the cultures with 10 µM uridine and 10 µM (+)-5-fluo-2´-deoxyuridine (Sigma, Deisenhofen, D) for 24 to 48 hours. In case of the *in vitro* ischemia experiments, the growth of non neuronal cells was not inhibited, only a medium change was performed. After 14-16 days in culture, cells were used for experiments.

Plating on 24-well microtiter plates. The cultures were plated on 24 well plates (Corning, Bodenheim, D) that, a day prior, were coated overnight at 37 °C with poly-L-ornithin

(15 µg/ml, dissolved in 10 mM sodium tetraborate solution, adjusted to pH 8,4 with HCL). After washing with sterile water and incubation with plating medium (see above), the dissociated cells were plated in the precoated culture wells (15-mm diameter, 0.43 $x10^6$ cells/well in 0,5 ml maintenance medium). Only 20 of 24 wells were plated with cells, leaving wells for background subtraction. Cells were maintained in a humidified 5 % CO_2/95 % air atmosphere at 37 °C. At 4 days in vitro, they were treated with 5 µM uridine and 5 µM (+)-5-fluo-2´-deoxyuridine for 48h to inhibit non-neuronal cell proliferation and shifted back to maintenance medium.

Immunostaining. Coverslips with neuronal cells were washed three times with phosphate buffered saline (PBS w/o calcium & magnesium, PAA, Cölbe, D) + 3 % bovine serum albumine (BSA, Fraction V, Sigma, Deisenhofen, D), to avoid nonspecific binding of the antibodies and than fixed and permeabilized with ice cold methanol at -20 °C for 30 min. After washing with PBS-BSA for three times (10 min, RT) cells were incubated with the primary antibodies for 1h. The coverslips were subsequently washed with PBS-BSA three times and thereafter incubated with the secondary antibody for 90 min at 37 °C in a humidified staining chamber. The secondary antibody Fluorescein Isothiocyanate-(FITC)-conjugated anti mouse IgG (Boehringer, Mannheim, D) was diluted 1:200 with PBS-BSA and mixed with the nuclear dye 4´,5-diamidino-2-phenylindole-dihydrochlorid (DAPI, final concentration 2 µg/ml). The cells were washed as previously described and mounted on micoscope slides using glycerine-MOWIOL (2.4 g MOWIOL 4-88 (Hoechst, Franfurt, D) + 6 g glycerin (Merk, Darmstadt, D) + 6 ml dest. water + 12 ml Tris pH 8.5 (Fluka, Deisenhofen, D) + 0.66 g Diazobicyclooctane (DABCO, Sigma, Deisenhofen, D). After drying overnight in the dark at 4 °C coverslips were sealed with nail varnish. The cells were viewed using phase contrast optics with an Leica DMR (Leica, Benzheim, D) fluorescence microscope equipped with a Photonic Science MonoCoolview integrating camera (Norwich, UK) connected to an Apple McIntosh based OpenLab image analysis system (ImproVision, Coventry, UK).

Measurement of cell death in a fluorescence multiwell reader. Quantitative measurements of cell death were performed using a modified Cytofluor II fluorescence multiwell plate scanner (Perseptive Biosystems, Farmingham, MA, USA). Briefly, this is a software-controlled device in which the optical apparatus consists of a quarz halogen lamp (spectral range 320-700 nm), two six-position filter wheels (to filter excitation and emission wavelengths), and an R1527 Hamamatsu photomultiplier tube (Hamamatsu, J), all coupled via

quartz optic fibers. The filter wheel is equipped with interference filters optimized for use with a given fluorescence probe. Presently, we use a filter combination aimed as exciting and recording propidium iodate (PI) fluorescence (530 ± 10 nm excitation and 630 ± 20 nm emission). Modification were made to the scanner to permit temperature control to within 0.2 °C. The casing was altered to contain copious styrofoam insulation. Changes in temperature were archived by mounting in the casing two modified thermoelectric heater/cooler assemblies taken from a cooler box (Igloo Cool-Mate, model 4502, Houston, TX, USA). These contained the thermoelectric devices, heat sinks, and fans. The fans circulated the air within the device to produce a uniform temperature throughout the chamber housing the microtiter plates. The thermoelectric assemblies were powered by a precision bipolar thermoelectric controller (Power Puncher BP 120, Alpha-Omega Instruments Corp., RI, USA) that permitted the temperature to be set and monitored. Monitoring was via a T-type thermistor placed at the level of the microtiter plate. A mercury lab thermometer was added to independently verify the accuracy of the temperature readings. Internal humidity was monitored with a household hygrometer and maintained above 65 % using a water bath containing a humidifier sponge inside the scanner. This kept fluid evaporation at the higher temperatures (37 °C) to < 5 % of the original culture well volume.

Manual counts of PI-labeled neurons. At the end of some experiments with 24 well plates, the plates containing PI-labeled cells were transferred to a Nikon Diaphot equipped with epifluorescence optics and viewed through a x 20 lens (Nikon CF UV-F; 20x) using a rhodamine filter cube (Nikon G-2A). Three microscope fields were chosen at random from each culture well and were photographed using a video camera (Hamamatsu C2400, Hamamatsu, J) interfaced to a digital image analysis software package (Image-1/AT; Universal Imaging Corp., West Chester, PA, USA). The numbers of PI-labeled cells were counted manually from each digital micrograph. This approach was chosen over direct observation through the microscope eyepieces to minimize the possibility that phototoxicity due to prolonged exposure to incident excitation light would alter the number of dead cells in a given well. A second observer replicated all manual counts to ensure count accuracy and minimal interobserver variability (< 5 %)

Experimental procedures: Fluorescence multiwell scanner. a) Online mode This mode was used to determine the time course of ongoing neuronal cell death following an excitotoxic challenge. Experiments were performed near room temperature as the cultures were shifted from the scanner to other areas within the same room for additional manipulations. All

manipulations were under sterile conditions. Typically, cultures were washed with 0.5 ml of HBBS containig 50 µg/ml propidium iodate, and a baseline fluorescence reading was taken. Subsequently, the solution in each well were switched to contain a given concentration of glutamate, and additional PI fluorescence measurements were taken at 1-h intervals for 24 h. Then, the plates were removed from the scanner and were subjected to manual cell counting or to lactate dehydrogenase (LDH) efflux determinations (see below). Raw PI fluorescence was background substracted using measurements taken from wells devoid of cultures containing neurotoxic agents. PI fluorescence was unaffected by adding excitatory amino acids or EAA receptor antagonists. Fluorescence values in arbitrary units can be converted to the fraction of neuronal cell death by normalizing them against the maximal background subtracted PI fluorescence of identical cultures exposed to a 60 min challenge of 1 mM NMDA resulting in near complete neuronal cell death after 24 h without affecting glial cells.
b) Endpoint mode To increase the number of 24-well plates tested within a given time (e.g. 24 h) and to focus on only a short excitatory amino acid challenge, we used an endpoint measurement mode to develop a high throughput screening system for testing of neuroprotective compounds. Neuronal cell cultures were washed with 0.5 ml of prewarmed HBBS containing 50 µg/ml PI, and after 10 minutes at 37 °C a baseline fluorescence reading was taken. Subsequently, the solution in each well were switched to contain a given concentration of different excitatory amino acids for 15 minutes in a humidified incubator at 37 °C and additional PI fluorescence measurements were taken. After switching the cell culture medium to EAA-free HBSS the well plates were shifted back to an incubator and cultured for 24 h at 37 °C followed by an additional fluorescence reading. Potential neuroprotective compounds were added with the EAA containing solution or at defined timepoints after the EAA challenge. Cultures were incubated with the drug containing medium throughout the experiment. Fluorescence values were normalized against background corrected changes of the control data which was set to 1 and expressed as arbitrary units.

Measurements of LDH release. In some experiments, PI fluorescence and LDH efflux measurements were compared at 24 h using a commercially available colorimetric assay (Boehringer, Mannheim, D). Cell death was expressed as the percentage of LDH activity produced by the maximal glutamate exposure (1 mM for 24 h) in cultures within the same microtiter plate.

Digital imaging of intracellular ion concentration (Ca^{2+}, H^+, Na^+) and mitochondrial membrane potential ($\Delta\Psi$). Intracellular changes in calcium, sodium and proton concentrations were monitored with the ratiometric fluorescent ion indicators fura-2, SBFI and BCECF (Molecular Probes, Leiden, NL), respectively. Neurons were loaded with membrane permeant acetoxymethylester (AM-ester) of the dyes for 60 min at 37 °C in the case of fura-2 (10 µM) and SBFI (10 µM) and for 15 min at room temperature for BCECF (5 µM) in a serum free Hepes buffered salt solution (HBSS). To increase the solubility of fura-2-AM and SBFI-AM, the stock solution of the dyes were mixed with an equal amount of a 20 % (w/v in DMSO) of the non-ionic detergent Pluronic F-127 (Molecular Probes, Leiden, NL). Cleavage of the AM-esters by nonspecific intracellular esterases resulted in the accumulation of the membrane impermeant free acids of the dyes. After washing the coverslips 3 times with normal HBSS, cells were incubated for another time of 15 min to allow complete cleavage of the esters.

Changes in the mitochondrial membrane potential were monitored with the fluorescence dye rhodamine-123 (rh-123), which accumulated in mitochondria on the basis of their membrane potential. Cells were loaded with 2 µM rh-123 for 15 min at room temperature, washed twice and used for the experiment. After washing with HBSS the coverslips were mounted in a temperature controlled flow-through chamber (Warner Inc., Science Products, Hofheim, D). The superfusion chamber was mounted on an inverted Zeiss Axiovert 100 TV (Zeiss, Oberkochen, D) microscope. Cells were superfused with prewarmed HBSS using a Warner in line heater at a rate of 2 ml/min for 10 minutes prior to starting the experiments. The temperature in the superfusion chamber was measured with a Pt-100 electrode and was set to 37 °C ± 0,5. Digital imaging was performed with the IonVision-system (ImproVision, Coventry, UK) equipped with an 75 W xenon excitation light source (Zeiss, Oberkochen, D) fitted to the microscope. The excitation wavelength was selected with an electronic filter wheel (Ludl, Cambridge UK) and excitation light was reduced by neutral density filters. Emission light was measured at 530 ± 20 nm with an intensified CCD camera (extended ISIS M, Photonic Science, Norwich, UK). Illumination of the cells was restricted to the time of data acquisition by the use of an electronic shutter. Frames were acquired routinely every 40 seconds and stored on an Apple McIntosh Quadra 800 Computer (Cupertino, CA, USA). Higher acquisition rates (up to 1 picture/2sec) were used at time points of special interest, for example during the application of glutamate. After the experiment, defined neurons were selected using custom build software and analyzed individually. For each experiment a number of 20-40 single neurons were analyzed and the resulting fluorescence changes were averaged. Fluorescence changes were normalized to the initial baseline fluorescence

determined within the first 2 minutes of data acquisition or fluorescence ratio values were estimated. In our experiments neurons loaded with the ratiometric fluorescent ion indicators like fura-2 and BCECF were viewed with an inverted fluorescence microscope with a 40x oil immersion objective.

The property of the ratiometric fluorescent dyes enables measurements of the intracellular ion concentration in single neurons independent of the intracellular concentration of the dye by using the ratio of fluorescence intensities measured at the two excitation wavelengths. Ratio images are computed by dividing on a pixel by pixel basis the A and B images of the monitored sequence. Therefore the resulting ratio images represent a picture of the cell in which the brightness at any location within the cell relates not to its superficial structure, but to the local value of calcium (Hafner, 1993). Because the absolute values of the calcium signals obtained were only of minor importance in our model, no calibrations of the fura-2 ratios were performed.

Experimental procedures: Digital imaging. Baseline fluorescence in standard HBSS was measured for 10 min and than the solution was switched to an appropriate EAA containing solution for 5 min Afterwards the neuronal cell culture was superfused with HBSS for an additional 60 min Cultures were superfused with the drug containing medium from the beginning of the EAA treatment throughout the experiment. The superfusion rate of 2 ml/min was maintained by a roler tube pump (IPN, Ismatec, Wertheim, D). The fluid level within the chamber was adjusted by a variable aspirator device which allowed a higher suction rate than the superfusion rate. Standard fluid content was 250 µl, resulting in a eightfold solution exchange per min.

a) Hypoglycemia/hypoxia: hypoglycemia was performed by superfusing cortical neurons with HBSS lacking any added glucose for 3 h. Afterwards, superfusion was changed to the normal glucose containing HBSS. The anoxic solution was supplied to the superfusion chamber via stainless steel capillaries. To prevent oxygen contamination of the buffers the chamber was closed and gassed with argon. Furthermore, the superfusion rate was increased to 5 ml/min. Control experiments showed that our cortical neurons tolerated the higher superfusion rate without any damage. Combined hypoglycemic/hypoxic conditions were carried out by superfusing neuronal cell cultures with glucose- and oxygen free buffer solutions. At the end of hypoglycemia/hypoxia cells were reoxygenated in the presence of 10 mM glucose.

b) In vitro ischemia studys: To mimic in vivo ischemic conditions, mixed glia and neuronal cell cultures on glass coverslips were placed in a PhysioControl microphysiometer (PTS, Freiburg, D). The system consists of a temperature controlled airtight stainless steel

incubation chamber with ports to connect miniatured electrodes for measuring temperature, extracellular pH and oxygen concentration directly above the cultured cells. The electrodes are connected to a specific computer controlled interface board and acquired data were stored on a custom build Pentium-based computer system (CT2000, Karlsdorf, D). The incubation chamber was mounted on a Zeiss Axiovert 100 TV fluorescence microscope and an inbuild window allows the observation of cells with transmitted light optics as well as the detection of fluorescence light. This enabled us to detect simultaneous changes of the intracellular ion and energy homeostasis and changes of the extracellular oxygen concentration as well as the extracellular pH.

c) Determination of cell viability: At the end of each experiment, cells were superfused with HBSS containing 50 µg/ml propidium iodate (PI) for a minimum of 10 min. Fluorescence images were collected after washout of the PI at excitation wavelengths 340 and 490 nm and emission at 530 nm. Afterwards, PI stained cells were related to the individual changes of their fluorescence signals during the experiment to determine specific differences between surviving and dead neurons.

Materials. HEPES-buffered salt solution (HBSS) was composed of the following (in mM): NaCl 124; KCl 4.9; $MgSO_4$ 1.3; KH_2PO_4 1.2; $CaCl_2$ 2.0; HEPES 25.0; Glucose 10.0 adjusted to pH of 7.4 with NaOH. Bicarbonate-buffered salt solution (BBSS) was composed of the following (in mM): NaCl 124; KCl 4.9; $MgSO_4$ 1.3; KH_2PO_4 1.2; $CaCl_2$ 2.0; H_2CO_3 25.0; with or without Glucose 10.0 adjusted to pH by gassing the solution with a mixture of 5% CO_2/95% O_2 for 30 min. Oxygen free HBSS was prepared by equilibrating the buffer solution with argon (99.998 %, Messer-Griesheim, Darmstadt, D) for more than 24 h under positive pressure (1 atm) in a special glas bottle. Rhodamine-123 was obtained from Sigma (Deisenhofen, D), aliquoted in dry dimethyl-sulfoxide, and frozen. Ionomycin and nigericin were dissolved in ethanol to give a stock of 10 mM. Cyclosporin A (Calbiochem, Bad Sodem, D) was dissolved in methanol, MK-801, CNQX, NBQX, ACPD in anhydrous dimethyl-sufoxide. In all cases, the final solvent concentration never exceeded 0.1 %. Glutamate, NMDA, kainate and ruthenium red were freshly prepared and dissolved in HBSS. In general, cell culture supplies were obtained from Life Technologies (Eggenstein, D) and neuroactive compounds from Biotrend (Köln, D). If not otherwise indicated, all other chemicals were of the highest grade available from Sigma (Deisenhofen, D) or Fluka (Deisenhofen, D). Nominally calcium free HBSS contained no added calcium and 100 µM EGTA. All drugs were tested for their interference with the used fluorescence dyes.

Data analysis and statistics. Custom software was used to transform the raw fluorescence data into display ready data and to perform simple statistical analysis on groups of cultures as defined by the user. Further data analysis and display, including linear regression analysis, were performed using MS Exel and the Sigma-Stat and Sigma Plot software packages (Jandel Scientific, San Rafael, Ca, USA). Results are expressed as mean ± SD. Statistical differences between experimental data within the same experimental group were calculated by a paired Student´s T-test. Differences between experimental groups were evaluated by a Wilcoxon-Mann-Whitney U test using the PC-based computer program TESTIMATE (IDV, Gauting, D). Values were considered significantly different when $P < 0.05$.

Results

I. Fluorescence multiwell reader

PI fluorescence increases with time and with magnitude of glutamate challenge. Pilot experiments revealed a minimal well-to-well variability in neuronal density. Therefore, entire concentration-response curves could be obtained in a single experiment by varying the concentration of glutamate between culture wells. In the representative experiment in fig. 1A, PI fluorescence increased with time and reached, within the first 12 h, a plateau that paralleled the magnitude of the glutamate challenge. Note that 50 µg/ml PI had no adverse effects as this was easily tolerated by control cultures (fig. 1A)

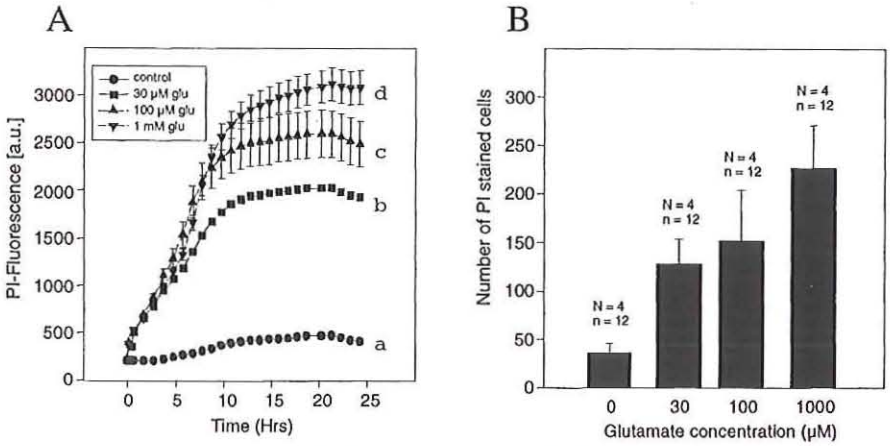

fig. 1. Representative measurements of the time course and extent of cell death in cultured cortical neurons using the multiwell plate reader. (A) Time course of propidium iodate staining measured by the fluorescence reader following application of different glutamate concentrations. Each symbol represents the averaged PI fluorescence intensity from four cultures. (B) Results of manual counts of PI-stained cells performed after the 24 h glutamate exposure, corresponding to the different concentration groups in A. Each bar represents the mean ± SD counts from three randomly selected microscope fields from each of four cultures. n = total number of microscope fields per group; N = number of cultures per group.

PI fluorescence intensity measurements using multiwell plate fluorescence scanner correlate highly with manual counts of PI-stained neurons. Manual counts of PI-stained neurons were performed in the cultures after the 24 h of PI fluorescence measurements. Dead neurons were easily visualized using conventional fluorescence optics. There was a strong linear relationship between the manual cell count and PI fluorescence measurements as performed by the scanner ($r = 0.958$, $p < 0.0001$; data pooled from 14 separate experiments using cultures from different dissections).

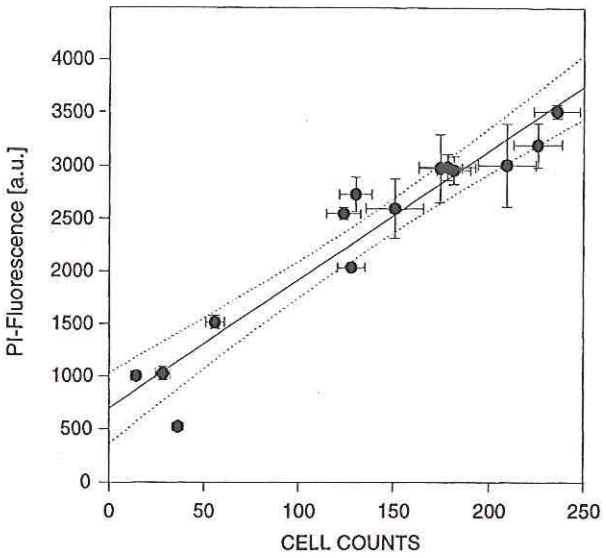

fig.2. Relationship between propidium iodide fluorescence labeling as measured by the multiwell plate reader and manual cell counts. Each symbol represents the mean PI fluorescence intensity value measured in a given glutamate exposure group plotted against the mean cell count in the same group (from 12 microscope fields in four cultures). Means are shown with their standard deviations. The solid and dotted lines show the best-fit curve and its 95 % confidence interval, respectively. There was a high correlation and a linear relationship between the number of dead cells (PI labeled) and the measured fluorescence (PI fluorescence = 699.6 + 12.2 x cell counts; $r = 0.958$, $p < 0.001$).

PI fluorescence intensity measurements using multiwell fluorescence scanner correlate highly with LDH release.

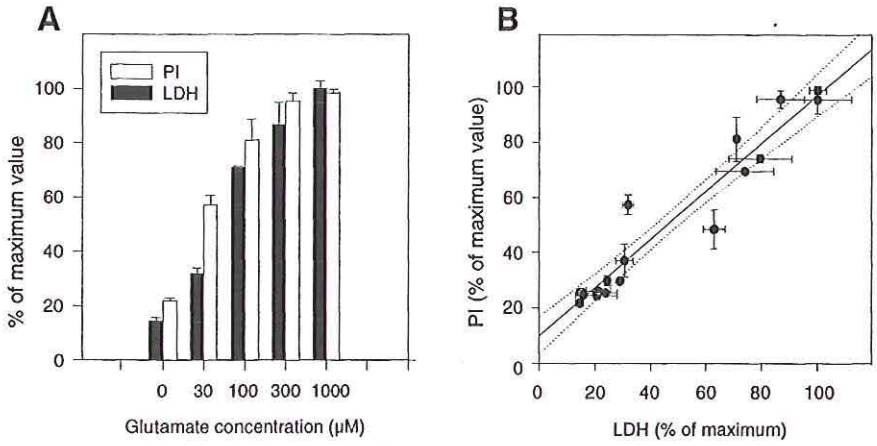

fig. 3. Propidium iodide fluorescence labeling, as measured by the multiwell plate fluorescence scanner, correlates higly with lactate dehydrogenase (LDH) release. Fluorescence and LDH release measurements were taken after a 24-h exposure of neurons to varying concentrations of glutamate. Measurements for each assay were normalized to their respective peak values. (A) Comparison of PI fluorescence and LDH measurements in a representative experiment in which glutamate exposure were performed for 60 min. Means ± SD are from two cultures per exposure group. (B) Relationship between PI fluorescence and LDH release combining data from four separate experiments similar to the one in A. Best fit least squares line (solid) is shown with its 95% confidence interval (dotted). $r = 0.964$, $p < 0.0001$.

LDH release is commonly employed as indicator of cell death in neurotoxicity studies (Koh & Choi, 1987). To compare the present approach with LDH measurements, the relative quantity of LDH release was determined in the same cultures subjected 24 h of sequential PI fluorescence measurements in the scanner. Like PI fluorescence intensity, LDH release also increased in a glutamate concentration dependent fashion. There was a high correlation between the two methods of cell death determination, but note that the PI-fluorescence shows a higher sensitivity at lower glutamate concentrations.

Dependence of neuronal cell death and duration of the glutamate exposure. As shown in fig. 4, a 15 min exposure to 300 µM glutamate, a concentration which is able to kill almost 100 % of all neurons after a 24 h incubation time (compare fig. 1) resulted in 80 % neuronal cell death as compared with the 24 h challenge. Therefore, a 15 min exposure of 300 µM glutamate was used as a standard excitotoxicity model in this multiwell approach.

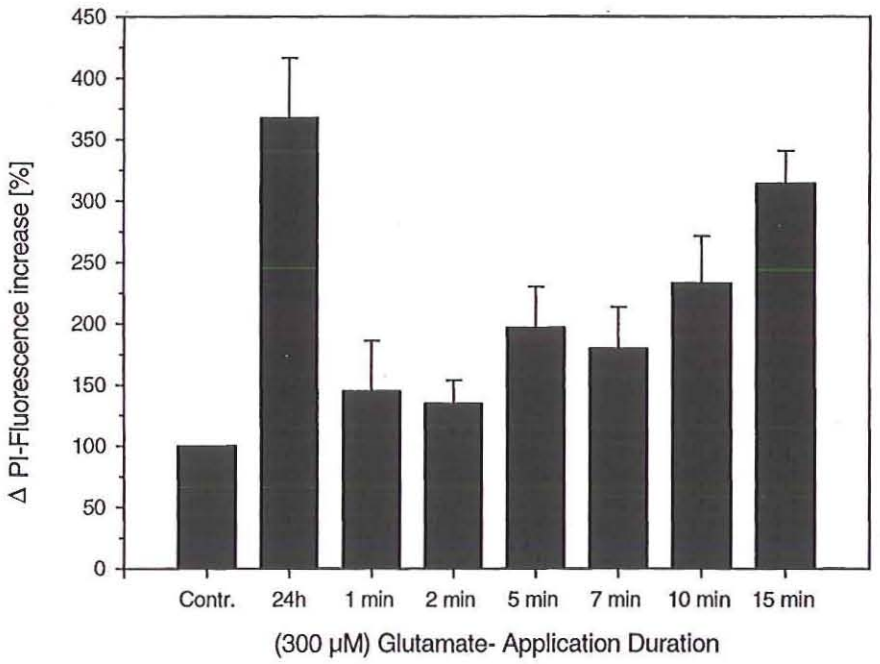

fig. 4. Dependency of the neuronal cell death on the duration of the glutamate challenge. Cell cultures were incubated with 300 µM glutamate for different time periods as indicated. PI measurements were performed 24 h after the insult. Means ± SD are from 5 independent experiments using averages from 4 wells each. PI fluorescence changes were normalized to the untreated controls.

Neuroprotective potential of glutamate antagonists. To assess the neuroprotective potential of glutamate antagonists, cell cultures were treated with the non-competitive NMDA-antagonist MK-801 and the AMPA/kainate antagonist CNQX. The drugs were administered to the cells simultaneously with glutamate (pretreatment-mode) or after the glutamate challenge (posttreatment-mode). As shown in fig. 5 only MK-801 had a significant neuroprotective effect. CNQX showed no marked neuroprotection in the pretreatment as well as in the posttreatment-mode.

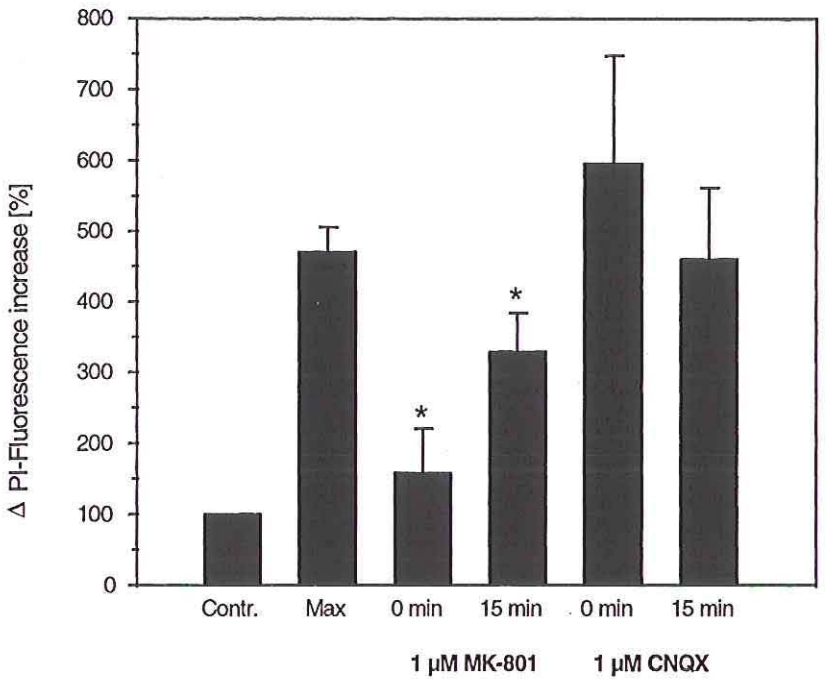

fig. 5. Neuroprotective potential of MK-801 (1 µM) depends on the time of application after glutamate challenge whereas CNQX (1 µM) was without effect. Cell cultures were incubated with 300 µM glutamate for 15 minutes. PI measurements were performed 24 h after the insult. Means ± SD are from 5 independent experiments using averages from 4 wells each. PI fluorescence changes were normalized to the untreated controls. * = statistical significant differences compared to the maximal PI fluorescence increase ($p < 0.005$)

Time dependent neuroprotection of MK-801 during and after a glutamate challenge. For a further characterisation of the neuroprotective potential of MK-801 and to determine the therapeutic window of the compound in this *in vitro* model, MK-801 was added at different time points during and after the exposure to 300 µM glutamate. Within the first 10 min MK-801 significantly counteracts the glutamate induced neuronal cell death (fig. 6). However, no neuroprotective effect of MK-801 was observed if administered at later time points.

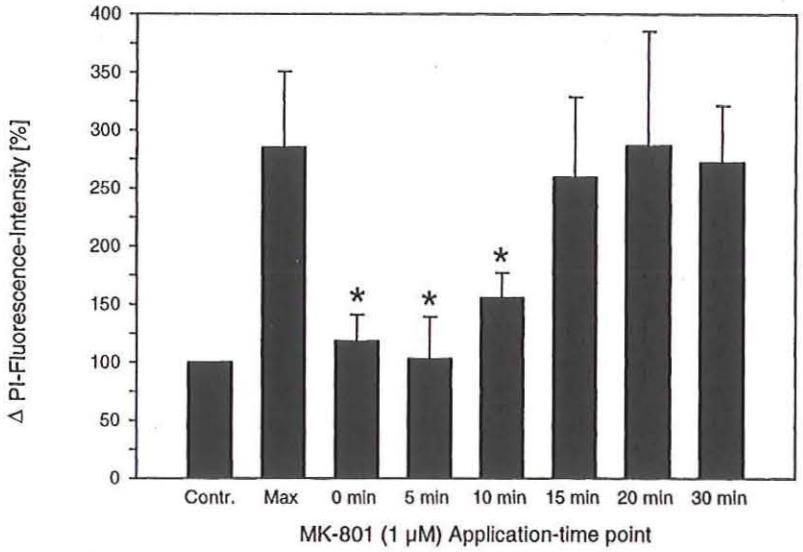

fig. 6. Neuroprotective potential of 1 µM MK-801 depends on the time point of application. Cell cultures were incubated with 300 µM glutamate for 15 minutes. PI measurements were performed 24 h after the insult. Means ± SD are from 5 independent experiments using averages from 4 wells each. PI fluorescence changes were normalized to the untreated controls. * = statistical significant differences compared to the maximal PI fluorescence increase ($p < 0.005$)

II. Digital Imaging

Principles. Fig 7 illustrates some of the information that can be revealed by studies at the single cell level that would not be apparent from population measurements: fig. 7A shows the distribution of free intracellular ion indicator in a linear greyscale representation of the fluorescence intensities. This illustration enabled us to localize the cells in order to monitor simultaneously the changes in intracellular ion concentrations from all individual cells in the field of view. After the experiment the software allowed to analyse each cell independently by generating a mask with defined regions of interests (ROI, fig. 7B) in order to measure the mean value of intracellular ions and the ratio value of the dye in each single cell by computing the average of the pixels in the region for every image in the experimental sequence. The ratio values in each of the ROI are plotted in fig. 7C. Note the most striking difference from previous population experiments that the individual cells do not respond to a stimulus with a simple monophasic ion increase, but give a series of discrete intracellular ion transients. It shows how surprisingly heterogeneous and pulsatile intracellular ion changes at the single cell level can be. This information is lost in population measurements due to the asynchronous nature of the individual responses to agonists. Even a small cell to cell variation of the time of onset can lead in a population measurement to a substantial underestimate of the rate of the

ion changes. This is shown in fig. 7D where we calculated the average of the individual responses of cells labeled in the mask. It is obvious that the response of those cells undergoing a second ion increase is lost in the analysis of the average values.

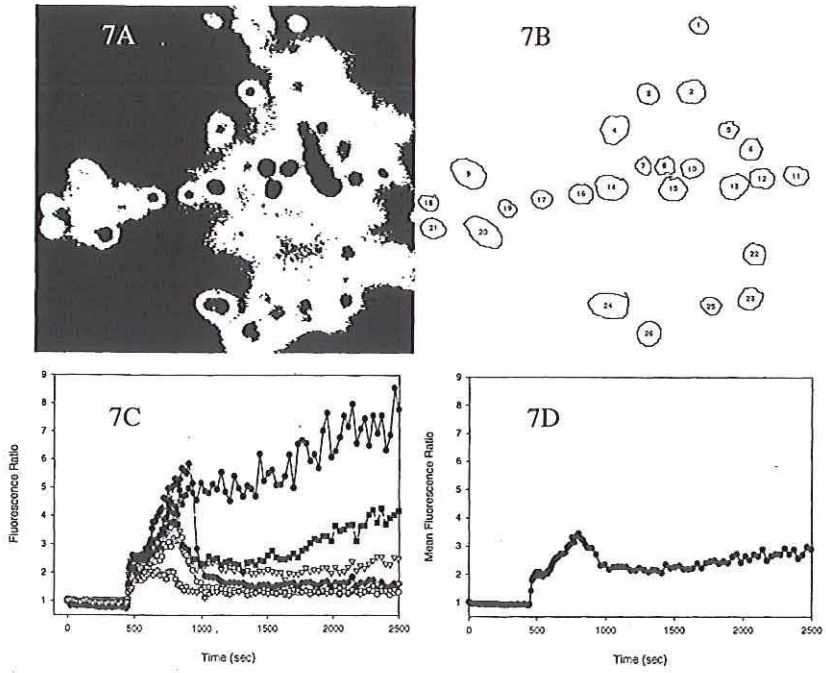

fig.7. Principle and advantage of single cell image analysis. For details see text above.

Single cell $[Ca^{2+}]_i$ measurements also circumvent problems associated with heterogeneous cell populations, allowing data to be obtained from an identifiable cell type, e.g. neurons versus glial-cells. To correlate the events of calcium increase and subsequent cell death in each individual cell we stained the cells with propidium iodate after the measurements. Because it is widely known, that mixed primary cortical neuronal cell cultures are inherently heterogeneous, we tried to minimize the resulting problem by the selection of specific groups of round-shaped cells (fig 8), which were identified as neuronal cells by immunostaining against the presence of specific neuronal markers (neurofilament 160, synaptophysin) and the absence of specific glial cell marker proteins like glial fibrillary acid protein (GFAP) and galactocerebroside. These specific round shaped cells are connected to each other by a network of neurofilaments stained positive to antibodies against neurofilament 160 but negativ to GFAP. GFAP stained cells, mainly astrocytes, are located inbetween the cortical

neuron clusters and in some cases below the neuronal cells. Because all fluorescencent dyes used stained neurons as well as glia cells, only groups of cortical neurons without cocultured glia cells were selected for fluorescence imaging.

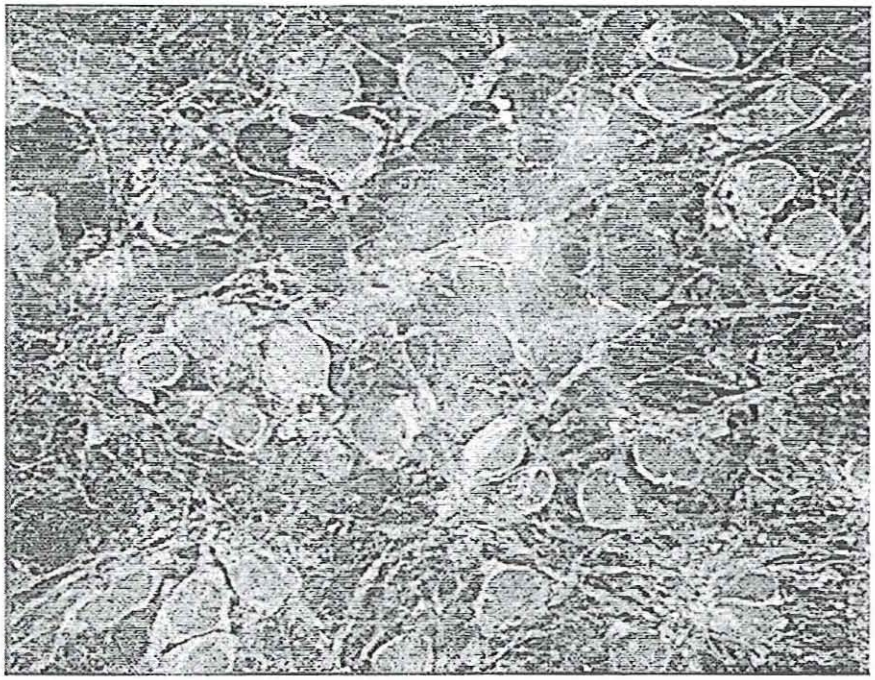

fig. 8. Cortical neurons stained with the intracellular pH-indicator BCECF. It shows the appearance of the cortical neurons in the fluorescence microscope. Round appearing cells were identified as neurons by immunostaining against neurofilament 160 in separate experiments (data not shown).

Basic characteristics of excitotoxicity:

Neuronal cultures exposed to glutamate undergo early swelling followed by cell death. The morphological changes accompanying the application of excitotoxins to cultured cortical neurons are well described (Rothman, 1985; Choi, 1987). Neurons exposed to 300 µM glutamate, for example, undergo cell swelling probably as a consequence of early influx of Na^+ and Cl^- and the accompanying changes in intracellular water content. Simultaneously, Ca^{2+} influx through glutamate receptor channels contributes to a loss of cell membrane integrity and subsequent cell lysis (see below). The sequence of events illustrated here is typical for this type of preparation and underlies the rationale for using a marker of cell membrane integrity (PI) as an index of cell death.

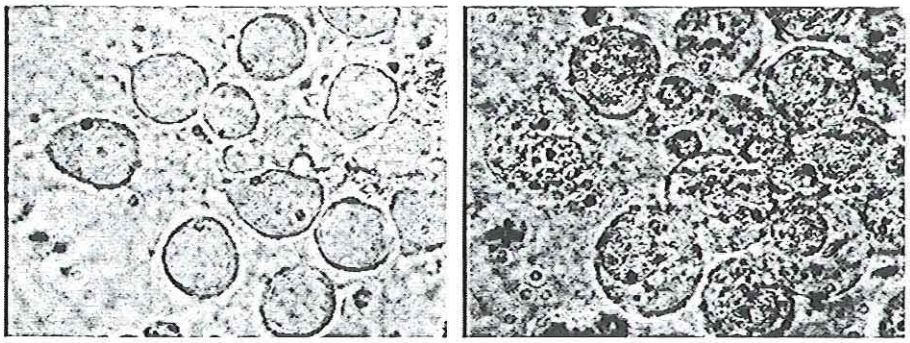

fig. 9. Glutamate induced swelling of cortical neurons. Cortical neurons were treated with 300 µM glutamate for 5 min. Photomicrographs were taken 10 min before and 2 h after glutamate treatment. Magnification = 200x.

Changes of the intracellular calcium concentration in cortical neurons induced by an excitotoxic challenge. 300 µM glutamate applied for 5 min to the neurons resulted in a rapid increase of the intracellular calcium concentration. The increase shows a biphasic pattern. An initial peak value is followed by a slight restoration and a secondary long-lasting increase of the intracellular calcium concentration in most of the neurons examined which indicated an intracellular calcium deregulation. Note, that not all of the neurons exhibit the secondary calcium overload.

In all cells that became positive labeled by PI, glutamate induced cell death was preceeded by a delayed intracellular calcium ($[Ca^{2+}]_i$) increase. Cortical neurons never recovered from this delayed $[Ca^{2+}]_i$ increase, which once initiated was only terminated by death.

To clarify which of the glutamate receptor subtype is responsible for the early calcium increase, cortical cell cultures were stimulated with either NMDA, kainate or ACPD. As shown in fig. 11 treatment with NMDA increased the intracellular calcium concentration to the same magnitude as glutamate but with a different time course.

NMDA was able to induce neuronal cell death in this model of excitotoxicity as measured with propidium iodate. Kainate (100 µM) also produced a rise in $[Ca^{2+}]_i$ in cortical murine neurons. However, most cells recovered from kainate induced $[Ca^{2+}]_i$ load and did not show delayed $[Ca^{2+}]_i$ rise as it was seen in many cells treated with glutamate.

Treatment of cortical neurons with ACPD, an agonist of the metabotropic glutamate receptors failed to induce a detectable increase in $[Ca^{2+}]_i$ (data not shown).

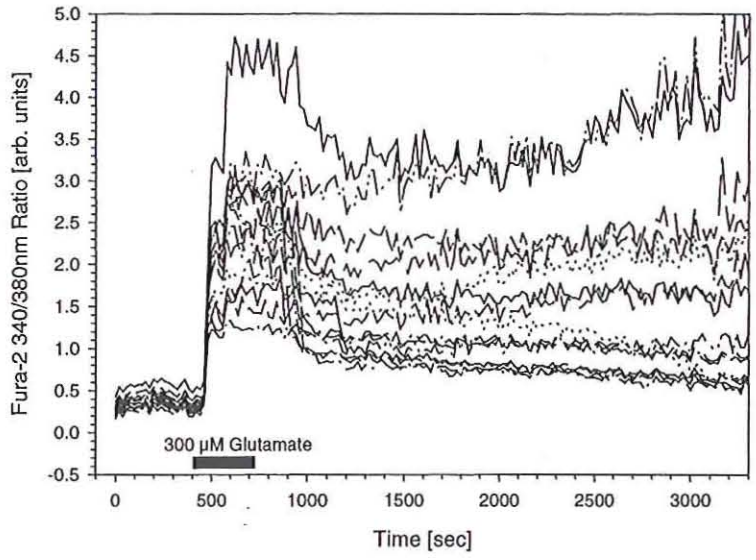

fig. 10. Glutamate evoked intracellular calcium increase in cultured cortical neurons at the single cell level. Representative traces out of six independent experiments. Fura-2 fluorescence ratios are expressed as uncalibrated arbitrary units.

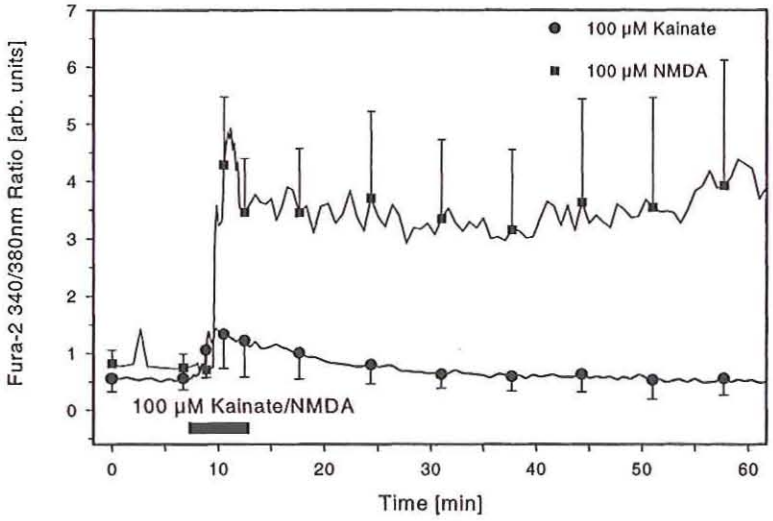

fig. 11. Changes of the intracellular calcium concentration in cortical neurons induced by the specific glutamate receptor agonists Kainate and NMDA. Means ± SD are from six independent experiments. Fura-2 fluorescence ratios are expressed as uncalibrated arbitrary units.

Changes of intracellular proton and sodium concentration in cortical neurons induced by an excitotoxic challenge.

- Exposure to glutamate, NMDA and kainate reduces the intracellular proton concentration $[pH]_i$ in murine cortical neurons. While the $[pH]_i$ started to recover during glutamate exposure, the $[pH]_i$ of most neurons treated with NMDA and kainate did not begin to recover until the application of the exitotoxins was terminated.

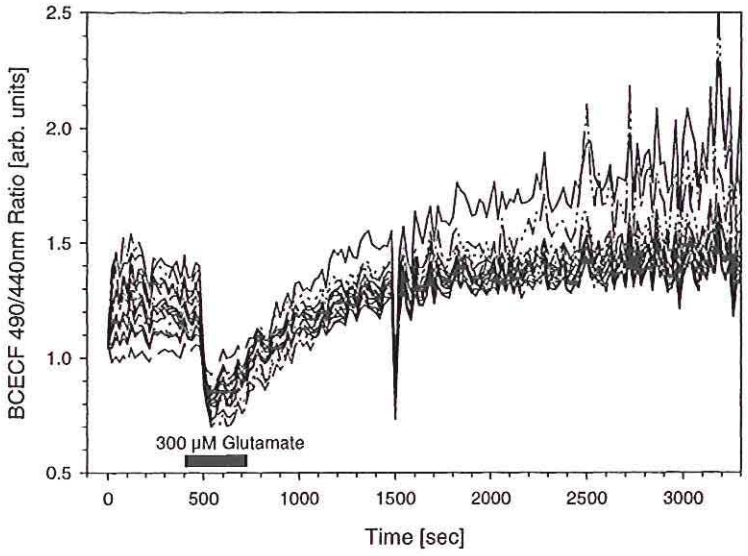

fig. 12. Glutamate evoked intracellular pH changes in cultured cortical neurons at the single cell level. Representative traces out of six independent experiments. BCECF fluorescence ratios are expressed as uncalibrated arbitrary units.

- Upon removal of glutamate, ratio values recovered to initial levels and continued to increase indicating an intracellular alkalinisation. The rate of recovery was slow compared to the initial drop since the ratios were continuously increasing until the end of the measurement, a maximum level for the alkalosis could not be determined. Following exposure to kainate, we observed little or no recovery of $[pH]_i$ in most of the neurons for up to 20 min.
- If MK-801 was co-administered with glutamate, the initial drop in the $[pH]_i$ was not effected but the later alkalinization was completely abolished (data not shown).

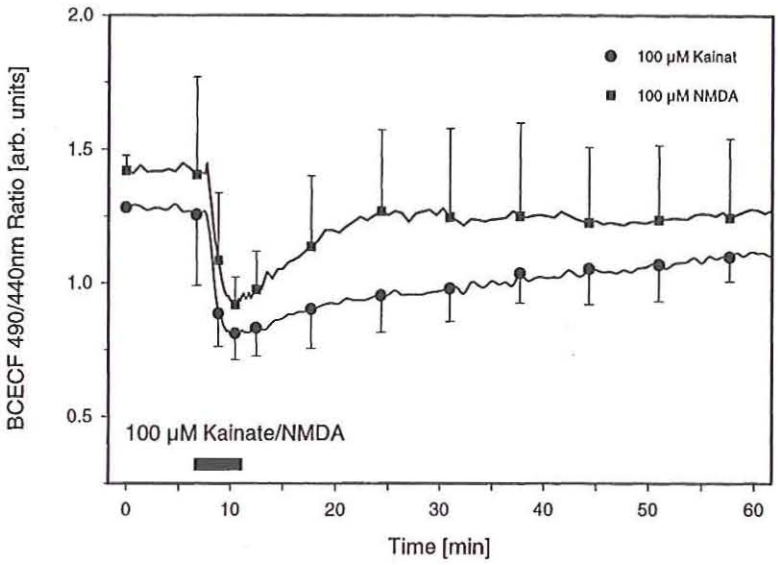

fig. 13. Changes of intracellular proton concentration in cortical neurons induced by specific glutamate receptor agonists kainate and NMDA. Means ± SD are from six independent experiments. BCECF flourescence ratios are expressed as uncalibrated arbitrary units.

- A prominent influx of Na^+ was also observed following glutamate receptor activation. Since the Na^+-H^+ antiporter has been implicated in the regulation of $[pH]_i$ in cortical neurons Na^+ fluxes or alterations in the Na^+ gradient may have contributed to the observed pH_i changes. To evaluate this possibility, we used the selective Na^+-H^+ antiporter blocker EIPA to inhibit antiporter activation. EIPA shows neither a marked effect on the initial glutamate induced acidification nor on the recovery period.
- The glutamate receptor mediated increase in the intracellular proton concentration requires extracellular calcium. Since glutamate receptor-gated ion channels are permeable to Ca^{2+} we examined whether Ca^{2+} influx is involved in the glutamate induced intracellular acidification. In the absence of extracellular calcium, the application of 300 µM glutamate resulted in little or no changes in $[pH]_i$ in all neurons used in these experiments.
- A neurotoxic administration of glutamate resulted in a rapid intracellular increase in sodium concentration followed by a normalization of the sodium concentration with time.
- Kainate but not NMDA produced a comparable increase in the intracellular sodium concentration. The glutamate induced influx of sodium was not blocked by MK-801 or TTX but showed sensitivety to CNQX (data not shown).

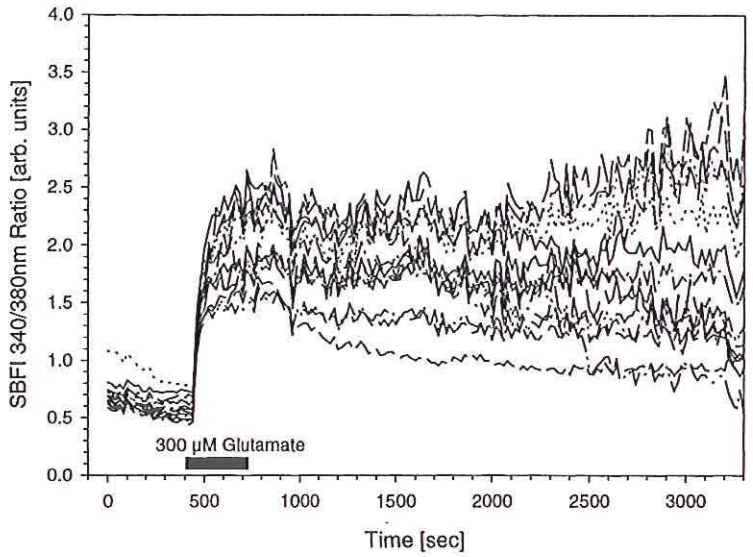

fig. 14. Glutamate evoked intracellular sodium increase in cultured cortical neurons at the single cell level. Representative traces out of six independent experiments. SBFI-2 fluorescence ratios are expressed as arbitrary units.

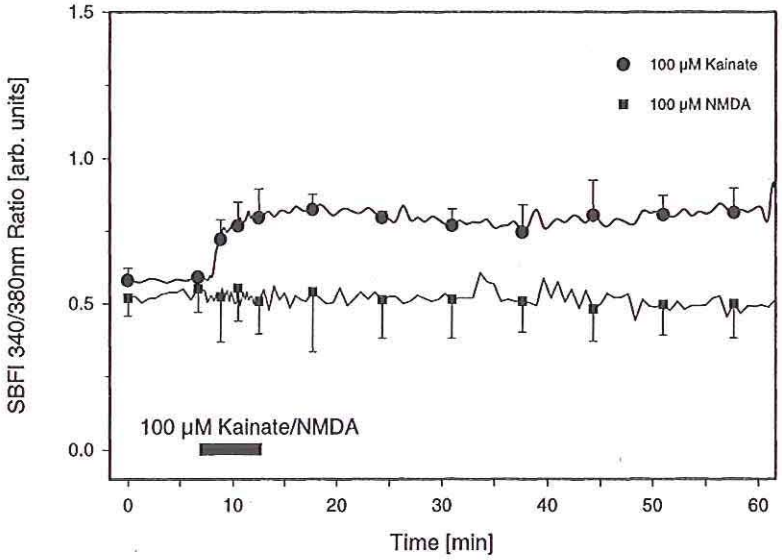

Fig. 15. Changes of the intracellular sodium concentration in cortical neurons induced by the specific glutamate receptor agonists Kainate and NMDA. Means ± SD are from six independent experiments. BCECF fluorescence ratios are expressed as uncalibrated arbitrary units.

Changes of the mitochondrial membrane potential in cortical neurons induced by an excitotoxic challenge. Rhodamine-stained mitochondria of selected cortical cells were located in neurites and somata but concentrated within the annular cytoplasm around the nucleus (fig.16). In this work, only those mitochondria in the perinuclear ring were analyzed.

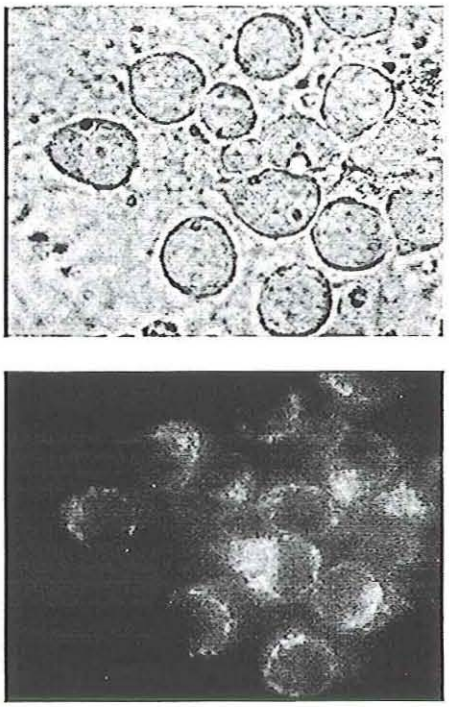

fig. 16. Appearance of cortical neurons using transmitted light and fluorescence microscopy. Cells were loaded with the selective mitochondrial stain rhodamine-123. Magnification was 640x.

Rhodamine-123 (rh-123) is well retained by mitochondria for several hours. Under control conditions there was only a loss of about 5 % of the initial fluorescence after a period of 2 hours. However, that decrease was not statistical significant different when compared to the starting value.

To test, if the collapse of mitochondrial membrane potential results in changes of the rh-123 fluorescence, we used nigericin, a protonophore known to equalize the intramitochondrial proton gradient and therefore leading to a depolarization of the inner mitochondrial membrane. As shown in fig. 17 a short exposure to 5 µM nigericin induced an 5-fold increase in rh-123 fluorescence followed by a reduction below initial values after removal of nigericin.

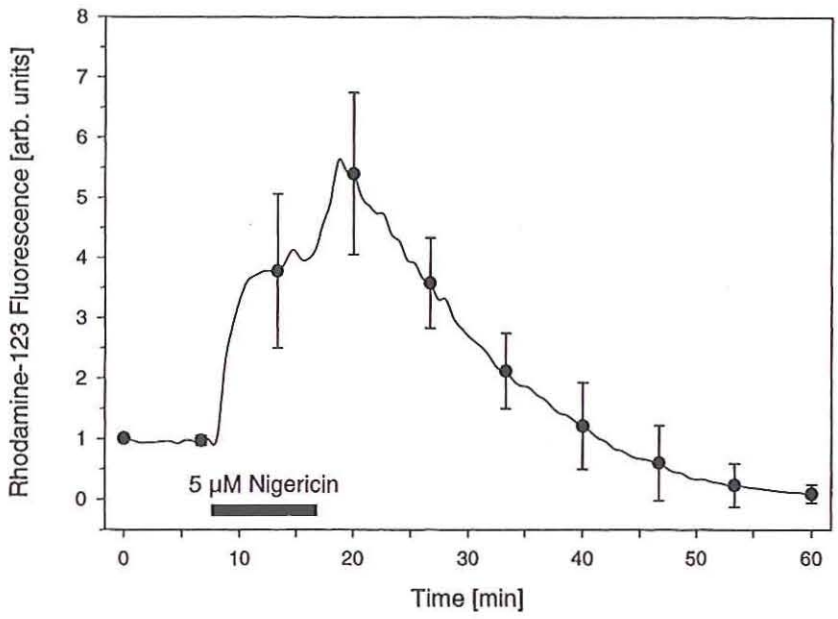

fig. 17. Changes of the mitochondrial membrane potential in cortical neurons induced by the specific protonophore nigericin. Means ± SD are from six independent experiments. Rh-123 fluorescence intensity changes are expressed as normalized arbitrary units.

Treatment of cortical cell cultures with 300 µM glutamate in the presence of Mg^{2+} (1.3 mM) for 5 minutes resulted in an early rapid increase of the rh-123 fluorescence indicating a depolarization of the mitochondrial membrane potential. Furthermore, glutamate induced mitochondrial depolarization is an unique feature of the selected cortical neurons. In all of the experiments performed all cortical neurons (up to 1000 analyzed neurons) first responded with an increase in the rh-123 fluorescence after a glutamate challenge which was than followed by a long-lasting decrease of the rh-123 fluorescence. After 2 hours, only 14 % of the initial fluorescence value remained which was statistical significant different (t-test, $P < 0.001$) from the fluorescence level at the beginning. It is known, that mitochondria which loose their ability to maintain a normal membrane potential are not able to accumulate rh-123. To elicit if the observed loss of rh-123 fluorescence after the glutamate challenge 1.) depends on the disruption of mitochondria and is 2.) accompanied with an ongoing cell death, we used propidium iodate (PI) at the end of the experiments to visualize dead cells.

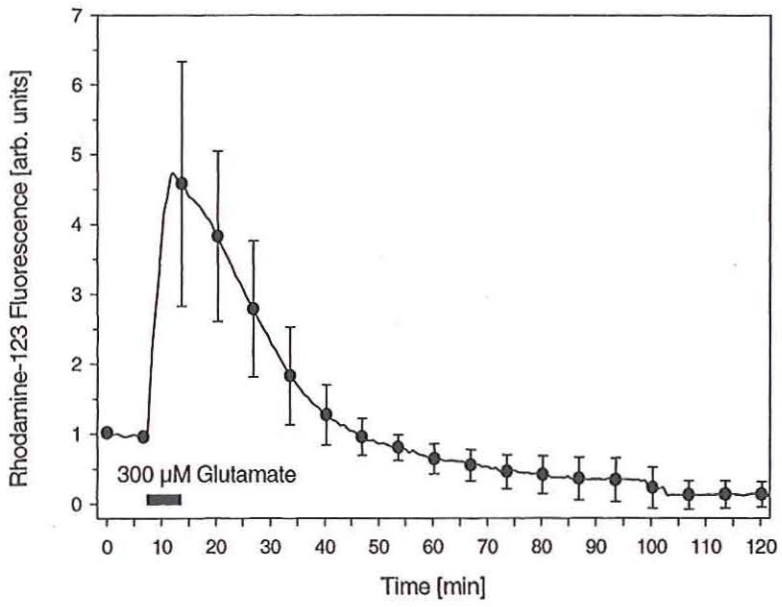

fig. 18. Changes of the mitochondrial membrane potential in cortical neurons induced by glutamate. Means ± SD are from six independent experiments. Rh-123 fluorescence intensity changes are expressed as arbitrary units normalized to the initial value.

The single cell analysis revealed two different response pattern of the glutamate induced changes rh-123 fluorescence which was dependent on the later fate of the neurons. As demonstrated in fig. 19 all cells positive stained for PI at the end of the experiments showed an early and complete loss of rh-123 fluorescence. In contrast, neurons which excluded PI 2 h after the glutamate challenge maintained 90 % of their initial fluorescence intensity. Therefore a rapid loss of the rh-123 fluorescence correlates highly with an early ongoing excitotoxic neuronal cell death.

Glutamate may be neurotoxic by activating multiple receptor subtypes e.g. NMDA, non-NMDA or metabotropic receptors.

To determine the contribution of the specific glutamate receptor sub-types to the observed changes in the mitochondrial membrane potential, we performed experiments using subtype specific glutamate receptor agonists such as NMDA, AMPA/kainate and ACPD. Neither kainate nor ACPD were able to produce a rapid mitochondrial depolarization. Whereas AMPA and ACPD were completely ineffective (data not shown), kainate induced a slow but long-lasting rise in the rh-123 fluorescence which was not restored upon removal of the drug.

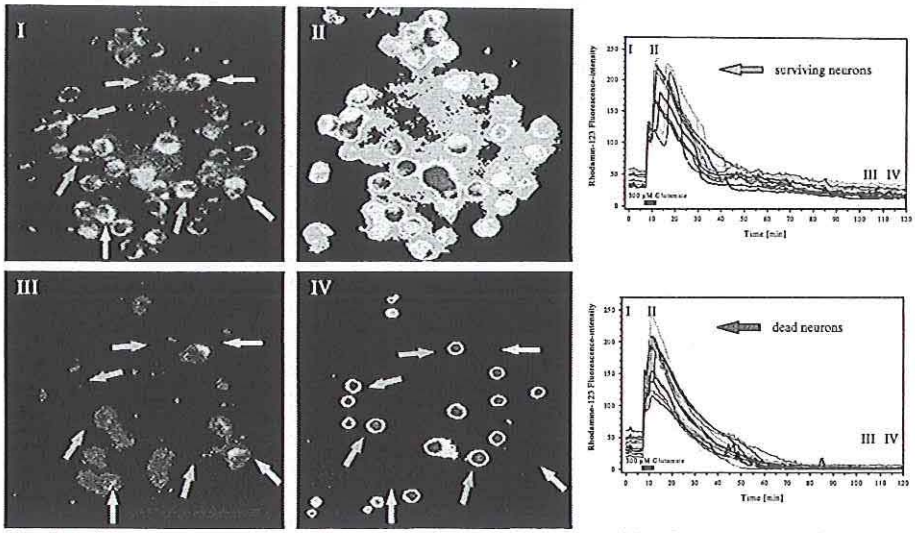

fig. 19. Different patterns of rh-123 fluorescence intensity changes resulting from a 300 µM glutamate challenge. Neurons which stained positive by the vital dye propidium iodate at the end of the experiment have completely lost their rh-123 fluorescence during the experiment. (I) rh-123 loaded cells at t=0 (II) increased rh-123 fluorescence as a response of the glutamate challenge (III) rh-123 fluorescence intensity at the end of the experiment. The fluorescence of some neurons completely disappeared (dark arrows) other maintained rh-123 fluorescence (light arrows) (IV) propidium iodate staining of dead neurons at the end of the experiment.

In contrast, NMDA evoked a rapid and pronounced increase in the rh-123 fluorescence that was followed by a subsequent loss of the dye. That pattern compared highly with the effect of glutamate.

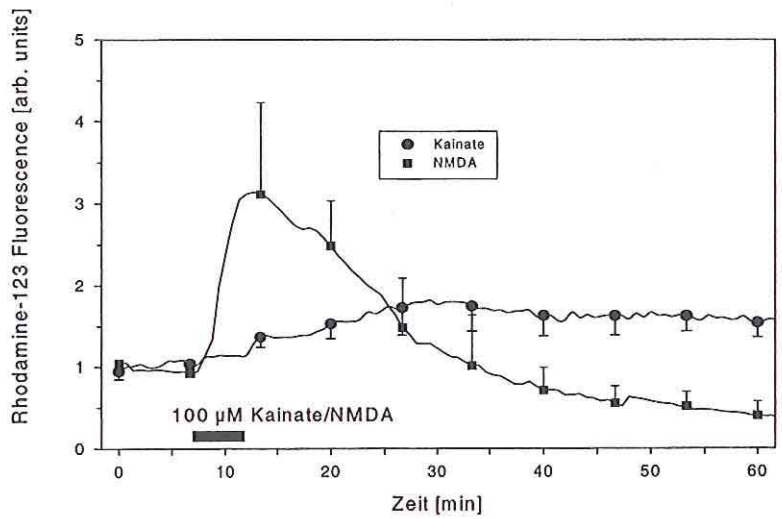

fig. 20. Changes of the mitochondrial membrane potential in cortical neurons induced by the specific glutamate receptor agonists Kainate and NMDA. Means ± SD are from six independent experiments. rh-123 fluorescence ratios are expressed as arbitrary units normalized to the initial value.

To test the hypothesis that the activation of the NMDA receptor channel is responsible for the observed depolarisation, we used MK-801 and CNQX to antagonize the NMDA- and AMPA/kainate-receptors. Co-application of 1 µM MK-801 with 300 µM glutamate completely prevents mitochondrial depolarization and all neurons analyzed survived. When applied together with glutamate, 10 µM CNQX had no protective effect on changes of the mitochondrial membrane potential and neuronal survival (data not shown).

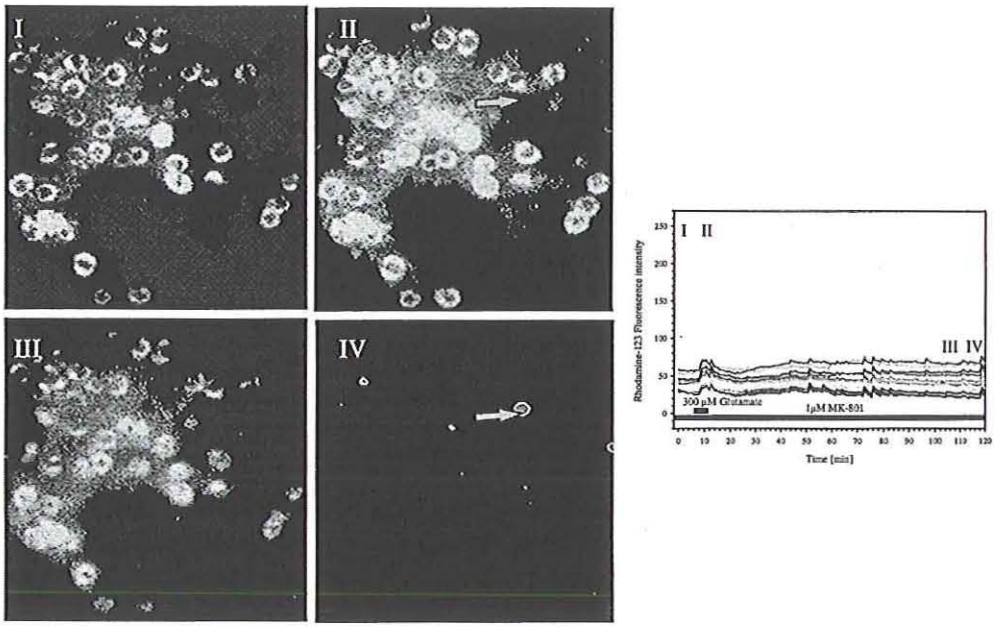

fig. 21. Protective action of MK-801 on rh-123 fluorescence intensity changes induced by a 300 µM glutamate challenge. (I) rh-123 loaded cells at t=0, (II) unaffected rh-123 fluorescence as a response of the glutamate challenge, (III) rh-123 fluorescence intensity at the end of the experiment. Note, that no neurons completely disappeared, (IV) PI staining of dead neurons at the end of the experiment. Note, that the stained nucleus (arrow) showed no corresponding rh-123 fluorescence at the beginning of the experiment.

It is speculated, that overstimulation of NMDA receptors leads to an uncontrolled influx of extracellular calcium into the neurons and that this may be the key event in excitotoxicity. Therefore, to test if intracellular calcium accumulation is due to the dissipation of the mitochondrial membrane potential, we conducted experiments in the absence of extracellular calcium. Under these conditions, application of glutamate caused only a slight increase of the rh-123 fluorescence. In contrast, the specific calcium ionophore ionomycine caused a marked increase in the rh-123 fluorescence and subsequent neuronal cell death (data not shown).

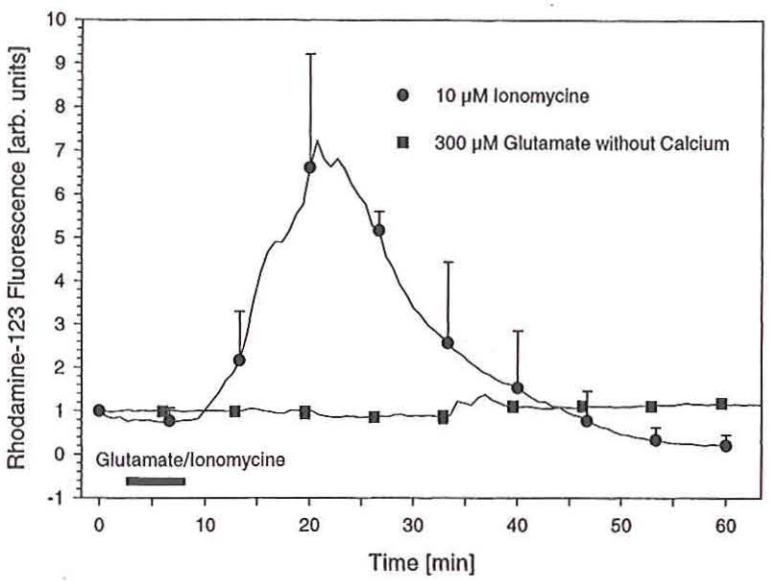

fig. 22. Calcium dependency of mitochondrial membrane potential depolarization. Changes of the mitochondrial membrane potential in cortical neurons induced by glutamate in the absence of extracellular calcium (circles) and the specific calcium ionophore ionomycine in the presence of extracellular calcium (squares). Means ± SD are from six independent experiments. Rh-123 flourescence ratios are expressed as arbitrary units normalized to the initial value.

We have tested a set of different chemical compounds and conditions on their ability to protect the mitochondria against glutamate induced depolarisation which were summarized in Tab. I:

Compound/conditions	Mode of action	Neuroprotection
MK-801	NMDA-antagonist	+
Ca^{2+}-free		+
Hypothermia (25 °C)		+
CNQX/NBQX	Kainate/AMPA-antagonist	-
Nimodipine	Ca^{2+}-channel blocker	-
TTX	Na^{+} -channel blocker	-
Dantrolene	intracel. Ca^{2+}-release inhibitor	-
Ruthenium Red	mito. Ca^{2+}-uptake blocker	-
Oligomycin/Rotenone	ATP-synthase/Resp. chain inhi	-
Cyclosporine A	PTP-inhibitor	-
Cyclohexemide	Proteine synth. inhibitor	-
U83836E	Antioxidant	-
Dithiothreitol	Reducing reagent	-
L-NAME	NO-synthase inhibitor	-

As shown in Tab. 1 only withdrawl of extracellular calcium, hypothermia or exposure to MK-801 have had a neuroprotective effect in cortical neurons after a 300 µM glutamate challenge.

Hypoglycemia/Hypoxia. Because the disruption of the mitochondrial membrane potential and the accompanied loss of the rh-123 fluorescence highly correlated with neuronal cell death, we used rh-123 fluorescence as a standard method to detect ongoing neuronal cell death. Furthermore, in case of hypoxia or ischemia depolarisation of the mitochondrial membrane potential is the earliest parameter to detect cellular oxygen definciency. First, we wanted to clarify if withdrawal of glucose in the presence of oxygen was able to damage cortical neurons. Therefore, neuronal cell cultures were superfused with HBSS lacking glucose for 2 h. Under those conditions no neuronal cell death was detectable (fig. 23) which was indicated by the persistent rh-123 fluorescence at the end of the experiment. In experiments using the fluorescence multiwell reader neuronal cell cultures are able to survive a hypoglycemic insult up to 12 h without any marked cell death (data not shown).

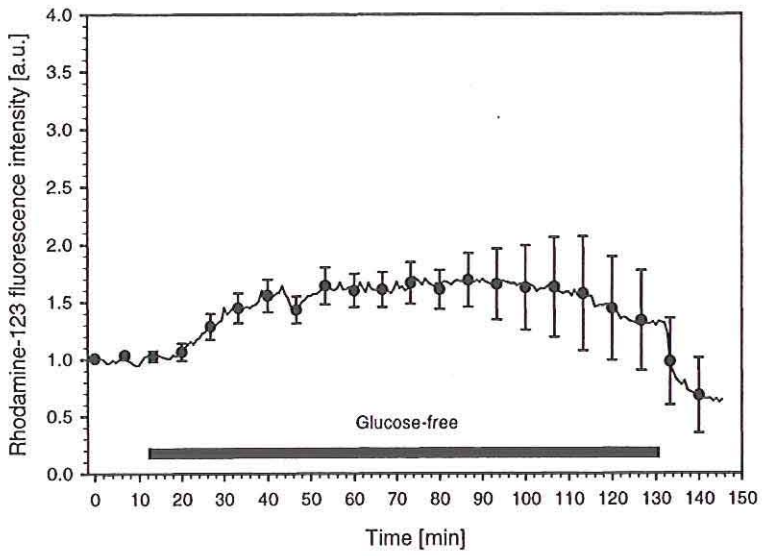

fig. 23. Mitochondrial membrane potential of cortical neurons during hypoglycemia. Means ± SD are from four independent experiments. Rh-123 fluorescence ratios are expressed as arbitrary units normalized to the initial value.

Superfusion of cortical neurons with oxygen free HBSS in the presence of glucose resulted in an early increase of the rh-123 fluorescence indicating mitochondrial depolarisation. During the anoxic superfusion period a slight decrease in the fluorescence intensity was detectable and followed by a complete normalization of the rh-123 fluorescence upon starting of reoxygenation. At the end of the experiments there was no significant loss of rh-123 fluorescence and none of the neurons showed positive PI staining.

However, the combined withdrawal of both glucose and oxygen had a more pronounced effect on neuronal survival. As shown in fig. 24 superfusion of neurons with oxygen and glucose free solution induced a marked decrease of the rh-123 fluorescence at the end of the experiment. The data were checked by PI counterstaining which identified some dead neurons at the end of the experiments. However, the majority of the neurons examined appeared swollen as observed by transmitted light microscopy.

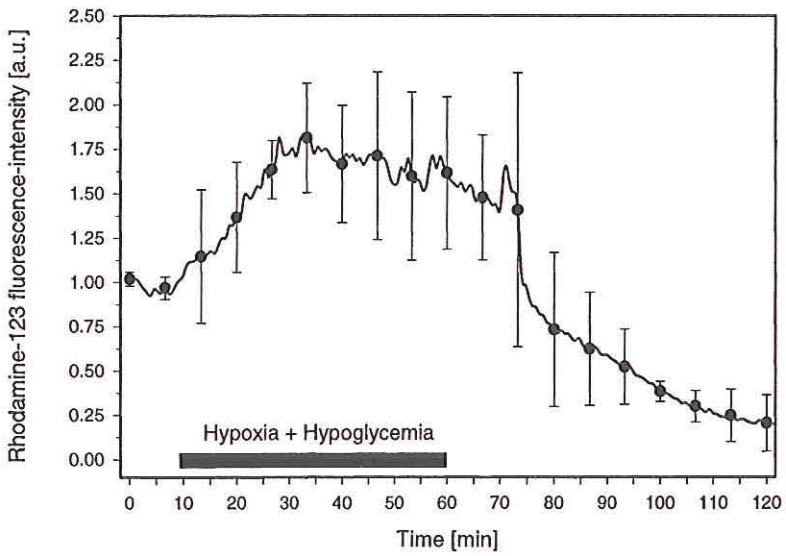

fig. 24. Mitochondrial membrane potential of cortical neurons during combined hypoglycemia/hypoxia. Means ± SD are from four independent experiments. Rh-123 fluorescence ratios are expressed as arbitrary units normalized to the initial value.

Model of *in vitro* ischemia. Because superfusion of neuronal cell cultures with hypoglycemic/hypoxic buffer solutions cannot resemble ischemia or stroke, we have started to set up *in vitro* ischemia experiments. Direct removal of metabolic substrates and oxygen (by

cellular self-consumption) should mimic the patho-physiological situation better than widely used chemical interruptions of cellular metabolism. For this purpose, we used a sealed microphysiometer, which allowed the detection and control of extracellular pH, oxygen concentration and temperature in combination with the determination of intracellular signals like the mitochondrial membrane potential or ion homeostasis. In this configuration we examined the effects of a stopped flow in the presence or absence of glucose on intracellular ion homeostasis and energy metabolism of cortical neurons which were co-cultured with glial cells. Switching from the superfusion mode to the stop flow mode in the absence of glucose at 37 °C caused a decrease in extracellular pH and oxygen concentration. Normally the extracellular oxygen concentration declined to zero within the first 30 min. Simultaneously with the complete consumption of oxygen mitochondrial membrane potential began to depolarize and the extracellular pH showed a marked increase. Upon reperfusion extracellular pH and oxygen levels normalized whereas rh-123 fluorescence started to decline below the initial level, indicating an ongoing neuronal cell death. At the end of the experiments neurons appeared swollen and granulated. Subsequently, neurons had lost their cell membrane integrity and stained positive with the vital dye propidium iodate (data not shown).

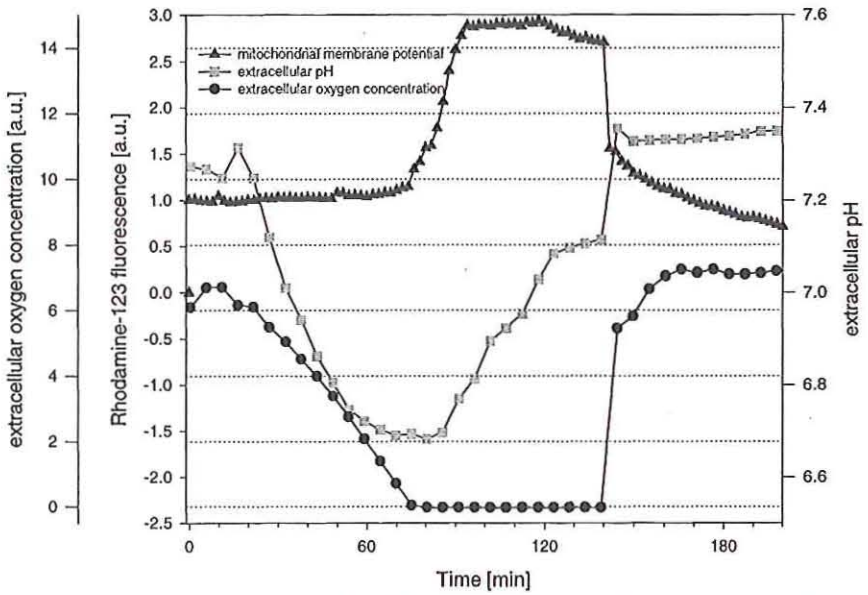

fig. 25. Simultaneous detection of extracellular pH, oxygen concentration and mitochondrial membrane potential during *in vitro* ischemia in the absence of glucose. Representative traces of five independent experiments. Superfusion was switched to glucose free conditions after 10 min and stop flow started at 20 min for 2 h.

When stop flow experiments were performed in the presence of glucose, a long-lasting intracellular acidification was observed. Depolarization of the mitochondrial membrane potential started up to 1h later as compared with the glucose-free ischemia. After reperfusion, all parameters were restored within minutes. Futhermore, ischemia induced neuronal cell death was not detected. Under those conditions expanding of the ischemic period to up to 4h was insufficient to produce detectable neurotoxicity (fig. 26).

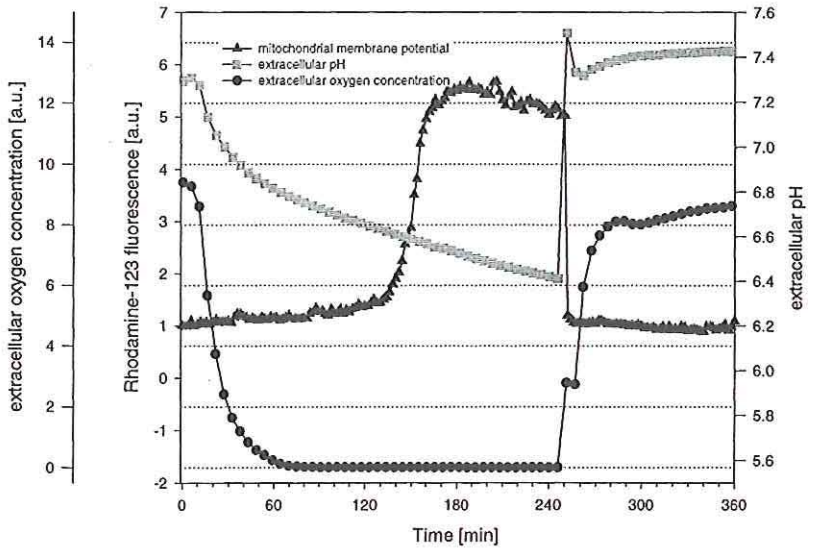

fig. 26. Simultaneous detection of extracellular pH, oxygen concentration and mitochondrial membrane potential during *in vitro* ischemia in the presence of glucose (10 mM). Representative traces of five independent experiments. Superfusion was switched to glucose free conditions after 10 minutes and stop flow started at 20 min for 4 h. Note the different time scale compared to the experiment shown in fig. 25.

Discussion

Fluorescence multiwell reader. The present assay provides a mean to perform cytotoxicity experiments at a precisely controlled temperature, taken into account the temperature sensitivity of excitotoxic phenomena, and serves the ability to study with precision the time course of cell death, which may be vary with different insults. The results obtained correlate highly with manual techniques (cell counting) and with other recognized methods to measuring cytotoxicity (LDH efflux).

The vital marker exclusion strategy has the advantage over vital dye retention that it is unaffected by healthy cells. Fluorescence vital markers such as PI, which increases its fluorescence upon entering cells and binding to DNA, are thus ideal for quantitative determination of cell death. PI and other DNA-binding dyes are relative resistant to photobleaching and are therefore amenable to repeated photoexcitation over prolonged periods as was done in the present report. Furthermore, these compounds are generally nontoxic to the cells over a period of many hours. Finally, fluorescence probes such as PI, when applied in correct quantities, provide for an excellent signal-to-noise ratio when measured in a multiwell plate scanner as described.

As shown in our glutamate experiments, this method is applicable in determine the time profile of ongoing neuronal cell death as well as the neuroprotective action of a glutamate receptor channel antagonist. The results obtained in the MK-801 posttreatment study showed a small therapeutic window for this compound in our *in vitro* model which supports *in vivo* findings of delayed neuroprotective actions of NMDA-receptor antagonists. Nevertheless, in contrast to many *in vivo* observations, CNQX failed to protect the neurons against a glutamate challenge. This is in line with the observation, that 100 µM kainate by itself failed to induce a marked cellular neurotoxicity. Taken together, in the described model the glutamate induced neuronal cell death is mainly due to the activation of NMDA receptor ion channels, therefore may reflect early ongoing neuronal cell death.

The use of a multiwell plate scanner permits a significant degree of automation, thereby removing any subjective element from the assessment of cell death. For this reason, this technique produces little variability among results obtained by different operators. The method is simple and is therefore easily learned by technical staff. Automation also results in large quantities of accurate and reproducible data being obtained, which is a time and cost-effective advantage over labor-intensitive manual cell-counting techniques. This method should have wide applicability to cell types other than neurons with minimal or no modification. By using this technique in the end point mode, a high throughput of multiwell

plates per day are possible making it useful as a tool for screening large amounts of potential neuroprotective compounds during pharmaceutical drug development.

The fluorescence multiwell plate reader used in our experiments is equipped with two filter wheels to switch between several excitation and emission wavelengths subsets within the same plate. The apparatus is thus especially amenable to studies combining the use of two or more fluorescent probes in the same cultures or in sister cultures within the same plate. Thus, studies are currently ongoing in our laboratory to examine simultaneously changes in cytoplasmic calcium and proton concentration using Ca^{2+} and H^+ intracellular indicators and cell death with fluorescent vital stains.

Fluorescence Imaging. We have demonstrated that a short exposure of murine cortical neurons to 300 µM glutamate, 100 µM NMDA and 100 µM kainate resulted in a rapid increase of the $[Ca^{2+}]_i$ whereas ACPD has no effect on $[Ca^{2+}]_i$. However, only glutamate and NMDA were toxic to neurons. These experiments also showed that $[Ca^{2+}]_i$ levels are not permanently elevated following transient exposure to excitotoxins. Prior to the observed delayed $[Ca^{2+}]_i$ deregulation, there was a period when neurons partly recovered their basal $[Ca^{2+}]_i$. Since active mechanisms are required to maintain low basal $[Ca^{2+}]_i$ levels this suggests that Ca^{2+} homeostasic mechanisms remain intact for certain but limited time. In agreement with the literature our results show that in cultured cortical neurons, secondary $[Ca^{2+}]_i$ overload is an early indicator of cell death (Thymianski, 1993a). The loss of mitochondrial membrane integrity and the subsequent loss of the oxydative phosphorylation may be the reason of the observed inability to maintain calcium homeostasis.

Hence, this recovery period may represent a therapeutic window during which neurotoxicity of an agonist may be reversed. The time dependent action of MK-801 in the posttreatment-mode supports this conclusion. The comparison of the time course of secondary calcium increase and the PI uptake suggests, that delayed secondary calcium load is more likely due to failure of Ca^{2+} homeostasic mechanisms as a result of the impaired mitochondrial ATP-production rather than a non-specific plasma membrane damage. In general our results agree with recently reported findings in cortical and hippocampal neurons with the exception that our experiments were performed at 37 °C compared to room temperature. This resulted in an earlier onset of the secondary calcium overload and supports the hypothesis that secondary $[Ca^{2+}]_i$ load indicates a temperature dependent irreversible deregulation of cellular calcium homeostasis.

We have observed that exposure of cultured murine cortical neurons to glutamate receptor agonists induced a rapid and pronounced intracellular acidification. This acidic shift can not be blocked by the Na^+-H^+ antiport inhibitor EIPA.

If the glutamate induced intracellular acidification observed in our experiments was due to H^+ entering neurons via glutamate receptor associated cation channels, the removal of external Ca^{2+} should fail to affect the increase in the intracellular proton concentration. Thus, removal of extracellular Ca^{2+} during exposure to glutamate blocks both, the cytosolic rise in Ca^{2+} and H^+, suggesting an important role for calcium in the neuronal acidification response. One explanation could be the ability of calcium ions to compete for intracellular H^+ binding sites or exchange for H^+ in intracellular organells like mitochondria. Blocking of the Na^+/H^+ exchanger with EIPA excludes the concomitant sodium load as a source for the increased proton concentration. Nevertheless, the exact source of protons responsible for the reduction in pH_i induced by excitotoxic stimuli is still unknown.

Hypoxia/Hypoglycemia. This study involved severe insults (hypoxia or ischemia) that resulted in almost complete inhibition of aerobic metabolism and depletion of the cellular ATP stores within 20-30 min. During severe ischemia, multiple avenues of cytosolic calcium elevation exist, including uptake via glutamate receptor ion channels, and release from intracellular stores. Although, the insult in the superfusion mode used in our experiments may not be as severe as those expected to occur in severe hypoxia/ischemia *in vivo*. This is assumed because superfusion of neuronal cell cultures does not involve significant extracellular lactic acidosis or accumulation of extracellular ions like potassium as well as bioactive amino acids like glutamate. Because these changes of the extracellular environment are considered to be very important in the sequence of neuronal cell death during stroke *in vivo*, that model may not represent the experimental set-up of choice in ischemia research. To exclude the disadvantages mentioned above, we developed a new experimental set-up. A closed microphysiometer-camber allowed us the detection and control of extracellular pH, oxygen content and temperature directly above the examined cells in combination with the determination of intracellular signals like the mitochondrial membrane potential or ion homeostasis. Furthermore, the extracellular fluid above the cell surface was reduced to less than 40 µl. Co-cultivation of neurons and glia cells should mimic in part the *in vivo* situation in the brain with respect to the important neuron-glia interactions.

Ischemia in the presence of glucose caused a rapid decrease in intracellular pH in cortical neurons and was followed by the depolarization of mitochondria when oxygen depletion was expanded. Obviously, the amount of energy supplied during ischemia was sufficient to keep the ATP-level in a state required for the maintenance of cellular membrane integrity typical for normoxic controls.

The new approach applied here allowed the simultaneous determination of extracellular signals like oxygen and proton concentration in combination with important intracellular parameters like calcium concentration and mitochondrial membrane potential in cortical neurons. Omission of glucose during ischemia was more deleterious. Reperfusion led to a normalization of all parameters examined when glucose was present during 2 h of ischemia but induced irreversible damages to the neuronal mitochondrial membrane potential and intracellular ion homeostasis in the absence of glucose. The initial changes of the extracellular pH during ischemia in the absence of glucose gave basically the same results as in the presence of glucose. The initial acidic shift may be due to an increased lactate accumulation in the extracellular fluid as a consequence of an activated glycolytic pathway. The consecutive alkalinisation of the extracellular milieu in experiments lacking glucose in the medium may represent the inhibition of glycolysis as a result from complete residual glucose metabolization.

Our recent studies focus on the determination of the extracellular concentrations of excitatory amino acids as well as the extracellular ion composition at various time-points during *in vitro* ischemia. This should give us a closer insight to the sequence of ongoing neuronal cell death. Comparison of those data with results from *in vivo* experiments (e.g. mikrodialysis) should validate that approach.

Conclusions

When using conventional endpoints in *in vitro* tests such as vital dye uptake, total cellular protein, or lactate dehydrogenase (LDH) release, the effects of a defined experimental insult on neuronal viability can only be evaluated at the end of an experiment. This approach precludes the study of neuronal physiology at the moment of lethal cell injury. Thus, we argue that deregulation of Ca^{2+} and energy metabolism (e.g. loss of the mitochondrial membrane potential) can be used as dynamic markers of cellular injury for the development of neuroprotective agents. The combination of the fluorescence multiwell reader based high throughput screening with digital imaging experiments on the single cell level revealed a useful tool for screening and characterisation of neuroprotective drugs because of the following:

- in addition to conventional endpoints they permit the assessment of cell function during the course of hypoxic/ischemic injury by measuring a variety of biochemical parameters in real time which may yield information about pharmacological properties of drugs at a resolution not possible *in vivo*.

- they permit the calculation of effective drug concentration and direct assessment of drug potency.
- the extracellular space is under experimental control which also allows the assessment of alterations in extracellular ionic compositions.
- they greatly increase the number of experiments which can be performed using a given number of animals. A gravid mouse with 12-14 fetuses prepared for cortical cultures can yield at least 10 - 12 multiwell culture plates and each plate may contain 24 - 48 individual cultures. If each experimental condition is prepared in quadruplicate a single dissection can provide more than 140 separate data points.

Presumably, animal experiments cannot be avoided completely because they allow to monitor the interactions of metabolites and their possible accumulations in different organs. However, the described approach can at least e.g. enlighten the neuroprotective effect of drugs or their critical concentrations and by that way avoid a large number of animal tests.

Acknowledgements. This work was supported by grants from the german Federal Ministry of Education, Science, Research and Technology (BMBF, BEO 0319520B) and Boehringer Ingelheim KG.

References

Choi D.W., Ionic dependence of glutamate neurotoxicity, Journal of Neuroscience, 7, 369-379, 1987

Choi D.W., Calcium-mediated neurotoxicity: relationship to specific channel types and role in ischemic damage, Trends in Neuroscience, 11, 465-469, 1988

Dugan L.L., Sensi S.L., Canzoniero, L.M.T., Handran S.D., Rothman S.M., Lin T.-S., Goldberg M.P. and Choi D.W., Mitochondrial production of oxygen species in cortical neurons following exposure to N-Methyl-D-Aspartate, Journal of Neuroscience, 15, 6377-6388, 1995

Dux E., Oschlies U., Uto A., Kusumoto M., Siklos L., Jo F. and Hossmann K.-A., Serum prevents glutamate-induced mitochondrial Calcium accumulation in primary neuronal cultures, Acta Neuropathologica, 92, 264-272, 1996

Fox G., Gallacher D., Shevde S., Loftus J.and Swayne G., Anatomic variation of the middle cerebral artery in the Sprague-Dawley rat, Stroke, 24, 2087-2093, 1993

Hafner, M., Visualization of calcium dynamics at fertilization of the sea urchin egg using fluorescent probes and digital imaging, Biological Research, 26, 429-440, 1993

Koh J.Y. and Choi D.W Quantitative determination of glutamate mediated cortical neuronal injury in cell culture by lactate dehydrogenase efflux assay, Journal of Neuroscience Methods, 20, 83-90, 1987

McAuley M.A., Rodent models of focal ischemia, Cerebrovascular and Brain Metabolism Reviews, 7, 152-180, 1995

McCormack J.D. and Denton R.M., Mitochondrial Ca^{2+} transport and the role of mitochondrial Ca^{2+} of energy metabolism, Developmental Neuroscience, 15, 165-173, 1993

Melzian D., Scheufler E., Grieshaber M. and Tegtmeier F. Tissue swelling and intracellular pH in the CA1 region of anoxic rat hippocampus; Journal of Neuroscience Methods, 65:183-7, 1996

Meyer F.B., Calcium, neuronal hyperexcitability and ischemic injury, Brain Research Reviews, 14, 227-243, 1989

Molinary G.F., Why model strokes?, Stroke, 19, 1195-1197, 1988

Oberpichler-Schwenk H. and Krieglstein J., Primary cultures of neurons for testing neuroprotective drug effects, Journal of Neural Transmission, [Suppl] 44, 1-20, 1994

Olney J.W., Toxic effects of glutamate and related amino acids on the developing central nervous system, in: Nyhan W.H., Heritable Disorders of Amino Acid Metabolism, New York: John Wiley, 501-512, 1974

Olney J.W., Brain lesions, obesity and other disturbances in mice treated with monosodium glutamate, Science, 164, 719-721, 1969

Orrenius S. and Nicotera P., The calcium ion and cell death, Journal of Neural Transmission, [Suppl] 43, 1-11, 1994

Petronilli V., Nicolli A., Costantini P., Colonna R. and Bernardi P., Regulation of the permeability transition pore, a voltage-dependent mitochondrial channel inhibited by cyclosporin A, Biochimica et Biophysica Acta, 1187, 255-259, 1994

Rothman S.M., The neurotoxicity of excitatory amino acids is produced by passive chloride influx, Journal of Neuroscience,5,1483-1489, 1985

Rothman S.M. and Olney J.W., Glutamate and the pathophysiology of hypoxic-ischemic brain damage, Annual Neurology, 19,105-111, 1986

Sattler R., Charlton M. P., Hafner M. and Tymianski M. Determination of the time course and extent of neurotoxicity at defined temperatures in cultured neurons using a modified multiwell plate fluorescence scanner.Journal of Cerebral Blood Flow and Metabolism. 17: 455-463, 1997

Tymianski M., Charlton M.P., Carlen P.L. and Tator C.H., Secondary Ca^{2+} overload indicates early neuronal injury which precedes staining with viability indicators, Brain Research, 607, 319-323, 1993a

Tymianski M., Charlton M.P., Carlen P.L. and Tator C.H., Source specificity of early calcium neurotoxicity in cultured embryonic spinal neurons, Journal of Neuroscience, 13, 2085-2104, 1993b

Tymianski M., Wallace M.C., Spigelman I., Uno M., Carlen P.L., Tator C.H. and Charlton M.P., Cell-permeant Ca^{2+} chelators reduce early excitoxic and ischemic neuronal injury in vitro and in vivo, Neuron, 11, 221-235, 1993c

White, R.J. and Reynolds, I.J., Mitochondria accumulate Ca^{2+} following intense glutamate stimulation of cultured rat forebrain neurones, Journal of Physiology, 498, 31-47, 1997

White, R.J. and Reynolds, I.J., Mitochondrial depolarization in glutamate stimulated neurons: an early signal specific to excitotoxin exposure, Journal of Neuroscience, 16, 5688-5697, 1996

Organotypic hippocampal slice cultures as an *in vitro* model for the investigation of neuroprotective drugs against ischemic damage

Jörg Breder, Clemens F. Sabelhaus, Ulrich H. Schröder, and Klaus G. Reymann

Leibniz Institute for Neurobiology
Laboratory of Neuropharmacology
POB 1860
39008 Magdeburg

Summary

Cerebral ischemia results in severe cell degeneration and consequently in loss of brain functions. In animal models of global ischemia the hippocampus has turned out to be one of the most vulnerable brain areas, and within the hippocampus the pyramidal neurons of the CA1 region are highly susceptible. These *in vivo* test systems cause substantial stress in form of pain and anxiety to the animals involved, giving rise to ethical problems and little public acceptance. *In vitro* models have been developed in order to overcome these problems. Dissociated cell cultures allow the strict control over environmental conditions and easy accessibility to manipulations but suffer from lacking the native neuronal circuitry as it is found *in vivo*. This major disadvantage can be at least partially circumvented by utilizing organotypic brain slice cultures. Organotypic cultures allow the investigation of delayed pathological processes after hypoxic/hypoglycemic insults and of the long-term effects of neuroprotective compounds. In the present report we describe the development of organotypic hippocampal slice cultures maintained on membrane filter inserts at the interface between tissue culture medium and atmosphere as an *in vitro* model for the investigation of neuroprotective drugs against ischemic damage. Ischemia was simulated *in vitro* by combined oxygen/glucose deprivation. Neuronal cell death as measured by propidium iodide uptake 24 h after the insult was compared with functional damage as estimated in the short-term range by electrophysiological recordings of field potentials. Pharmacological validation was achieved by testing the effects of cytoprotective compounds with different effector mechanisms. Bearing in mind that OSC prepared from neonate rats may not represent the situation found in the adult CNS, they provide an experimental *in vitro* system that is well suited to complement *in vivo* preparations and dissociated cell cultures in studying long-term pathophysiological processes of neurodegenerative diseases.

Introduction

Stroke is one of the leading causes of mortality and a major cause of long-lasting physical and mental disability in western industrialized countries. Pharmaceutical companies are therefore making substantial efforts to develop drugs which are able to protect the brain from neurodegeneration following an ischemic insult. Animal models that mimic the neuropathological consequences of stroke are utilized in the search for putatively protective compounds. In animal models of global ischemia the hippocampus has turned out to be one of the most vulnerable brain areas, and within the hippocampus the pyramidal neurons of the CA1 region are highly susceptible (for review see Schmidt-Kastner and Freund, 1991). These *in vivo* test systems cause substantial stress in form of pain and anxiety to the animals envolved, giving rise to ethical problems and little public acceptance. Besides this the complex system of animal models bears problems in controlling critical parameters such as brain temperature and blood pressure. Moreover, the beneficial effects of potentially neuroprotective drugs may be masked by poor permeability through the blood-brain barrier. To overcome these problems, *in vitro* models have been developed to investigate the various aspects of cellular degeneration following hypoxia/hypoglycemia. Dissociated cell cultures offer the advantages of strict control over environmental conditions and easy accessibility to manipulations (Banker and Cowan, 1977; Banker and Cowan, 1979). On the other hand, however, they suffer from lacking the native neuronal circuitry as it is found *in vivo*. This major disadvantage can be at least partially circumvented by utilizing organotypic brain slice cultures (Gähwiler, 1981; Stoppini et al., 1991), in which the neuronal connectivity occuring *in situ* is well preserved. Since they are long-lived, they allow the investigation of delayed pathological processes after hypoxic/hypoglycemic insults and the long-term effects of neuroprotective compounds.

Two main alternative techniques are currently used to prepare and maintain organotypic slice cultures (Gähwiler et al., 1997). In roller tube cultures the slices are embedded in a collagen matrix or a plasma clot on glass coverslips and slowly rotated in medium-containing tubes resulting in periodic feeding and air supply (for reviews see Crain, 1976; Gähwiler, 1988). In interface or membrane filter cultures the slices are maintained stationary on porous membranes at the interface between atmosphere and cell culture medium (Stoppini et al., 1991). Both techniques yield cultures that retain the characteristic cytoarchitecture of the tissue of origin to a large extent and display cellular differentiation. The main difference between them is the final thickness of the slices, roller tube cultures always turning out thinner than interface cultures. Due to their flattening to a quasi-monolayer and their growth on glass coverslips, roller tube cultures are preferable for experiments that require optimal optical conditions and access to single neurons. Interface cultures offer advantages when a three dimensional struc-

ture is desired. This is the case for the investigation of entire neuronal populations e.g. for the recording of field potentials. For these purposes the interface method was chosen for the studies described in the present report. Organotypic hippocampal slice cultures (OSC) were developed as *in vitro* model for the investigation of neuroprotective drugs against ischemic damage and the study of the underlying physiological and cellular mechanisms.

Abbreviations

1S,3R-ACPD: 1S,3R-aminocyclopentane-1,3-dicarboxylic acid, ACSF: artificial cerebrospinal fluid, AMPA: α-amino-3-hydroxy-5-methyl-4-isoxazole propionic acid, CNQX, 6-cyano-7-nitroquinoxaline-2,3-dione, DIV: days *in vitro*, DMSO: dimethylsulfoxide, EPSPs: excitatory postsynaptic potentials, HEPES: N-(2-hydroxyethyl)piperazine-N'(2-ethanesulfonic acid), MEM: minimal essential medium, NBQX: 2,3-dihydroxy-6-nitro-7-sulfamoyl-benzo(F)quinoxaline, NMDA: N-methyl-D-aspartate, OGD: oxygen/glucose deprivation, OSC: organotypic hippocampal slice culture(s), PBS: phosphate buffered saline, PFA: paraformaldehyde, PI: propidium iodide, PS: population spike(s), TCM: tissue culture medium, TTX: tetrodotoxin, U-83836E: (-)2-((4-(2,6-di-1-pyrrolidinyl-4-pyrimidinyl)-1-piperazinyl)methyl)-3,4-dihydro-2,5,7,8-tetramethyl-2H-1-benzopyran-6-ol-dihydrochloride.

Materials and Methods

Sources of materials. MEM-Hanks' (w/o L-glutamine, w/o $NaHCO_3$) was purchased from Biochrom (Berlin, Ger); Hanks' balanced salt solution (HBSS), horse serum (heat inactivated), MEM-Hanks' (incl. 25 mM HEPES, 2 mM L-glutamine, w/o $NaHCO_3$) from Gibco (Eggenstein, Ger). Gases (CO_2, O_2, 95% N_2/5% CO_2, 95% O_2/5% CO_2) were obtained from Linde (Leuna, Ger); NaCl from Fluka (Buchs, CH); KCl, $MgSO_4$, $CaCl_2$, PFA, sucrose (saccharose) from Merck (Darmstadt, Ger); KH_2PO_4, D-glucose from Serva (Heidelberg, Ger); D-mannitol, $NaHCO_3$, PI from Sigma (Deisenhofen, Ger). TTX was purchased from Alexis (Grünberg, Ger); U83836E from Biomol (Hamburg, Ger); nimodipine from RBI (Natick, MA, USA); 1S,3R-ACPD, CNQX, (+)-MK 801 maleate, NBQX from Tocris (Bristol, UK).
6-well-multiplates (Nunclon®) and Anopore® tissue culture inserts (25 mm diameter, 0.02 µm pore width), which were used for most preparations, were obtained from Nunc (Wiesbaden, Ger). In some preparations Millicell®-CM culture plate inserts (30 mm diameter, 0.4 µM pore width) obtained from Millipore (Eschborn, Ger) were used.

Solutions. Stock solutions of compounds were prepared as follows: 1S,3R-ACPD (1mM) in equimolar NaOH, CNQX (100mM) in DMSO, NBQX (100mM) in DMSO, nimodipine (100 mM) in methanol, (+)-MK 801 maleate (10 mM) in H_2O, PI (10 mM) in H_2O, TTX (10 mM) in equimolar acetic acid, U83836E (100 mM) in H_2O.

Preparation of OSC. 9-10-days-old Wistar rats (Institute breeding stock) were killed by decapitation. The brain was quickly removed and placed into ice-cold preparation medium (MEM-Hanks', incl. 25 mM HEPES, 2mM L-glutamine, w/o $NaHCO_3$, pH 7.35) perfused with O_2. Both hippocampi were isolated and transverse slices (350 µm) were prepared using a McIlwain tissue sectioner (The Mickle Laboratory Engineering Co., Guildford, UK). If necessary slices were separated from one another in preparation medium under a binocular. Intact slices were transfered onto membrane inserts (3-4 slices per insert) in 6-well-plates with 1.2 ml/well tissue culture medium (TCM, 50% MEM-Hanks', w/o L-glutamine, 25% HBSS, 25% horse serum, 350 mg/l $NaHCO_3$, 12.5 mM HEPES, pH 7.4). OSC were maintained in an incubator at 1% CO_2 and 36°C. TCM was changed completely three times/week.

Induction of hypoxia/hypoglycemia. After 12-15 days *in vitro* (DIV) OSC were transfered to 6-well-plates containing 1 ml/well of artificial cerebrospinal fluid (ACSF, composition in

mM: NaCl 124, KCl 4.9, $MgSO_4$ 1.3, $CaCl_2$ 2, KH_2PO_4 1.2, $NaHCO_3$ 25.6, D-glucose 10, pH 7.4). Hypoxia was induced by incubating OSC in a moistened gas mixture of 95% N_2/5% CO_2 in an incubator at 37°C for 10-30 min in ACSF. In order to induce hypoglycemia ACSF was substituted by modified ACSF containing mannitol (10 mM) instead of glucose. Drugs were applied either in ACSF 1 h before and in modified ACSF during hypoxia/hypoglycemia or throughout the entire experiment, 1 h before hypoxia/hypoglycemia until propidium iodide (PI) staining. After hypoxia/hypoglycemia OSC were incubated in TCM under normoxic conditions for another 24 h.

Quantification of neuronal cell death. 24 h after hypoxia/hypoglycemia OSC were stained with PI (10 µg/ml) for 2 h. PI fluorescence was elicited at 510-560 nm and recorded at >610 nm on an inverted fluorescence microscope (Nikon, Düsseldorf, Ger). Images were captured using a CCD camera (Visitron Systems, Eichenau, Ger), stored on CD, and subsequently analysed on a PC with an image analysis software (LUCIA M, Nikon).
The neuronal regions of control OSC could easily be identified from transmission images. Due a pronounced darkening of OSC after hypoxia/hypoglycemia (Fig. 4c), however, the areas of the CA1 and CA3 subfields could not be unequivocally demarcated. Thus, for the quantification of neuronal damage the percentage of CA1-CA3 area expressing PI fluorescence above background level was calculated in relation to the total area of each OSC. The mean values of 3-4 OSC treated under identical conditions were calculated and normalized against standard damage in order to compensate variations in PI fluorescence between different experiments. Each experiment contained a condition in which OSC were subjected to 30 min hypoxia/hypoglycemia and no compound applied. The mean percentage of fluorescing CA1-CA3 area of this condition was taken as standard damage. Percentages of fluorescing CA1-CA3 area obtained from other conditions are expressed as percentage of this standard damage.

Electrophysiological characterization of OSC. After 2-10 DIV OSC were transfered on their membrane inserts to an interface type recording chamber (Institute workshop), constantly perfused at 1 ml/min with ACSF and exposed to a moist carbogen atmosphere (95% O_2/5% CO_2) at 35±1°C. Population spike (PS) responses were evoked by stimulation of the perforant path, mossy fibers or Schaffer collaterals with stainless steel electrodes and recorded with glass microelectrodes (1-4 MΩ) in the stratum granulare of the dentate gyrus or the stratum pyramidale of the CA3 or CA1 region, respectively.

Electrophysiological experiments. After 7-10 DIV PS responses were evoked by stimulation of the Schaffer collaterals and recorded in the stratum pyramidale of the CA1 region. Test stimuli (biphasic current pulses, 0.1 msec per half wave) were adjusted to elicit a PS of about 66% of its maximum amplitude. The PS amplitude was evaluated by calculating the voltage difference between the negative peak and the positive one preceding it. Since the amplitude of the PS correlates over a wide range with the number of firing neurons (Andersen et al., 1971), it may serve as a measure of functional neuronal integrity. After the PS amplitude had been stable for at least 30 min (baseline) hypoxia/hypoglycemia was induced by changing the carbogen atmosphere of the chamber to a gas mixture consisting of 95% N_2/5% CO_2 in the presence of ACSF that contained 10 mM mannitol instead of glucose. After 4-20 minutes of hypoxia/hypoglycemia normal oxygen and glucose supply was re-established. The restitution of PS was monitored for one hour. Test compounds were bath applied 10 min before 18 min hypoxia/hypoglycemia and washed out immediately thereafter in the respective experiments.

Histological staining. OSC on membrane inserts were fixed in cold PFA (4% in 0.1 mM PBS, pH 7.4) for 30 min and subsequently rinsed in PBS (0.1 mM, pH 7.4). After being carefully removed from the membrane inserts OSC were incubated in graded sucrose buffers (10%, 20%, 30% sucrose in PBS, 30 min each). Subsequently they were mounted on a flat stage of frozen cryo-embedding compound (Microm, Walldorf, Ger) on a cryotome (Microm). Sections of 15-20 µM thickness were mounted on glass slides (Superfrost®, Menzel, Braunschweig, Ger) and air-dried for at least 3-4 h. Life/death staining was performed with toluidine blue/fuchsin acid according to standard procedures (Romeis et al., 1989).

Statistics. The normalized values of neuronal cell death and the values of PS recovery obtained from independent experiments are given as mean ± s.e.m. The Mann-Whitney *U*-test was used to compare the neuronal damage of differently treated OSC, i.e. hypoxia/hypoglycemia vs control or drug treatment vs no drug treatment, respectively.

Results

Development of OSC. From each animal 20-30 OSC could be obtained, which were cultivated by 3-4 on individual membrane inserts. During the first week in culture slices reorganize and flatten from 350 µM to about 150 µM, which can be followed up in bright field microscopy (Fig. 1). On the day of preparation the slices are opaque, with the neuronal layers transparent. During the reorganization period the OSC become dark and seem to be covered by dark spots. After about one weak the spots disappear and the OSC become transparent with the neuronal regions easily identifiable.

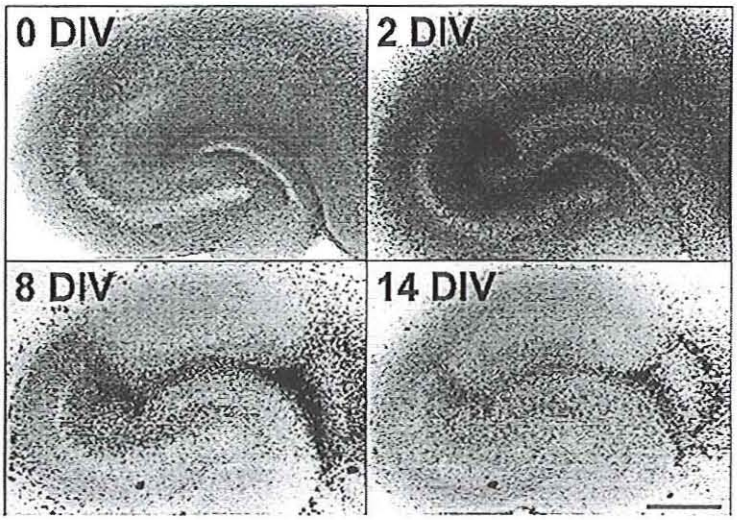

Fig. 1. Development of an OSC during the first two weeks in culture. At the day of the preparation (0 DIV) the neuronal regions of the hippocampal slice are clearly distinguishable. During the reorganization period (2 DIV) the OSC become covered by dark spots. After 8-14 DIV, when the reorganization period has finished, OSC of good quality appear light and transparent. There are no more dark spots detectable on the neuronal layers, which can easily be identified. Scale bar: 0.5mm.

In the course of the reorganization period the pyramidal cells displace resulting in a pronounced broadening of the neuronal regions, especially the CA1 region (Fig. 2). Glial cells form an outgrowth zone around the OSC and are most likely also reponsible for the firm attachment of the slice cultures to the porous membranes (Buchs et al., 1993). OSC retained viability for more than 6 weeks as was proved by healthy appearance in bright field microscopy and intact electrophysiological connectivity (Sabelhaus et al, in prep.).

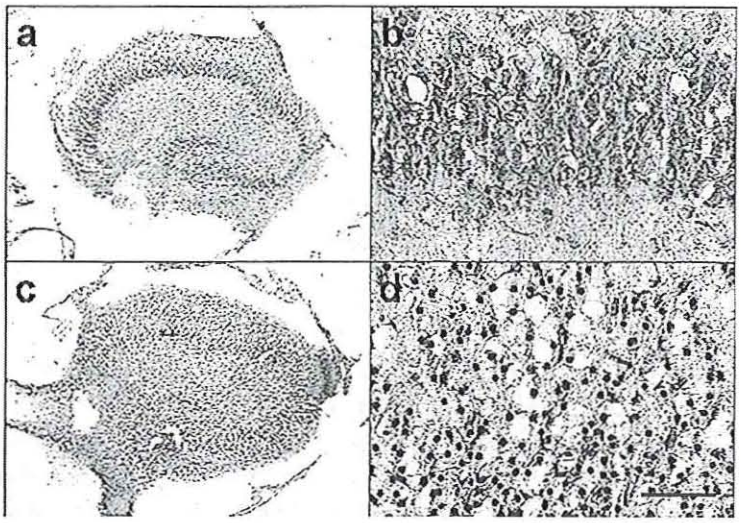

Fig. 2. Fuchsin acid/toluidine blue staining of OSC. a) The pyramidal fields and the dentate gyrus are easily recognizable in slice cultures. b) The pyramidal CA1 neurons have displaced to a width of several cell layers. c) 24 h after 30 min hypoxia/hypoglycemia pyramidal cells in the CA1 and CA3 area are damaged. d) Nuclei in the CA1 neurons appear pyknotic after hypoxia/hypoglycemia, the cytoplasms is vacuolized. Scale bar: 0.5mm (a, c), 0.05mm (b, d).

The intrinsic electrophysiological connectivity is well preserved in OSC. Stimulation in the subiculum evokes PS in the dentate gyrus, the CA3 and the CA1 region of the hippocampus, respectively. PS can be evoked in the CA3 and CA1 regions after stimulation of the mossy fibers in the hilus of the dentate gyrus (orthodromic recordings). Antidromic responses consisting of PS and excitatory postsynaptic potentials (EPSPs) were recorded in the granular cell layer of the dentate gyrus after stimulation of the mossy fibers. Stimulation of Schaffer collaterals elicits PS in CA1 region. Paired pulse inhibition (20 msec pulse interval) demonstrates intact inhibitory synaptic transmission in CA1 region. The intrinsic connectivity also shows features of maturation during the first week in culture. Extracellular recordings of EPSPs and PS can be evoked already after 2-3 DIV, but full amplitude of recordings developes only until DIV 4-5.

Sensitivity of OSC to oxygen/glucose deprivation. After 14 DIV, when the reorganization of the OSC had finished, experiments were performed to determine the adequate treatment for inducing measurable neuronal damage. Damage was induced by depriving the OSC from oxygen (hypoxia) or from oxygen and glucose (hypoxia/hypoglycemia) for 10-30 min. Hy-

poxia without glucose deprivation induces only minor neuronal damage, not significantly different from control cultures (Fig. 3). Hypoxia/hypoglycemia on the contrary induces increasing neuronal damage, when lasting for 20 or 30 min, whereas 10 min of hypoxia/hypoglycemia did not induce any measurable damage. 60 min of hypoxia/hypoglycemia result in slightly enhanced damage compared to 30 min oxygen/glucose deprivation, but often also comprises cells outside the hippocampal neuronal layers. For this reason and as 30 min hypoxia/hypoglycemia resulted in nearly maximal neuronal damage this treatment of OSC was considered as adequate for purposes of investigating neuroprotective drug effects.

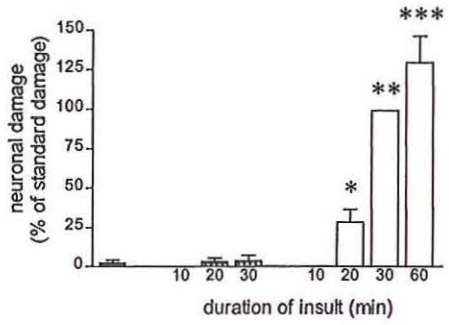

Fig. 3. Neuronal damage measured as PI uptake after hypoxia (hatched bars) and hypoxia/hypoglycemia (open bars). Hypoxia (w/o glucose deprivation) induces only light neuronal damage, similar to control cultures (filled bars), even when the incubation lasts 30 min. 10 min of hypoxia/hypoglycemia do not induce any measurable damage, whereas 20 and 30 min of hypoxia/hypoglycemia induce increasing neuronal damage. 60 min of hypoxia/hypoglycemia result in slightly increased damage compared to 30 min, which is taken as standard damage. *: $p<0.05$, **: $p< 0.01$, ***: $p<0.001$ vs control (Mann-Whitney *U* -test).

After hypoxia/hypoglycemia OSC exhibited neuronal cell death especially in the CA 1 region (Fig. 4), but also extending into the CA3 region in some OSC. Already directly after the hypoxic/hypoglycemic period a reduction of transmission light properties was detectable. Due to this darkening of the entire OSC, the areas of the CA1 and CA3 subfields could not be unequivocally demarcated (cf. Material and Methods). Untreated control OSC did not show significant PI uptake or such darkening. In order to validate the PI staining method, OSC were subsequently fixed for histological examination. Neuronal damage of OSC that had suffered an ischemic insult became visible as cytoplasmic vacuolization and pyknosis of pyramidal cell nuclei (Fig. 2).

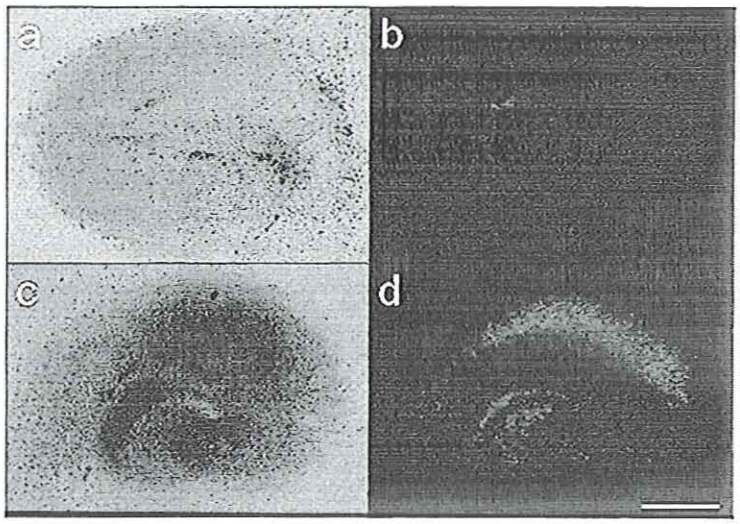

Fig. 4. Transmission images (a,c) and PI-fluorescence micrographies (b,d) of a control culture (a,b) and a culture 24 h after a hypoxic/hypoglycemic insult (c,d). Hypoxia/hypoglycemia results in a loss of light transmission and PI uptake by damaged neurons especially in the CA1 area, but also in CA3 and DG subfields of the hippocampus. Scale bar: 0.5mm.

In electrophysiological experiments performed after 7-10 DIV PS were evoked by stimulation of Schaffer collaterals and recorded in the stratum pyramidale of the CA1 region. The amplitude of PS was used as a measure of functional neuronal integrity. Hypoxia/hypoglycemia resulted in the disappearance of the PS within 3-4 min. During the following reoxygenation period the PS amplitude recovered to about 20-90% after one hour depending on the duration of hypoxia/hypoglycemia (Fig 5, 6a control). 12 min hypoxia/hypoglycemia did not result in a sustained loss of synaptic transmission, neither in acutely isolated slices from 20 day old rats nor in OSC. About 18 min hypoxia/hypoglycemia were necessary to obtain a PS recovery of about 50% in OSC. An oxygen/glucose deprivation of 20 min resulted in a pronounced decrease of synaptic recovery. For acutely isolated slices from adult rats only 4 min hypoxia/hypoglycemia are sufficient to obtain 50% PS recovery.

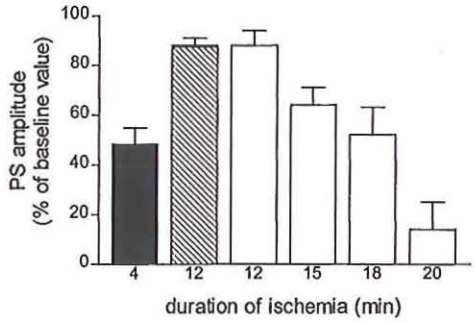

Fig. 5. Recovery of synaptic transmission after hypoxia/hypoglycemia. Acutely isolated slices of adult rats (filled bar), of 20-days-old rats (hatched bars) and OSC (open bars) subjected to various periods of hypoxia/hypoglycemia. Restitution of PS in the CA 1 region was monitored for 60 min after the insult.

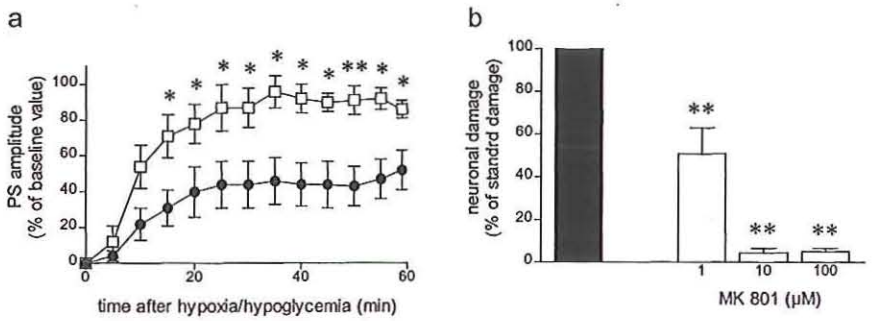

Fig 6. The NMDA receptor antagonist MK 801 protects OSC from ischemic injury. a) Recovery of synaptic transmission after 18 min hypoxia/hypoglycemia is significantly ameliorated by 10 mM MK 801 (open symbols) compared to unprotected OSC (filled symbols). b) MK 801 (open bars) decreases the amount of neuronal cell death dose-dependently. Filled bar: w/o MK 801, *: $p<0.05$, **: $p<0.01$ vs hypoxia/hypoglycemia w/o MK 801 (Mann-Whitney *U*-test).

Pharmacological validation of of OSC for testing neuroprotective drugs. For pharmacological validation of the OSC as *in vitro* model cytoprotective compounds with different effector mechanisms were tested, which have been reported to be neuroprotective in other *in vivo* and *in vitro* systems (Tab. 1). As it is widely accepted that glutamate is involved in the pathogenesis of ischemic cell damage (Rothman and Olney, 1986; Choi, 1988), inhibitors of the different glutamate receptor subtypes were tested in our model system. The non-competitive NMDA receptor antagonist MK 801 exerted neuroprotection on OSC, both measured as

increased PS amplitude after 18 min hypoxia/hypoglycemia and as decreased PI uptake (Fig. 6). The AMPA/kainate receptor antagonists CNQX and NBQX and the mGluR I receptor agonist 1S,3R-ACPD failed to protect OSC from ischemic injury both measured as synaptic recovery and PI uptake.

Tab 1. Validation of OSC with neuroprotective compounds exhibiting different effector mechanisms.

effector mechanism	compounds	concentration	damage parameter	protection
NMDA receptor-antagonist	MK 801	10 µM 1-100 µM	PS recovery PI uptake	yes yes
AMPA/kainate receptor antagonist	CNQX, NBQX	10 µM	PI uptake	no
mGluR I agonist	1S,3R-ACPD	100 µM	PS recovery PI uptake	no no
Na^+ channel blocker	TTX	10 µM	PI uptake	yes
Ca^{2+} channel blocker	nimodipine	10 µM	PI uptake	no
free radical scavenger	U83836E	10 µM	PI uptake	no

Na^+ influx during anoxia is responsible for some of the acute injury seen in CNS (Rothman and Olney, 1986). To test whether voltage-gated Na^+ channels are involved in mediating neuronal damage in OSC the Na^+ channel blocker TTX (Urenjak and Obrenovitch, 1996) was applied to OSC during hypoxia/hypoglycemia. TTX (10 µM) exerted significant and dramatic neuroprotective effects on OSC.

The Ca^{2+} channel blocker nimodipine, which has proven to be neuroprotective in dissociated cell cultures (Krieglstein et al., 1996) had no protective effect on OSC after hypoxia/hypoglycemia.

As free oxygen radicals are involved in neuronal damage following ischemia, the radical scavenger U83836E which is neuroprotective in a rabbit model of trauma (Wilson et al., 1995) was tested in our model system, but U83836E had no protective effect on OSC.

Discussion

Preparation and maintainance of OSC. Organotypic hippocampal cultures possess the differentiated morphological and physiological characteristics, comprising cellular composition, neuronal organization and intrinsic connectivity, of the hippocampus at the day of preparation and appear to undergo further maturation in culture to attain many adult-like qualities (Bahr et al., 1995; Caesar and Aertsen, 1991). On the other hand, all extrinsic afferent fibers and projections oriented in the longitudinal direction of the hippocampus are transsected in the course of tissue preparation and degenerate. With increasing age of the neonate rats the slice cultures are prepared from, the architecture of the hippocampal formation is better retained (Bahr et al., 1995; Buchs et al., 1993).

Our OSC were prepared from 9-10-days-old neonate rats. At that age, functional synaptic connections have already been established, particularly in the CA1 area. But many important characteristics of the mature brain are still lacking and may develop only during the following weeks. An extensive cellular and synaptic reorganization can be found during the first week in culture (Caesar and Aertsen, 1991; Muller et al., 1993; Buchs et al., 1993). Compared to roller tube cultures (Gähwiler, 1981), however, these changes are less pronounced in interface cultures and the preservation of the three dimensional tissue structure is superior (Stoppini et al., 1991).

The proliferation of glial cell appears to be very limited in interface type OSC and they do not cover or overgrow OSC permanently. In contrast to other culture methods it is therefore not necessary to include cytosine arabinoside in the culture medium to suppress astroglial growth. During the first week in culture a transient increase in glial cells can be observed, which is probably related to the removal of degenerated cells, produced during the dissection process (Buchs et al., 1993). This glial cell activity may be the cause for the darkening of our OSC and the appearance of dark spots during the reorganization period. Predominantly astrocytes accumulate at the border between slice and porous membrane (Stoppini et al., 1991). They extend processes into the membrane, thus anchoring the slices into the membrane. It is speculated that they may form a kind of barrier between culture medium and tissue (Buchs et al., 1993).

OSC maintained according to the interface technique flatten considerably during the first week *in vitro* although they remain several cell layers thick. The accessibility of individual neurons, e.g. for intracellular electrophysiological recordings, might therefore be not as good as in roller tube cultures. In any case, the neuronal layers of the hippocampal formation can easily be visualized in bright field and fluorescence microscopy.

Extracellular electrophysiological recordings revealed that the main intrinsic connectivity of the native hippocampus is retained in OSC. This trisynaptic cascade reorganizes during the first days in culture, as can be observed from the maturation of the electrophysiological connectivity. Additionally aberrant connections form in OSC as can be seen from the antidromic response in the granular cell layer of the OSC after the stimulation of the mossy fibers. The IPSPs/EPSPs in the field potentials probably have their origin in the backpropagation of mossy fibers into the dendritic field of the dentate gyrus granular cells. This situation may mimic the missing innervation from the entorhinal cortex via the perforant path which was interrupted during the slice preparation.
In summary our findings demonstrate that OSC maintained on membrane inserts are quite useful for microscopic and electrophysiological studies on populations of neurons.

Sensitivity of OSC to oxygen/glucose deprivation. Combined oxygen/glucose deprivation is accepted to mimic closely ischemic conditions *in vivo* (Goldberg and Choi, 1990; Goldberg and Choi, 1993). Oxygen/glucose induced cell death has been described as neuron specific, since astrocytes are not affected (Strasser and Fischer, 1995). Thus, hypoxia/hypoglycemia was chosen the most reliable method to simulate cerebral ischemia in our *in vitro* model system.
Electrophysiological recordings of the PS in the CA1 pyramidal cell layer after stimulation of the Schaffer collaterals were taken as a measure of the functional viability. The recovery of synaptic transmission at 1 h after the insult was adjusted to a half maximal value by varying the duration of oxygen/glucose deprivation. By this means we were able to observe both protective and detrimental effects of tested compounds. The PS amplitude recovered to about 50% after 18 min hypoxia/hypoglycemia. In comparison with the acutely isolated slices from adult rats a 4-5 times longer oxygen/glucose deprivation was necessary to adjust the recovery of synaptic transmission at about 50% of the baseline value recorded before the insult. No difference in the susceptibility could be observed between OSC and acutely isolated slices from age-matched rats, indicating that the susceptibility depended on the overall age of tissue and was not affected by culture conditions. These observations support the generally accepted findings that the susceptibility to ischemic conditions of neuronal tissue from adult organisms is higher than that from juveniles (Frank, 1985).
In the long-term range, neuronal cell death was quantified measuring the uptake of PI 24 h after the ischemic insult. Hypoxia/hypoglycemia was induced in a gasifiable incubator for 10-30 min. This method allows the induction of ischemia in a series of organotypic cultures at the same time. Thus we were able to increase the number of experiments and different experimental conditions considerably.

The susceptibility of OSC to hypoxia/hypoglycemia measured both by electrophysiology and by PI uptake was very similar. Oxygen/glucose deprivation lasting for 18 and 30 min, respecively, resulted in reliable neuronal damage. Our OSC seem to be more susceptible to hypoxia/hypoglycemia than OSC of another laboratory, which reported that 60 min hypoxia/hypoglycemia were necessary to obtain significant neuronal damage measured by PI uptake (Strasser and Fischer, 1995). Since Strasser and Fischer use animals only 3-days-old for preparing OSC it may be concluded that the age of the rats may contribute decisively to the susceptibility of the OSC. Other factors that influence the severeness of damage after an ischemic insult may be the degree of oxygen deprivation obtained in the hypoxic/anoxic chamber and the rat strain used for preparation.

Pharmacological evaluation of OSC. For pharmacological validation of the OSC as *in vitro* model cytoprotective compounds with different effector mechanisms were tested, which have been neuroprotective in other *in vivo* and *in vitro* systems. To ensure suffient diffusion into the OSC, all compounds were applied in the medium in 6-well-plates for 1 h before hypoxia/hypoglycemia or perfused for 10 min before hypoxia/hypoglycemia in the recording chamber.

It is widely accepted that glutamate is mainly involved in the pathogenesis of ischemic cell damage (Rothman and Olney, 1986; Choi, 1988). The contribution of different glutamate receptor subtypes to ischemic damage seems to be age-dependent. NMDA receptors appear to be primarily responsible for ischemia-induced excitotoxic neuronal injury in the developing CNS (McDonald et al., 1987; Olney et al., 1989) whereas both NMDA and non-NMDA receptors are likely to contribute to ischemic neurodegeneration in the adult brain (Mosinger et al., 1991; Sheardown et al., 1990; Gill et al., 1992; Gill, 1994). In our model-system the NMDA receptor antagonist MK 801 turned out to be protective both tested in the short-term (restitution of synaptic transmission within 1 h after hypoxia/hypoglycemia) and the long-term range (PI uptake 24 h after the insult). This result coincides well with other *in vivo* and *in vitro* models of cerebral ischemia (Gill et al., 1991; Newell et al., 1995; Vornov et al., 1994; Hatfield et al., 1992; Pringle et al., 1997).

The AMPA/kainate receptor antagonists CNQX and NBQX were not protective in our model system. In *in vitro* models of cerebral ischemia utilizing OSC the involvement of AMPA/kainate receptors in neuronal damaged is controversely described (Pringle et al., 1997; Strasser and Fischer, 1995, Laake et al., 1996) The obvious differences in the protective effects of CNQX, which was used as antagonist may at least in part be due to the severity of the ischemic insult, the OSC are subjected to. Strasser and Fischer (1995) reported that CNQX exerted a protective effect only when the ischemic period was short enough to result only in

partial neuronal cell death, whereas it was not protective when the insult lasted longer. Pringle et al. (1997) reported on neuroprotective effects of CNQX also after 60 min hypoxia/hypoglycemia, whereas Laake et al. (1996) did not find any protective effects of CNQX, as we did. These fact appears to be very intriguing since both NMDA and AMPA receptors are reported to be well maintained in OSC from 11-days-old rats compared to neonate and adult hippocampal membranes (Bahr et al., 1995). Since the expression of AMPA receptors increased steadily with increasing age in the rat telencephalon (Hall and Bahr, 1994), it can not be ruled out that the rats we prepared OSC from were too young.

The same may be true for the mGluRs. mGluRs are decisively envolved in neuronal damage after hypoxia in adult rats (Riedel et al., 1996) and hippocampal slices from adult rats (Opitz et al., 1994; Opitz and Reymann, 1993). In our model system the mGluR class I agonist 1S,3R-ACPD which improves the synaptic transmission in hippocampal slices from adult rats after hypoxia/hypoglycemia (Opitz and Reymann, 1993) had no protective effect.

Na^+ influx during anoxia is responsible for some of the acute injury seen in CNS (Rothman and Olney, 1986). To test whether voltage-gated Na^+ channels are involved in mediating neuronal damage in OSC the Na^+ channel blocker TTX was tested and exerted significant and dramatic neuroprotective effects on OSC. This finding corroborates data obtained in other *in vivo* and *in vitro* models of ischemia, where it was demonstrated that damage following insults could be prevented by addition of TTX (Urenjak and Obrenovitch, 1996; Pringle et al., 1997; Vornov et al., 1994).

The L-type Ca^{2+} channel blocker nimodipine, which has proven to be neuroprotective in dissociated cell cultures (Krieglstein et al., 1996) had no protective effect on OSC after hypoxia/hypoglycemia. In another report (Pringle et al., 1996) it was demonstrated that the dihydropyridine nifedipine and other Ca^{2+}-channel blockers were not protective against damage induced by hypoxia/hypoglycemia, although it was determined that extracellular calcium was essential for the generation of ischemic damage. It was speculated that neuroprotective effects of dihydropyridines may be mediated through vascular calcium channels or indirectly through actions in other brain regions.

Lazaroids such as the 21-aminosteroid U-83836E are a new class of superoxide and free radical lipid peroxidation inhibitors. U-83836E prevents hydrogen peroxide-induced F2 isoprostane production in renal proximal tubular cells (Salahudeen et al., 1995), prevents free radical mediated effects of oxyhemoglobin on vascular smooth muscle (Vollrath et al., 1995), and reduces secondary brain injury in a rabbit model of cryogenic trauma (Wilson et al., 1995). As U83836E had no protective effect in our model system the generation of free radicals seems to play only a minor role in neuronal damage after hypoxia/hypoglycemia in OSC.

The pharmacological validation of our in vitro model indicates that OSC are quite reliable for the investigation of neuroprotective drug effects with some restrictions resulting from the neonate age of the rats the OSC are prepared from.

Reduction of animal consumption. Since 20-30 slices were obtained from each rat, which were cultivated by 3-4 on individual membrane inserts, up to 6-8 different conditions, e.g. different compounds or different concentrations of one compound, could be tested using slice cultures of a single animal. For the prescreening of possibly neuroprotective compounds this would mean a reduction of animal consumption by a factor of about 8 compared to *in vivo* methods.

Acknowledgements

The authors wish to thank H. Herold and A. Böcker for expert technical assistance and Dr. P. Hendrich-Noack for critically reading the manuscript.
This study was supported by BMBF grant 0319998B and LSA 2507A/0086H.

References

Andersen P, Bliss TV, Skrede KK (1971) Unit analysis of hippocampal polulation spikes. Exp Brain Res 13: 208-221.

Bahr B, Kessler M, Rivera S, Vanderklish PW, Hall RA, Mutneja MS, Gall C, Hoffman KB (1995) Stable maintenance of glutamate receptors and other synaptic components in long-term hippocampal slices. Hippocampus 5: 425-439.

Banker GA, Cowan WM (1977) Rat hippocampal neurons in dispersed cell culture. Brain Res 126: 397-342.

Banker GA, Cowan WM (1979) Further observations on hippocampal neurons in dispersed cell culture. J Comp Neurol 187: 469-493.

Buchs P-A, Stoppini L, Muller D (1993) Structural modifications associated with synaptic development in area CA1 of rat hippocampal organotypic cultures. Dev Brain Res 71: 81-91.

Caesar M, Aertsen A (1991) Morphological organization of rat hippocampal slice cultures. J Comp Neurol 307: 87-106.

Choi DW (1988) Glutamate neurotoxicity and diseases of the nervous system. Neuron 1: 623-634.

Crain SM (1976) Neurophysiologic studies in tissue culture. Raven Press, New York.

Frank L (1985) Effects of oxygen on the newborn. Fed Proc 44: 2328-2334.

Gähwiler BH (1981) Organotypic monolayer cultures of nervous tissue. J Neurosci Methods 4: 329-342.

Gähwiler BH (1988) Organotypic cultures of neural tissue. Trends Neurosci 11: 484-489.

Gähwiler BH, Capogna M, Debanne D, McKinney RA, Thompson SM (1997) Organotypic slice cultures: a technique has come of age. Trends Neurosci 20: 471-477.

Gill R (1994) The pharmacology of alpha-amino-3-hydroxy-5-methyl-4-isoxazole propionate (AMPA)/kainate antagonists and their role in cerebral ischaemia. Cerebrovasc Brain Metab Rev 6: 225-256.

Gill R, Brazell C, Woodruff GN, Kemp JA (1991) The neuroprotective action of dizocilpine (MK-801) in the rat middle cerebral artery occlusion model of focal ischaemia. Br J Pharmacol 103: 2030-2036.

Gill R, Nordholm L, Lodge D (1992) The neuroprotective actions of 2,3-dihydroxy-6-nitro-7-sulfamoyl-benzo(F)quinoxaline (NBQX) in a rat focal ischaemia model. Brain Res 580: 35-43.

Goldberg MP, Choi DW (1990) Intracellular free calcium increases in cultured cortical neurons deprived of oxygen and glucose. Stroke 21: III75-7.

Goldberg MP, Choi DW (1993) Combined oxygen and glucose deprivation in cortical cell culture: calcium-dependent and calcium-independent mechanisms of neuronal injury. J Neurosci 13: 3510-3524.

Hall RA, Bahr BA (1994) AMPA receptor development in rat telencephalon: [3H]AMPA binding and western blot studies. J Neurochem 63: 1658-1665.

Hatfield RH, Gill R, Brazell C (1992) The dose-response relationship and therapeutic window for dizocilpine (MK-801) in a rat focal ischaemia model. Eur J Pharmacol 216: 1-7.

Krieglstein J, Lippert K, Poch G (1996) Apparent independent action of nimodipine and glutamate antagonists to protect cultured neurons against glutamate-induced damage. Neuropharmacology 35: 1737-1742.

Laake JH, Rundén E, Brodal P, Ottersen OP (1996) In vitro ischemia and phosphatase 1/2a inhibition cause selective neuronal death in hippocampal slice cultures. Soc Neurosci Abstr 22: 1897.

McDonald JW, Silverstein FS, Johnston MV (1987) MK-801 protects the neonatal brain from hypoxic-ischemic damage. Eur J Pharmacol 140: 359-361.

Mosinger JL, Price MT, Bai HY, Xiao H, Wozniak DF, Olney JW (1991) Blockade of both NMDA and non-NMDA receptors is required for optimal protection against ischemic neuronal degeneration in the in vivo adult mammalian retina. Exp Neurol 113: 10-17.

Muller D, Buchs P-A, Stoppini L (1993) Time course of synaptic development in hippocampal organotypic cultures. Dev Brain Res 71: 93-100.

Newell DW, Barth A, Papermaster V, Malouf AT (1995) Glutamate and non-glutamate receptor mediated toxicity caused by oxygen and glucose deprivation in organotypic hippocampal cultures. J Neurosci 15: 7702-7711.

Olney JW, Ikonomidou C, Mosinger JL, Friedrich G (1989) MK-801 prevents hypobaric-ischemic neuronal degeneration in infant rat brain. J Neurosci 9: 1701-1704.

Opitz T, Reymann KG (1993) (1S, 3R)-ACPD protects synaptic transmission from hypoxia in hippocampal slices. Neuropharmacology 32: 103-104.

Opitz T, Richter P, Reymann KG (1994) The metabotropic glutamate receptor antagonist (+)-alpha-methyl-4-carboxyphenylglycine protects hippocampal CA1 neurons of the rat from in vitro hypoxia/hypoglycemia. Neuropharmacology 33: 715-717.

Pringle AK, Benham CD, Sim L, Kennedy J, Iannotti F, Sundstrom LE (1996) Selective N-type calcium channel antagonist omega conotoxin MVIIA is neuroprotective against hypoxic neurodegeneration in organotypic hippocampal-slice cultures. Stroke 27: 2124-2130.

Pringle AK, Iannotti F, Wilde GJ, Chad JE, Seeley PJ, Sundstrom LE (1997) Neuroprotection by both NMDA and non-NMDA receptor antagonists in in vitro ischemia. Brain Res 755: 36-46.

Riedel G, Opitz T, Reymann KG (1996) Blockade of metabotropic glutamate receptors protects hippocampal neurons from hypoxia-induced cell death in rat in vivo. Prog Neuropsychopharmacol Biol Psychiatry 20: 1253-1263.

Romeis B, Denk H, Künzle H, Plenk H Jr, Rüschoff J, Sellner W (1989) Mikroskopische Technik. Urban und Schwarzenberg, München.

Rothman SM, Olney JW (1986) Glutamate and the pathophysiology of hypoxic-ischemic brain damage. Ann Neurol 19: 105-111.

Salahudeen A, Badr K, Morrow J, Roberts J 2nd (1995) Hydrogen peroxide induces 21-aminosteroid-inhibitable F2-isoprostane production and cytolysis in renal tubular epithelial cells. J Am Soc Nephrol 6: 1300-1303.

Schmidt-Kastner R, Freund TF (1991) Selective vulnerability of the hippocampus in brain ischemia. Neuroscience 40: 599-636.

Sheardown MJ, Nielsen EO, Hansen AJ, Jacobsen P, Honoré T (1990) 2,3-Dihydroxy-6-nitro-7-sulfamoyl-benzo(F)quinoxaline: a neuroprotectant for cerebral ischemia. Science 247: 571-574.

Stoppini L, Buchs P-A, Muller D (1991) A simple method for organotypic cultures of nervous tissue. J Neurosci Methods 37: 173-182.

Strasser U, Fischer G (1995) Quantitative measurement of neuronal degeneration in organotypic hippocampal cultures after combined oxygen/glucose deprivation. J Neurosci Methods 57: 177-186.

Strasser U, Fischer G (1995) Protection from neuronal damage induced by combined oxygen and glucose deprivation in organotypic hippocampal cultures by glutamate receptor antagonists. Brain Res 687: 167-174.

Urenjak J, Obrenovitch TP (1996) Pharmacological modulation of voltage-gated Na^+ channels: a rational and effective strategy against ischemic brain damage. Pharmacol Rev 48: 21-67.

Vollrath B, Chan P, Findlay M, Cook D (1995) Lazaroids and deferoxamine attenuate the intracellular effects of oxyhaemoglobin in vascular smooth muscle. Cardiovasc Res 30: 619-626.

Vornov JJ, Tasker RC, Coyle JT (1994) Delayed protection by MK-801 and tetrodotoxin in a rat organotypic hippocampal culture model of ischemia. Stroke 25: 457-464.

Wilson JT, Gross CE, Bednar MM, Shackford SR (1995) U83836E reduces secondary brain injury in a rabbit model of cryogenic trauma. J Trauma 39: 473-477; discussion 477-479.

In vitro models of the blood-brain barrier for the investigation of cerebroprotective agents

Katharina Mertsch, Reiner F. Haseloff, Matthias L. Schroeter and Ingolf E. Blasig

Forschungsinstitut für Molekulare Pharmakologie,

Alfred-Kowalke-Str. 4, 10315 Berlin

Abstract

The blood-brain barrier (BBB) formed by brain capillary endothelial cells (BEC) under the influence of astrocytes (AC) has been neglected in the treatment of blood flow disturbances of the brain, such as ischemia and related injury. On the other hand, these cells can be reached easily by systemic administration of a drug. Among others (i.e., accumulation of cellular Ca^{2+}, energy deficiency), reactive oxygen species play an important pathogenic role under ischemic conditions. Therefore, a test hierarchy was developed based on BEC, AC and cocultures of both, which allows to characterize a potentially protective agent with respect to: radical scavenger activity, cytotoxicity, cytoprotectivity against oxidative (hypoxic) stress, and protectivity on the tightness of a cell culture model of the BBB under hypoxic conditions. Moreover, the permeability of test compounds through the BBB model can be determined to predict the permeation of substances into the brain. This test system was validated using neuroprotective agents of different classes and various radical scavengers as research standards. The research strategy described here is expected to partly replace animal experiments in the development of novel neuroprotective drugs.

Introduction

Brain endothelial cells (BCE), being mainly influenced by astrocytes (AC) with respect to the formation of the blood-brain barrier (BBB; Risau et al., 1990; Dehouk et al., 1990; Giese et al., 1995), possess tight junctions and are characterized by low pinocytosis and very low

paracellular permeation. During cerebral ischemia, brain microvessels generate an enhanced amount of free radicals (Grammas et al., 1993; Mertsch et al., 1995), which can disturb the function of the BBB (Evans, 1993; Giese et al.; 1995). Both BEC and AC have been reported to generate reactive oxygen species (ROS) due to hypoxia and following reoxygenation (Betz, 1993; Mertsch et al., 1995). Hypoxia reduces the activity of antioxidatively acting enzymes of BEC, such as superoxide dismutase (SOD), glutathione peroxidase and catalase (Plateel et al., 1995; Schroeter et al., 1997).

Pharmacological interventions directed to the cells of the BBB have been neglected so far. Therefore, the aim of this project was to establish *in vitro* methods by using cells of the BBB for the investigation of potentially neuroprotective agents. Methods have been developed mainly on the cellular level. The investigations have been performed in monocultures of BEC and in cocultures of BEC and AC. As a model of the BBB, BEC are cultivated on one side and AC on the other side of a filter insert. There is the possibility to study the influence of other types of cells (e.g., those occurring *in vivo* close to the BBB) which can be cultivated on the bottom of the well. On the cellular level, opening of the BBB, increase of ROS-induced peroxidation of membrane lipids (LPO) and viability after hypoxia and reoxygenation have been investigated. Various types of potentially protective compounds have been included into the investigations. Among these were neuroprotective agents, such as Ca^{2+} channel blockers, NMDA- and AMPA receptor antagonists or compounds affecting free radical reactions as, for instance, radical scavengers. The results demonstrate the potential of *in vitro* models of the BBB to characterize the activitiy of neuroprotective drugs on the level of the BBB during and following oxidative stress.

Materials and Methods

Reagents, materials and kits. Ham's F10, α-medium, Dulbecco's modified Eagle's medium (DMEM) were purchased from Biochrom (Berlin, Germany), fetal bovine serum (FBS), glutamine, bovine fibroblast growth factor (bFGF), geneticin, trypsin/ethylenediaminetetraacetic acid (EDTA) and collagen type I for BEC from Boehringer Mannheim (Germany), FBS for AC from Gibco BRL (Eggenstein, Germany), glutamine, amphotericin B, penicillin/streptomycin and trypsin/EDTA for AC from Biochrom. Phosphate buffered saline (PBS) was purchased from Biochrom. BEC were cultivated on Corning flasks (Corning,

Dunn, Asbach, Germany), AC on Falcon flasks (Heidelberg, Germany). 6-well plates, filters for 6-well plates (polyethylene terephthalate, 0.45 μm pore size, 1.6×10^6 pores/cm^2) and 75 cm^2 culture flasks from Falcon were used. 24-well plates and cryotubes were purchased from Greiner (Frickenhausen, Germany). Immuncytochemistry was performed for Factor VIII, glial fibrillary acidic protein (GFAP), vimentin, desmin, α-smooth muscle actin (LSAB DAKO, Hamburg, Germany). Activities of γ-glutamyltranspeptidase (γGT) and alkaline phosphatase (ALP) were measured by Sigma kits. Isolectin *Bandereia simplicifolia* (positive for microglia) and oligodendrocyte specific marker O4 were purchased from Sigma.

Dimethylsulfoxide (DMSO), Na-fluorescein and hypoxanthine were from Sigma. [^{14}C]-sucrose and [^{3}H]-dichlorkynurenic acid were obtained from NEN (Brussels, Belgium). Phosphoric acid, NaOH and methanol were from Baker (Gross-Gerau, Germany), thiobarbituric acid from Merck (Darmstadt, Germany). Malondialdehydbis(diethylacetal) was from Merck-Schuchardt (Hohenbrunn, Germany), xanthine oxidase from Boehringer Mannheim (Germany) 5,5-dimethylpyrroline-1-oxide (DMPO) from Aldrich (Steinheim, Germany), diethylenetriaminepentaacetic acid (DETAPAC) and pyridine from Fluka (Buchs, Switzerland). Water used for cleaning equipments or preparation of solutions was purified with MilliRO and MilliQUF from Millipore, Eschborn, Germany. Carbogen (95% O_2/5% CO_2) and Nelson gas (95% N_2/5% CO_2) were purchased from Messer Griesheim (Berlin, Germany).

Test substances. U83836E {(-)-2-[[4-(2,6-di-1-pyrrolidinyl-4-pyrimidinyl)-1-piperazinyl] methyl]-3,4-dihydro-2,5,7,8-tetramethyl-2H-1-benzopyran-6-ol (dihydrochloride)}; kindly provided by Dr. Hall, Kalamazoo/MI, USA, Upjohn Comp.}, trolox C (6-hydroxy-2,5,7,8-tetramethylchroman-2-carbonic acid; LaRoche, Basel, Switzerland), α-tocopherol (Serva, Heidelberg, Germany), mannitol (Sigma), MK 801 (NMDA-receptor antagonist, kindly provided by Boehringer Ingelheim), nimodipine (Ca-channel antagonist, Research Biochemicals International, Natick, USA), NBQX (6-nitro-7-sulphamoylbenzo[f]quinoxaline-2,3-dione, AMPA receptor antagonist; Calbiochem, Bad Soden, Germany) were used. NN 1 (4,4,5,5-tetramethyl-2-(4-trimethylammoniophenyl)-2-imidazoline-1-oxyl methyl sulfate) was obtained from the Institute of Organic Chemistry (Novosibirsk, Russia).

Cloned immortalized rat brain endothelial cells (RBE4). RBE4 cells kindly supplied by Prof. P.O. Couraud (Paris, Frankreich) were cultivated according to Roux et al. (1994) in Ham's F10/α-medium 1:1, 10% FBS, 2 mM glutamine, 1 ng bFGF, 300 µg/ml geneticin on collagen I coated (1.7 µg/cm^2) plastics. Subcultivation of cells between 40th and 55th passage was performed twice a week: cells were washed with PBS for about 5 min, EDTA (0.02%) was added for 2 min, trypsin/EDTA (0.05%/0.02%, Boehringer Mannheim) was added for 2-5 min. Cells were frozen in cell medium (see above), containing 10% DMSO by reducing the temperature for 1°C per minute. At -70°C cells were transferred into liquid nitrogen. Endothelial origin of cells was characterized by phase contrast microscopy, factor VIII staining and staining procedures for ALP and γGT. Cell cultures were characterized morphologically by light microscopy (IMT 2, Olympus, Hamburg, Germany); monolayers with giant cells or abnormal cell morphology were not used for coculture experiments (Mertsch et al., 1997).

Porcine BEC were isolated according to Mertsch et al. (1995). Briefly, 6-8 brains were placed in PBS (without Ca^{2+}, Mg^{2+}), washed, covered with 70% ethanol and flamed. Brains were minced after discarding the meninges and mixed for 2-3 hours (37°C, approx. 60 rpm) with dispase II (5 mg/ml, *B. polymyxa*, Boehringer Mannheim). Density gradient centrifugation (5800×g for 10 min at 4 °C) was performed with 15% dextran solution (mol. wt. 500,000; Sigma). The pellet was dissolved in PBS (with Ca^{2+}, Mg^{2+}), collagenase/dispase (from *Achromobacter ioghages/B. polymyxa*, Boehringer Mannheim, 1 mg/ml) was added, and mixed for 1.5-2 h (37°C, 10 rpm). The resulting mixture was centrifuged (1000×g, 4°C, 10 min) and dissolved in medium 199 (Biochrom) with 16% FBS (Gibco) containing 2 mM glutamine, 100,000 I.U. penicillin, 100 µg/ml streptomycin, 2.5 µg/ml amphotericin (Biochrom). Cells were cultivated in 6- or 24-well-plates (Greiner), covered with gelatine (Sigma) for 2 h before plating (approx. 10^7 cells per 145 cm^2). Every second day cells were washed with PBS (37°C) to remove erythrocytes and covered again with medium, up to 10 days. Endothelial origin of cells was verified by Factor VIII staining. Activities of ALP and γGT were determined. Immunological tests were performed for vimentin and GFAP, neuron-specific enolase and 4-prolylhydroxylase activities (Dako) to exclude the presence of AC, neurons and fibroblasts, respectively. Subcultivation of porcine BEC was accomplished according to Dehouk et al. 1990) by trypsinization of pure endothelial cell islands 5-6 days after primary isolation (trypsinization as for RBE4). Cells were allowed to reach confluence

during the 4th-5th passage. Cells of the 7th or 8th subculture were frozen in liquid nitrogen and preserved for experiments (cf. AC).

Astrocytes. AC from neonatal rats were isolated according to Booher & Sensenbrenner (1972; Giese et al., 1995). Briefly, neonatal rats (1-2 days old) were killed by cervical dislocation, brains were removed and cortex was isolated. After removal of meninges, tissue was given through a nylon sieve (pore size, 100 µm) into DMEM with 10% FBS, 2 mM glutamine, 100 I.U./ml penicillin, 100 µg/ml streptomycin, 2.5 µg/ml amphotericin (Biochrom). AC isolated from one animal were prepared with 13 ml of DMEM and transferred into a 75 cm^2-cell culture flask. Medium was changed each third day. After reaching confluence, cells were shaken overnight in a Certomat shaker at 130 rpm (Braun-Melsungen, Germany) to remove microglia and oligodendrocytes. Next morning, medium was changed and cells were cultivated to confluence again. Cells were verified for GFAP, Isolectin *Bandereia simplicifolia* (positive for microglia) and for the oligodendrocyte-specific marker O4. If not used immediately, AC were frozen in liquid nitrogen (1 cryotube for the amount of cells harvested from 75 cm^2): cells were trypsinized (trypsin/EDTA solution, 0.25%/0.25%, Biochrom), centrifuged at 1000×g for 10 min (4K10, Sigma, Osterode, Germany). The cell pellet was dissolved in FBS (Biochrom) with 5% of DMSO and filled in cryo tubes. After 1 h at 4°C, cells were frozen for 4 h at -20°C and than placed into the gas phase of liquid nitrogen overnight. Next morning, cells were put into liquid nitrogen. For thawing the cells, cryo tubes were put into a water-containing tube (37°C). Suspension was immediately transferred to DMEM with 10% FBS and centrifuged for 10 min with 1000×g (4K10, Sigma). The supernatant was discharged and cells were plated for growth control in 75 cm^2 culture flask. If the cell density was 75% after 48 h, coculture experiments were started (Mertsch et al., 1997).

Coculture. RBE4 and astrocytes were cultivated separately on the two sides of Falcon filter inserts, coated with rat tail collagen I. AC ($6x10^4$ cells/cm^2) were seeded on filters upside down (in DMEM with 10% FBS, 2 mM glutamine, 100 I.U./ml penicillin, 100 µg/ml streptomycin, 2.5 µg/ml amphotericin B). After 3-4 h, filters were turned around into the right position. 3 days after seeding of astrocytes, RBE4 cells were seeded on the other side of the filter ($1.8x10^5$ cells/cm^2). The endothelial side of filters was prepared prior to cultivation procedures by coating with collagen (Boehringer Mannheim, collagen I, preparation as described by the

manufacturer, 1.7 µg/cm^2). After reaching confluence, medium of RBE4 cells was replaced by a medium with 5% FBS and without growth factor. Measurement of the transendothelial electrical resistance (TEER, above 250 Ω/cm^2) were performed to check that permeability studies could be started (approx. 2-3 days after confluence). TEER was measured using an ohmmeter (World Precision Instruments, Sarasota, USA) connected to special electrode sticks (Mertsch et al., 1997).

Pericytes, oligodendrocytes, microglia. Pericytes were isolated according to Frey et al. (1991) and cultivated in 84% M199 (Biochrom) with 16% FCS, 2 mM glutamine, 100 I.U./ml penicillin, 100 µg/ml streptomycin, 2.5 µg/ml amphotericin. Oligodendrocytes were isolated according to Milner (1996) and cultivated in DMEM with 10% FCS, 4 mM glutamine, 100 µg/ml bovine serum albumine (BSA), 2 mg/ml gentamycin, 400 ng/ml thyroxin, 5 ng/ml Na-selenin, 400 ng/ml 3,3',5'-triiodo-L-thyronine, 6.2 ng/ml progesteron, 16 µg/ml putriscine, 5 g/ml insulin, 50 µg/ml transferrin, 2 mg/ml $NaHCO_3$. Coculture of BEC/AC (both on filter) with another type of cell was performed in 6-well-plates with pericytes, oligodendrocytes or microglia on the bottom of the same well. Permeability studies, measurement of TEER and staining procedures were performed 48 h after the addition of one of the latter cell type.

Permeation studies. Permeation studies were performed 2-3 days after confluence of RBE4 cells, 10 min after addition of Na-fluorescein (50 µM), [^{14}C]-sucrose (0.1 µCi/2 ml PBS) and/or [^{3}H]-dichlorkynurenic acid (0.1 µCi/2 ml PBS) to the top of the filter insert. Fluorescence (λ_{exc}= 488 nm, λ_{em}= 512 nm) or radioactivity (scintillation measurement) were determined in samples from both donor and receptor chamber (Mertsch et al. 1997). During incubation, cells were kept at 37° C and 30 rpm (Certomat, Braun Melsungen, Germany). The permeability coefficient was calculated according to Dehouk et al. (1995). The clearance volume was calculated by dividing the amount of compound in the receptor chamber (lower compartment) by the concentration in the donor chamber (upper compartment). The average volume cleared was plotted versus time. The slope of the clearance curve was denoted Pt, where P is the permeability surface area product (in ml/min). The slope of the clearance curve for the control filter (only astrocytes at the filter downside) was denoted Ptc. P was calculated from 1/P=1/Pt-1/Ptc. and divided by surface area of filters: 4.2 cm^2 (Falcon-filters) to get endothelial permeability (Mertsch et al., 1997).

Cytotoxicity. The neutral red assay (Borenfreund & Puerner, 1985; Mertsch et al., 1995) was used to determine toxicity of a test substances. RBE4 ($8x10^4/cm^2$) and AC ($2x10^5/cm^2$) were seeded on 24-well plates; toxicity in coculture was studied with RBE4 growing on filters and AC growing on the bottom of the same well as described above (see coculture). After 24 h, each substance was added in different concentrations (24 h incubation, 4 wells/concentration, 4-6 plates per substance). Cells were washed with PBS, incubated with neutral red (50 µg/ml in Hams F10/α-medium with 10% FBS, 2 h at 37°C), and washed again. The dye (absorbed by viable cells only) was extracted (50% ethanol/50% a.d., 10 min shaking) and measured at λ = 540 nm using a microtiter plate reader (Cambridge Technology 7500, USA). The inhibitory concentration of a compound, reducing the viability by 50% (IC_{50} value), was calculated from the linear part of the concentration response curve.

Cytoprotection. For protection studies, 6-well plates were seeded as given for the cytotoxicity test. 72 h after seeding, cells were washed, and the test substance dissolved in PBS were added (1 ml) in non-toxic concentration. The solvents were: ethanol (0.1%, nimodipine), DMSO (0.5%, MK 801), BSA (0.05%, U83836E), ethanol (0.1%, NBQX), NN1 (PBS), desferal (PBS), SOD (PBS). Cells were scraped off after 2h of hypoxia and 30 min of reoxygenation, and lipid peroxidation was determined. For permeability studies, 1 ml of PBS was placed in the well before filters with 1 ml test substance were added. Following 30 min of hypoxia and 30 min of reoxygenation, permeability measurement was performed as described.

Hypoxia and reoxygenation. Investigations were carried out on 6-well plates in a rotating water bath (37°C; GFL, Burgwedel, Germany). For the experiments, cells were washed twice with PBS (without glucose, pH 7.1). 1 ml of the PBS was added to each of the 6 wells or filters. PBS was saturated with Nelson gas for 30 min before use (for the hypoxia group); pO_2 was 20 mm Hg before starting the experiment (Oxymeter, Oxi538, WTW, Weilheim, Germany). For permeation studies using the BBB model, plates were gassed with Nelson gas for 30 min (hypoxia) and with Carbogen during the following 30 min of reoxygenation. Each well was gassed separately. For the normoxic control, plates were kept in the incubator for 60 min. For biochemical studies, the hypoxic period was prolonged (2 h) followed by 30 min of reoxygenation (control incubation 2.5 h). For analysis of LPO, cells were scraped off in 600 µl of PBS (without Ca^{2+}/Mg^{2+}) immediately after reoxygenation and frozen in liquid nitrogen until analysis. For permeation studies, filter inserts were immediately transferred from

hypoxia equipment (and the control from incubator) to prepared 6-well plates containing 2 ml PBS. Then, 2 ml of PBS with Na-fluorescein was added to the top of the filter.

Analysis of LPO and protein content. As a product of LPO, the content of malondialdehyde (MDA) was determined. For this purpose, 400 µl of cell suspension were mixed with 0.75 ml phosphoric acid (150 mM), 0.25 ml thiobarbituric acid (42 mM) and 0.1 ml water, and boiled for 60 min. The reaction was stopped by cooling the samples in an ice bath. An equal volume of NaOH solution (4.5 ml NaOH in 45.5 ml methanol) was added immediately before analysis on a Shimadzu HPLC (LC-10A, Kyoto, Japan) equipped with a spectrofluorometric detector RF-10A and a HPLC column Supelcosil 150x4 mm LC-18-S (Supelco, Sigma-Aldrich, Deisenhofen, Germany). A 50 mM potassium phosphate buffer solution (pH 6.8) with 40% methanol was used as eluent (Mertsch et al., 1995). The standard was malondialdehyde-bis(diethylacetal). Preceding experiments were performed under control conditions (using PBS only in the absence and presence of cells, respectively) in the presence and absence of the substances to exclude interference of the compounds investigated with the MDA assay. Protein determination was performed by a Lowry Kit (P5656, Sigma, Deisenhofen, Germany).

Test for $^{\bullet}OH$-scavenger activity. Components of the test system were 10 mM DMPO, 0.05 mM $FeSO_4$, 0.1 mM H_2O_2, 14 mM HCl, 93 mM NaCl, 1.24 M pyridine. EC_{50} is defined to be the concentration of the test compound that inhibited the electron spin resonance (ESR) signal intensity of DMPO/$^{\bullet}OH$ by 50%. The tested compounds were dissolved in NaCl or pyridine according to their solubility. The reaction was started in the presence of the compounds tested by addition of ferrous ions. Percentage values of signal inhibition were determined as the mean of 3 independent concentration-response curves, the relative deviation of the mean value was ≤ 15%.

Test for $^{\bullet}O_2^-$-scavenger activity. Components of the test system were 0.4 U/ml xanthine oxidase, 13.67 mM HCl, 0.4 mM hypoxanthine, 1.24 M pyridine, 7.4 mM NaCl, 1.0 mM DETAPAC and 0.1 M DMPO. The tested compounds were dissolved either in NaCl or pyridine according to their solubility. The reaction was started in the presence of the tested compounds by addition of xanthine oxidase. The $^{\bullet}O_2^-$-scavenging activity was quantified by the decrease of ESR signal intensity (low-field line) of the DMPO superoxide adduct (DMPO/$^{\bullet}OOH$); the EC_{50} value corresponds to half-maximum inhibition of DMPO/$^{\bullet}OOH$ for-

mation. Percentage values of signal inhibition were determined as the mean of 3 independent concentration-response curves, the relative deviation of the mean value was ≤ 15%.

ESR spectroscopy. ESR experiments were performed at room temperature using a Bruker ECS 106 X-band spectrometer (Karlsruhe, Germany; equipped with a high sensitivity rectangular-mode cavity ER 4102 ST). The following standard conditions were used: modulation frequency, 100 kHz; modulation amplitude, 0.1 mT; field set, 347.5 mT; scan range, 10 mT; microwave power, 20 mW.

Statistics. If not stated otherwise, statistics were performed with Man-Whitney test using the program Sigma-Stat (Jandel Co., San Rafael, CA, USA). Toxicity tests were calculated using Hill-kinetics (4 parameters, Sigma Stat).

Results

***In vitro*-models of the blood-brain barrier.** Five different models were developed and compared regarding their applicapability as an *in vitro*-model of the BBB (characterization of paracellular tightness). Table 1 shows the permeability coefficients through the respective endothelial monolayers for different markers impermeable into the brain. The lowest permeability was achieved using the coculture model of primary porcine BEC and AC grown on opposite sides of the filter (cellular contact via filter pores); similar permeability coefficients were found for fluorescein, sucrose and dichlorkynurenic acid. The TEER of this model was 358±39 Ωcm^2. Nearly the same tightness was obtained by using subcultivated porcine BEC or immortalized rat BEC clone (RBE4), when cultivated with AC on the same filter. The TEER was determined to be 416±27 Ωcm^2 for the model with RBE4 and AC, grown on the two sides of the filter. Lower tightness/higher permeability were observed in filter-cultivated monolayers of RBE4 or porcine BEC, when AC were cultivated on the bottom of the same well. However, these cocultures showed lower paracellular permeability as compared to the respective monocultures.

Table 1: Permeability coefficients (P) for sodium fluorescein, [^{14}C]sucrose and [^{3}H]dichlorkynurenic acid (DKA) for different *in vitro* models of the blood-brain-barrier.

model	P (x10^{-4} cm/min) Na-fluorescein	P (x10^{-4} cm/min) [^{14}C]sucrose	P (x10^{-4} cm/min) [^{3}H]DKA	reference
PBEC/AC-filter	4.2±0.4	6.2±0.9	2.3±0.3	Giese et al., 1995
BBEC/AC-well		7.5	3.7(inulin)	Dehouk et al., 1995
BBEC		19.0	9.8	Dehouk et al., 1995
RBE4/AC-filter	6.60±0.85 n=8	4.58±0.66 n=7	6.65±0.90 n=7	
RBE4/AC-well	13.14±0.86 n=16	14.53±1.06 n=5	13.65±0.56 n=5	
BEC/AC-filter	9.20±1.65 n=3	8.70±0.95 n=3	5.40±1.50 n=3	
BEC/AC-well	7.30±1.79 n=3	19.0±1.05 n=3	9.70±0.25 n=3	

PBEC, porcine primary brain endothelial cells; AC, astrocytes; BBEC, bovine brain endothelial cells; RBE4, immortalized rat brain endothelial cells; BEC, subcultivated porcine brain endothelial cells in 10th passage; AC-filter, astrocytes cultivated on the filter; AC-well, astrocytes cultivated on the bottom of the 6-well-plate. Mean±SEM.

RBE4 and subcultivated porcine BEC (data not shown) expressed Factor VIII, γGT and ALP to a lower degree as found in primary rat or porcine BEC. There was a higher expression of ALP and γGT in BEC (10th passage) as compared to RBE4 (45th-50th passage). Cocultivation of RBE4 and AC on the two sides of a filter (cellular contact) led to a significant increase in ALP and γGT compared to the coculture with AC on the bottom of the same well (no cellular contact). In parallel, a decrease was observed in the permeability by approx. 100%. The effect of other cell types grown on the bottom of the same well was also investigated in the coculture using filters with cellular contact. There was an enhancement of the expression of ALP and γGT by pericytes, microglia and in partivular by oligodendrocytes under these conditions. However, neither the permeability nor the TEER changed considerably (Table 2, data regarding TEER not shown).

Table 2: Comparison of different *in vitro* BBB models.

Model	Permeability	γ-Glutamyl-transpeptidase	Factor VIII	Alkaline Phosphatase
RBE4 solo	288%	+	++	+
RBE4/ AC-filter	100%	++↑	++	++↑
RBE4/ AC-well	199%	++↑	++	++↑
RBE4/AC-filter+oligo (AM)	100%	+++↑	++	++↑
RBE4/AC-filter+oligo (OM)	100%	++++↑↑	++	++↑
RBE4/AC-filter+PC	100%	+++↑	++	++↑
RBE4/AC-filter+MG	100%	+++↑	++	++↑

RBE4/AC-well, astrocytes growing on 6-well; RBE4/AC-filter, astrocytes growing on filter upside down; RBE4/AC-filter+oligo (AM), astrocytes growing on filter, oligodendrocytes growing on well with astrocyte medium; RBE4/AC-filter+oligo (OM), astrocytes growing on filter, oligodendrocytes growing on well with oligodendrocyte medium; RBE4/AC-filter+PC, astrocytes growing on filter, pericytes growing on well with astrocyte medium; RBE4/AC-filter+MG, astrocytes growing on filter, microglia growing on well with astrocyte medium.
↑ increase due to coculture

Cocultivation with AC also enhanced the activity of ALP (Fig. 1a) and of γGT (Fig. 1b) in RBE4 and in subcultivated porcine BEC.

Cytotoxicity. Table 3 presents data on the toxicity of standard substances (frequently applied for studies of cytotoxicity and neuroprotection) in monocultures of RBE4 and AC, respectively, and in cocultures of both. The highest IC_{50}-value was found for ethanol (submolar range) whereas U83836E showed the lowest value (submillimolar range). Monocultures of the cells seemed to be more vulnerable than cocultures both of RBE4 and AC, as demonstrated using MK 801.

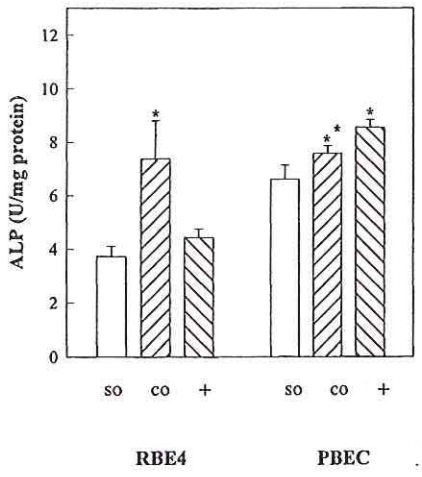

Fig. 1a: Content of alkaline phosphatase in porcine brain endothelial cells (10th passage) and RBE4 in mono- (so) and coculture with astrocytes, growing at the other side of the filter (co) and at the bottom of the 6-well-plate (+). n=6, mean ± SEM, * significantly different as compared to monocultures ($p<0.05$).

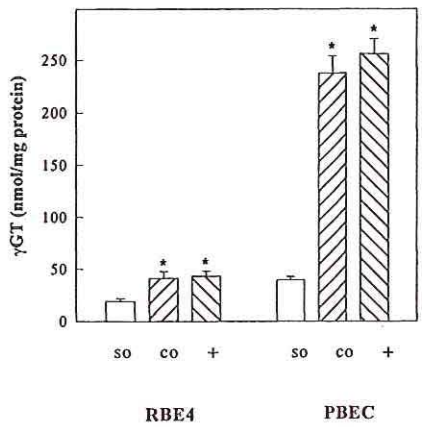

Fig.1b: Content of γ-glutamyltranspeptidase in porcine brain endothelial cells (10th passage) and RBE4 in mono (so) and coculture with astrocytes, growing at the other side of the filter (co) and at the bottom of the 6-well-plate (+). n=6, mean ± SEM, * significantly different as compared to monocultures ($p<0.05$).

Radical scavenger activity. As shown in Table 4, there were strong differences in the ability of the compounds tested to act as radical scavengers. The highest potential for inhibition of the formation of DMPO/˙OH was found for U83836E (approx. 3 orders of magnitude more effective as compared to mannitol). Other compounds did not exert any radical scavenger activity (tetrodotoxin, Ca^{2+} antagonists) or the EC_{50}-value was within the cytotoxic concentration range of the respective compound (NBQX, MK 801). Only nisoldipin was found to exert a low inhibitory activity on the formation of DMPO/˙OOH.

Table 3: Cytotoxicity of toxicological standards and neuroprotective agents in mono- and cocultures of brain endothelial cells (RBE4) and astrocytes (AC)

substance	monoculture		coculture		
	IC_{50} (mM)		Concentration tested (mM)	Cytotoxicity relative to monoculture (%)	
	RBE4	AC		RBE4	AC
Standards					
Ethanol	366±186	629±25	600	14%	10%
Acetylsalicylic acid	9.51±1.44	24.0±0.6	10	41%	26%
4-Acetamidophenol	5.49±1.57	2.44±0.45			
Amitryptilin	0.047±0.002	0.043±0.01			
Neuroprotective agents					
U83836E	0.032±0.001	0.050	0.03	69%	31%
Nimodipin	>0.200	>0.200			
MK 801	0.469±0.015	0.418±0.007	0.4	4%	44%
NBQX	0.350	0.350			

Mean±SEM.

Cellular injury after hypoxia/reoxygenation. After 2 h of hypoxia followed by 30 min of reoxygenation, the cellular content of MDA (indicating radical-induced lipid peroxidation and lipid membrane injury) increased in RBE4 cells from 0.76±0.02 nmol/mg protein (normoxic control) to 2.60±0.04 nmol/mg protein, in AC from 1.24±0.04 nmol/mg protein to 1.70±0.08 nmol/mg protein. RBE4 were more sensitive than AC, exhibiting, in contrast to AC, accumulation of MDA already upon hypoxia (Fig. 2). The permeability coefficient for fluorescein increased four- to five-fold already after 30 min hypoxia and 30 min reoxygenation when compared to the control cells kept in incubator (Fig. 3).

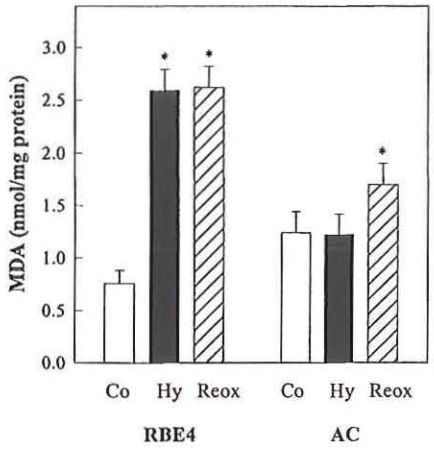

Fig. 2: Effect of the lazaroid U83836E on lipid peroxidation in RBE4 and astrocytes following hypoxia (95% N_2/ 5% CO_2, 2h) and reoxygenation (95%O_2/5%CO_2, 30 min). Mean ± SEM, n=6. Reoxygenation is significantly different as compared to control ($p<0.05$), * statistically significant as compared to reoxygenation ($p<0.05$).

Cytoprotective effects of neuroprotective agents and radical scavengers. Fig. 3 presents data on protective effects of test substances with different modes of action on the permeability of the BBB model after a short-time hypoxia (30 min) and reoxygenation (30 min). U83836E significantly prevented the increase of permeability after reoxygenation in the model using RBE4 cocultivated with AC on the two sides of the filter as compared to untreated cocultures after reoxygenation. Protective effects were also found for SOD, the iron chelator desferal and the nitronyl nitroxide NN1. MK 801, nimodipine and NBQX did not protect against the permeability increase following hypoxia/reoxygenation. Moreover, there was an inhibition of the posthypoxic increase in the MDA content of RBE4 in the presence of U83836E (Fig. 4).

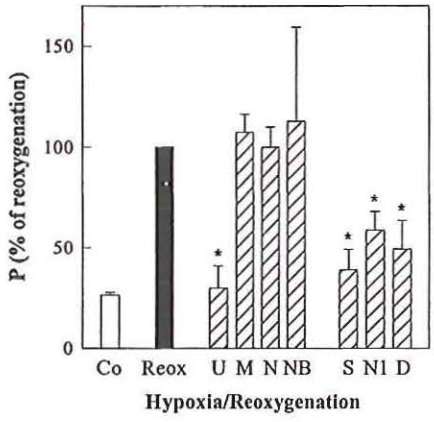

Fig. 3: Effects of neuroprotective agents and radical scavengers on permeability changes in the RBE4/AC coculture model due to hypoxia (95%N_2/5%CO_2, 30 min) and reoxygenation (95%O_2/ 5%CO_2, 30 min). Mean ± SEM, n=3-6. Reoxygenation is significantly different as compared to control, $p<0.01$, * significantly different as compared to reoxygenation, $p<0.05$.

Test substances: U, U83836E (1 µM); M, MK801 (10 µM); N, nimodipine (10 µM); S, superoxide dismutase (50 U/ml); D, desferal (0.8 mM); NB, NBQX (10 µM); N1, 4,4,5,5-tetramethyl-2-(4-trimethylammoniophenyl)-2-imidazoline-1-oxyl methyl sulfate (10 µM).

Discussion

In stroke, the BBB is opened within the first hours after the onset of the injury. The damage in the core of the infarcted region is often irreversible already after the first hour. However, in the penumbra a potential protection seems to be possible, and the cells of this region may respond to pharmacological treatment. It is an important aspect of ischemic processes in the brain that ischemic intervals may result in severe deteriorations of neuronal function many hours after the begin of the disturbances. Therefore, the development of protective strategies for the BBB may help to improve the treatment of stroke. To model the ischemic BBB without cerebral or vascular influences for pharmacological investigations, a suitable cell culture system is necessary.

Table 4: Radical scavenger activity of standard antioxidants and neuroprotective agents

Compound	Antioxidative activity towards $\bullet O_2^-$	Antioxidative activity towards •OH
	EC_{50} (µM)	EC_{50} (µM)
superoxide dismutase	0.008	not determined
$MnCl_2$	1	not determined
troxerutin	300	not determined
NN 1	22[§]	not determined
mannitol	not determined	1300
α-tocopherol	not determined	1650
U-83836E	not detectable[*]	5.0
MK 801	—	4000
Nimodipin	not detectable	not detectable
Nisoldipin	200	not detectable[**]
NBQX	—	55
Tetrodotoxin	not determined	not detectable[***]
Cysteine	460	9.7

Radical scavenger activity was „not detectable" when precipitation of the compound from the solvent mixture prevented measurement at higher concentrations.
[*] small activity at concentrations ≥ 500 µM, [**] small activity at concentrations ≥ 5 mM, [***]no activity up to 5 µM, [§] value recalculated from data given by Haseloff et al., 1997

BBB models. The present study compares the tightness of different *in vitro* models of the BBB. Permeability coefficients of standard substances, frequently used in BBB studies and impermeable to the brain, are comparable to the results of Dehouk et al. (1995) investigating models with BEC on the filter and AC on the bottom of the same well. The lowest permeability is achieved when BEC and AC are cocultivated separately on the opposite sides of a filter. Primary BEC seem to be superior concerning the tightness compared to subcultivated and immortalized cells, respectively. However, isolation of primary cells is time consuming and results in cells with low proliferation rates. It is known that BEC (and even primary cultivated cells) undergo dedifferentiation in culture (Pardridge et al., 1990). Cocultivation with AC may reduce this dedifferentiation and may prevent the loss of a variety of proteins and receptors specific for the BBB (DeBault and Cancilla, 1980; Joo, 1992; Dehouk et al., 1990). Therefore, the best compromise for modeling the BBB is the use of BEC lines in coculture with AC allowing cellular contacts through the filter. If necessary, for instance for certain biochemical studies and to exclude cell contacts, coculture of AC at the bottom of the same well also results in sufficiently tight monolayers of BEC.

Porcine BEC (10th passage) can easily be cultivated in large amount. They express markers specific for the endothelium of the brain, being more pronounced compared to those of RBE4. However, the properties of the porcine cells are not stable during further passages. RBE4 are more susceptible to changes of cultivation conditions (media, serum, coating). The low permeability coefficients for the coculture with AC is maintained for a limited time (1-2 days). RBE4 cells are immortalized cells with a higher proliferation rate as compared to the porcine cell line. An advantage of RBE4 is the stable cultivation virtually without limitation: the markers ALP, γGT and Factor VIII are present at least up to the 58th passage, although to a lower degree than in the 43th-50th passage used here for the experiments. Primary BEC and the subcultures have to be characterized for each preparation and subcultivation, respectively. In conclusion, a stable cell line or cell clone, such as the RBE4, with a sufficient degree of differentiation and good proliferation properties are recommended to be used as a cell culture model of BBB.

A 3-cell system has been established to study the influence of specific cell types occurring in the surrounding of the BBB *in vivo*. For that purpose, pericytes, microglia or oligodendrocytes were cultured at the bottom of the well containing the filter membrane carrying BEC/AC.

This system is very difficult to maintain. Pericytes, oligodendrocytes and microglia have to be used as primary cells. However, their isolation is very time consuming and their growth characteristics are different from those of BEC and AC. Therefore, it is not possible to establish this 3-cell coculture permanently, because it is very difficult to handle the time schedules of the different culture in a reproducible manner. Permeability and TEER are not changed in any of the 3-cell models. However, the expression of ALP and of γGT is improved in the BEC. The latter, localized at the luminal and abluminal part of the cell membrane, is assumed to be of relevance for the transport function from blood to brain (Frey et al. 1991; Dehouk et al. 1997).

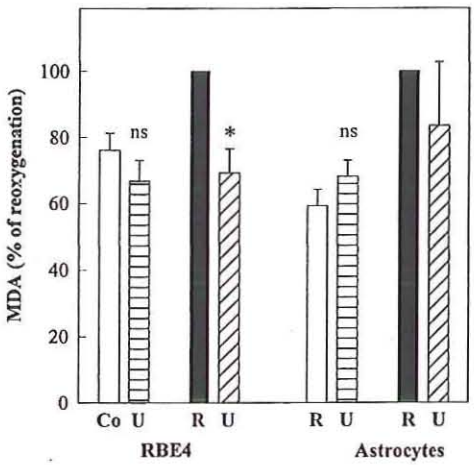

Fig. 4: Lipid peroxidation in RBE4 and AC after hypoxia (95%N_2/5%CO_2, 2h) and reoxygenation (95%O_2/5%CO_2, 30 min). Co, control (normoxia); U, addition of 10 μM U83836E; R, hypoxia/reoxygenation. Mean ± SEM, n=5. * significantly different as compared to control, $p<0.05$.

Hypoxia and reoxygenation injury. BEC are highly susceptible to acute oxidative injury (Grammas et al., 1993; Mertsch et al., 1995). Hypoxia and reoxygenation result in opening of the different coculture (AC) models of the BBB. This is consistent with earlier reports (Giese et al., 1995). During hypoxia and reoxygenation, BEC and AC as well may release high amounts of H_2O_2 (Kondo et al., 1996) and superoxide (Terada, 1996) which is disproportionated to H_2O_2 by SOD. By this means, SOD decreases radical-mediated processes, however, a sufficient catalase activity is essential (Zöllner et al., 1997) since H_2O_2 seems to be an important mediator of oxidative injury (Horwitz et al., 1996). Adhesion of circulating neutrophils to endothelial cells as a result of pathological processes, such as ischemia and reperfusion, can amplify oxidative stress via additional formation of H_2O_2, hydroxyl radicals and superoxide (Siflinger-Birnboim et al., 1993; von Asmuth et al., 1995).

Transient changes in the organization of the cytoskeleton caused by ROS were observed in endothelial cells and led to angiogenic response, reduction of permeability and formation of intracellular gaps (Hastie et al., 1997; Crawford et al., 1996).

The RBE4/AC model with cells cultivated on the two sides of a filter has been used for reoxygenation experiments. The content of MDA is increased in both RBE4 and AC, indicating lipid peroxidation and membrane damage (Mertsch et al., 1995). These processes are initiated by free radicals generated during hypoxia/reoxygenation of RBE4 cells (Mertsch et al., 1997). The susceptibility of BEC to reoxygenation-mediated injury is greater as compared to AC, probably due to a more potent endogenous radical defence of AC. The permeability coefficient increases after short-time hypoxia and reoxygenation about five-fold. These alterations and the changes in the content of MDA enable experiments to investigate substances thought to be protective against injury caused by hypoxic conditions.

Test for radical scavenger activity and cytotoxicity. For estimation of the non-toxic concentration range of a compound to be tested in cytoprotection studies, it is necessary to determine its cytotoxicity. The results demonstrate that BCE should be used for this purpose, which generally seem to be more vulnerable against unspecifically acting agents. However, substances specifically influencing receptors of AC, such as AMPA receptors (i.e. NBQX) should be tested in this cell type, too. In general, cytotoxicity tests are not necessary in coculture because the sensitivity is decreased under cocultivation conditions. It has been shown that concentrations of an agent below 10% of its IC_{50}-value estimated in the toxicity test can be used for cytoprotection studies. As ROS play a pathogenic role in oxidative stress the radical scavenger activity of an agent can be of additional therapeutic benefit and should be tested. For this purpose, an ESR spin trapping test has been developed.

Test for cytoprotection. $^{\cdot}O_2^-$ was shown to be an important factor increasing the paracellular permeability in a monolayer of BCE, suggesting oxidant-dependent mechanisms of barrier injury (Shukla et al., 1993). H_2O_2 exerted noxious effects on cells and cellular matrices and caused LPO, DNA strand breaks and protein oxidation (Floyd, 1990). In the present study, SOD very effectively protected the *in vitro* BBB from barrier opening due to hypoxia/ reoxygenation-induced injury. Protective effects of SOD following hypoxia were found *in vivo* (Ercan et al., 1992), for hippocampal slice cultures (Horakova et al., 1997) and *in vitro* in

peripheral endothelial cells (Palluy et al., 1991) and neurons (Kinoshita et al., 1991). After hypoxia and reoxygenation, the activated arachidonic acid cascade and the Ca^{2+}-induced conversion of xanthine dehydrogenase to xanthine oxidase may produce increasing amounts of superoxide (Betz et al., 1993). In general, ROS may open BBB and radical scavenger may effectively prevent breakdown of BBB due to hypoxia/reoxygenation.

The pool of cytotoxic ferrous ions was reported to be increased during postischemic reperfusion injury *in vivo* (Voogd et al., 1992) enabling occurrence of the Fenton reaction. Subsequent radical reactions are involved in oxidative protein damage (Caraceni et al., 1997). Thus, chelating agents may react in a protective manner. Indeed, the permeability increase is reduced by the chelator desferal during hypoxia/reoxygenation, supporting the involvement of Fe^{2+} in the hypoxia-injured BBB. The protective effects of desferal and SOD against oxidative stress are in good agreement with previous results in hepatocytes (Lefebvre et al., 1995) and human umbilicial endothelial cells (Shatos et al., 1990).

The nitronyl nitroxide NN1 protects both viability (preliminary experiments, data not shown) and tightness of BEC during hypoxia/reoxygenation. NN1, originally designed as NO scavenger, effectively reacts with $^{\cdot}O_2^-$ (Haseloff et al., 1997). It is concluded that the protective effects of NN1 observed here are due to a SOD-mimetic activity of this compound.

The highest protective activity is found for U83836E, a compound containing a chromanol ring similar to α-tocopherol (Hall, 1994). The antioxidative activity of this lazaroid was confirmed by high radical scavenging activity as detected by ESR spectroscopy, reduction of LPO both in BEC and AC during hypoxia/reoxygenation, and reduced reoxygenation-induced permeability increase of the RBE4/AC model. The enantiomer of U83836E, the derivative U78517F exerting a similar radical scavenger activity, is also protective *in vivo* with respect to LPO, edema formation and protection on BBB after cerebral ischemia (Hall et al., 1991; McIntosh et al., 1992). This underlines that, rather than specific receptor-mediated mechanisms, the inhibition of radical-induced processes is responsible for the cerebroprotective action of U83836E (Hall et al., 1991).

Oxidative stress enhances Ca^{2+} influx into the cell, further disturbing cell function (Doan et al., 1994). High intracellular Ca^{2+} concentrations severly disturb Ca^{2+}-regulated processes and

may lead to cell death (Disterhoft et al., 1993). The protectivity of the Ca^{2+} channel antagonist nimodipine was shown in neurons following depolarization (Baer et al., 1993), kainate toxicity (Gepdiremen et al., 1997) and *in vivo* during ischemia (Lemons et al., 1993; Ichihara et al., 1996). However, there are contradictory results *in vivo* (Calle et al., 1993). In the present study, protective effects were not found for the Ca^{2+} antagonist nimodipine at the *in vitro* BBB. This result could be explained by reports in the literature indicating that there are effects exerted by nimodipine which are different from its influence on Ca^{2+} homoeostasis (Lemons et al., 1993, Danks et al., 1992).

The NMDA receptor antagonist MK 801 was reported to diminish hypoxia-induced dysfunction of neurons in hyppocampal slices (Domenici et al., 1993; Barth et al., 1996) and *in vivo* (De Riu et al., 1995; Katoh et al., 1997). This effect is attributed to a reaction at the glycine-site of the NMDA receptor which is excessively stimulated by hypoxia (Priestley et al., 1990). Moreover, blockade of the l-type Ca^{2+} is discussed to protect neurons in hippocampal slices because AMPA and kainate-induced neuronal toxicity has been prevented without any action at the NMDA receptor (Schurr et al., 1995). In the present study, MK 801 does not exert any protective effects at the *in vitro* BBB based on immortalized BEC. Protection was found by MK 801 against the hypoxia/reoxygenation-mediated increase of permeability (Giese et al., 1995) using a coculture model of primary porcine BEC and AC. This contradiction may result from the loss of NMDA receptors in RBE4, which can be found in primary BEC (Koenig et al., 1992). On the other hand, BEC injured by hypoxia are protected by MK 801 neither concerning viability, LDH release nor energy loss (Gobbel et al., 1994). This agrees with additional experiments which did not show any reduction of LPO caused by hypoxia/reoxygenation in the presence of MK 801 using different BEC.

For NBQX, no protection of tightness is found in the BBB model. NBQX is an AMPA receptor antagonist providing protection to neurons (Lippert et al., 1994). However, this compound also failed to protect BEC from hypoxia-induced injury in other studies (Gobbel et al., 1994).

In summary, results presented suggest a participation of ROS in opening of the BBB due to oxidative stress. The breakdown of the barrier after hypoxia/reoxygenation is reduced very effectively by the radical-scavenging lazaroid U83836E, the SOD-mimetic nitronyl nitroxide

NN1, the iron chelator desferal and by SOD itself indicating therapeutic applications of antioxidants to maintain the integrity of the BBB during cerebral ischemia. SOD and desferal have been shown for the first time to protect the BBB *in vitro* from radical-induced opening. Both nitroxides and lazaroids are new approaches to protect BBB from permeability disturbances induced by ROS. In conclusion, the test system developed in this study allows to select new protective agents preventing functional and biochemical disturbances of the BBB against ischemic injury under special consideration of ROS. Moreover, the models of the BBB introduced here provide the possibility to study the permeability of low-molecular weight compounds found to be active in neuropharmacological investigations.

Acknowledgement. This work was supported by BMBF BEO003115A/B. The authors would like to thank H. Kettenmann and S. Lyons for providing oligodendrocyte and microglia cultures.

References

Arroyo C. M., Carmichael C.J., Bouscarel B., Liang J.H. and Weglicki W.B. Endothelial cells as a source of oxygen-free radicals. An ESR-study. Free Rad Res Commun: 9: 287-296, 1990.

Audus K.L., Guillot F.L. and Braughler J.M. Evidence for 21-aminosteroid association with the hydrophobic domains of brain microvessel endothelial cells. Free Rad. Biol. Med. 11: 361-371, 1991.

Barth A., Barth L., Newell D.W. Combination therapy with MK 801 and alpha-phenyl-tert-butyl-nitrone enhances protection against ischemic neuronal damage in organotypic hippocampal slice cultures. Exp. Neurol. 141: 330-336, 1996.

Baer P.R., Renkema G.H., Veraart C.M., Hol E. M., Gispen W.H. Nimodipine protects cultured spinal cord neurons from depolarization-induced inhibition of neurite outgrowth. Cell

Calcium 14: 293-9, 1993.

Betz A.L. Oxygen free radicals and the brain microvasculature. The blood-brain barrier. Ed. W.M. Pardridge. Raven Press, Ltd. New York, p.302-320, 1993.

Borenfreund E. and Puerner J.A. Toxicity determined *in vitro* by morphological alterations and neutral red absorption. Toxicol. Lett. 24: 119-124, 1985.

Booher J. and Sensenbrenner M. Growth and cultivation of dissociated neurons and glial cells from embryonic chick, rat and human brain in flask cultures. Neurobiology 2: 97-105, 1972.

Calle P.A., Paridaens K., DeRidder L.I., Buylaert W.A. Failure of nimodipine to prevent brain damage in global brain ischemia model in the rat. Resuscitation 25: 59-71, 1993.

Caraceni P., DeMaria N., Ryu H.S., Colantoni A., Roberts L., Maidt M.L., Pye Q., Bernardi M., Van Thiel D.H., Floyd R.A. Proteins but not nucleic acids are molecular targets for the free radical attack during reoxygenation of rat hepatocytes. Free Rad. Biol. Med. 23: 339-344, 1997.

Crawford L.E., Milliken E.E., Irani K., Zweier J., Becker L.C., Johnson T.M., Eissa N.T., Crystal R.G., Finkel T., Goldtschmidt-Clermont P. Superoxide-mediated actin response in post-hypoxic endothelial cells. J. Biol. Chem. 271/13: 26863-26867, 1996.

DeBault LE and Cancilla PA. Gamma-glutamyl transpeptidase in isolated brain endothelial cells: induction by glial cells *in vitro*. Science; 207: 653-655, 1980.

Danks A.M., Hammond D.N., Wainer B.H., VanBuskirk R.G., Isaacson R.L. Cellular alterations produced by the experimental increase in intracellular calcium and the nature of protective effects from pretreatment with nimodipine. Brain Res. Mol. Brain Res. 16: 168-172, 1992.

Dehouk M.-P., Meresse S., Delorme P., Fruchart J.-C. and Cecchelli R. An easier, reproducible and mass-production method to study the blood-brain barrier *in vitro*. J. Neurochem. 54: 1798-1801,1990.

Dehouk M.-P., Dehouk B., Schluep C., Lemaire M. and Cecchelli R. Drug transport to the brain: comparison between *in vitro* and *in vivo* models of the blood-brain barrier. Eur. J. Pharm. Sci. 3: 357-365, 1995.

Dehouk M.P., Vigne P., Torpier G., Breittmayer J.P., Cecchelli R., Frelin C. Endothelin-1 as a mediator of endothelial cell-pericyte interactions in bovine brain capillaries. J. Cer. Blood Flow and Metab. 17: 464-9, 1997.

DeRiu P.L., Demontis M.P., Anania V., Caria M.A., Mameli O., Becchiu A., Tolu E. Brain electrobiogenesis protection induced by nimodipine and MK 801 during acute hypoxia in hypertensive rats. Pharmacol. Res. 31: 169-173, 1995.

Disterhoft J.F., Moyer J.R., Thompson L.T., Kowalska M. Functional aspects of calcium-channel modulation. Clin. Neuropharm. 16/1: S12-24, 1993.

Doan T.N., Gentry D.L., Taylor A.A. and Elliott S.J. Hydrogen peroxide activates agonist-sensitive Ca^{2+}-flux pathways in canine venous endothelial cells. Biochem. J. 297: 209-215, 1994.

Domenici M.R., Longo R., Carolis A.S., Frank C., Sagratella S. Protective actions of 21-aminosteroid and MK 801 on hypoxia-induced electrophysiological changes in rat hippocampal slices. Eur. J. Pharmacol. 233: 291-3, 1993.

Ecran Z.S., Ilhan M., Oguz H., Turker R.H. Superoxide dismutase and allopurinol prevent the pressor effects of angiotensin II and histamine in the guinea pig isolated perfused lung exposed to hypoxia. Gen. Pharmacol. 23/6: 1149-1151, 1992.

Evans P.H. Free radicals in brain metabolism and pathology. Brit. med. Bull. 49: 577-587, 1993.

Frey A., Meckelein B., Weiler-Güttler H., Möckel., Flach R., Gassen H.G. Pericytes of the brain microvasculature express gamma-glutamyltranspeptidase. Eur. J. Pharm. 202: 421-9, 1991.

Floyd R.A. Role of oxygen free radicals in carcinogenesis and brain ischemia. FASEB J. 4: 2587-2597, 1990.

Gepdiremen A., Sonmez S., Batat I., Esrefoglu M., Duzenli S., Suleyman H. Nimodipine improves kainic acid induced neurotoxicity in cerebellar granular cell culture: a double-blind dose-response study. Fundam. Clin. Pharmacol. 11: 117-120, 1997.

Giese H., Mertsch K. and Blasig I.E.: Effect of MK 801 and U83836E on a porcine brain capillary endothelial cell barrier during hypoxia. Neurosci. Lett. 191: 169-172, 1995.

Gobbel G.T., Chan T.Y., Gregory G.A., Chan P.A. Response of cerebral endothelial cells to hypoxia: modification by fructose-1,6-biphosphate but not glutamate receptor antagonists. Brain Res. 653: 23-30, 1994.

Grammas P., Liu G.-J., Wood K. and Floyd R.A. Anoxia/reoxygenation induces hydroxyl free radical formation in brain microvessels. Free Rad. Biol. Med. 14: 553-557, 1993.

Hall E.D., Braughler J.M., Yonkers P.A., Smith S.L., Linseman K.L., Means E.D., Scherch H.M., Von Voigtlaender P.F., Lahti R.A. and Jacobsen E.J. U78517F: a potent inhibitor of lipid peroxidation with activity in brain injury and ischemia. J Pharm. Exp. Therap. 258: 688-694, 1991.

Hall E.D.: Generation and detection of hydroxyl radical following experimental head injury. In: Annals of the New York Academy of Sciences Vol 738. Eds. Chiueh CC, Gilbert DL and Colton CA, p.15-24, 1994.

Hastie L.E., Patton W.F., Hechtman H.B. and Shepro D. Filamin redistribution in an endothelial cell reoxygenation injury model. Free Rad. Biol. Med. 22/6: 955-966, 1997.

Haseloff R.F., Zoellner S., Kiriljuk I.A., Grigor'ev I.A., Reszka R., Bernhardt R., Mertsch K., Roloff B. and Blasig I.E. Superoxide-mediated reduction of the nitroxide group can prevent detection of nitric oxide by nitronyl nitroxides. Free Rad. Res. 26: 7-17, 1997.

Horakova L., Stolc S., Chromikova Z., Pekarova A., Derkova L. Mechanisms of hyppocampal reoxygenation injury. Treatment with antioxidants. Neuropharmacology 36/2: 177-184, 1997.

Horwitz L.D., Wallner J.S., Decker D.E. and Buxser S.E. Efficacy of lipid soluble, membrane-protective agents against hydrogen peroxide cytotoxicity in cardiac myocytes. Free Rad. Biol. Med. 21: 743-753, 1996.

Ichihara S., Tsuda Y., Hosomi N., Kitadai M., Matsou H. Nimodipine improves energy metabolism and blood rheology during ischemia and reperfusion in the gerbil brain. J. Neurol. Sci. 144: 84-90, 1996.

Joo F. The cerebral microvessels in culture: an update. J Neurochem 1992; 58: 1-17.

Katoh H. Sima K., Nawashiro H., Wada K., Chigasaki H. The effect of MK 801 on extracellular neuroactive amino acids in hippocampus after closed head injury followed by hypoxia in rats. Brain Res. 758: 153-62, 1997.

Kinoshita A., Yamada K., Kohmura E., Hayakawa T. Human recombinant superoxide dismutase protects primary cultured neurons against hypoxic injury. Pathobiology 59/5: 340-344, 1991.

Koenig H., Trout J.J., Goldstone A.D., Lu C.Y. Capillary NMDA-receptors regulate blood-brain barrier function and breakdown. Brain Res. 588: 297-303, 1992.

Kondo T., Kinouchi H., Kawase M. and Yoshimoto T. Differential response in the release of hydrogen peroxide between astroglial cells and endothelial cells following hypoxia/reoxygenation. Neuroscience Lett. 215: 103-106, 1996.

Lefebvre V., Buc-Calderon P. Desferal prevents against cell lysis induced by hydrogen peroxide to hypoxic hepatocytes: a role for free iron in hypoxia-mediated cell injury. Chem. Biol. Interact. 94: 37-48, 1995.

Lemons V., Chehrazi B.B., Kauten R., Hein L., Wagner F.C. The effect of nimodipine on high energy phosphates and intracellular pH during cerebral ischemia. J. Neurotrauma 10: 73-81, 1993.

Lippert K., Welsch M., Krieglstein J. Over-additive protective effect of dizocilpine and NBQX against neuronal damage. Eur. J. Pharm. 253: 207-213, 1994.

McIntosh T.K., Thomas M., Smith B. and Banbury M. The novel 21-aminosteroid U74006F attenuates cerebral edema and improves survival after brain injury in the rat. J. Neurotrauma 9: 33-46, 1992.

Mertsch K., Grune T., Siems W.G., Ladhoff A., Saupe N. and Blasig I.E. Hypoxia and reoxygenation of brain endothelial cells *in vitro*: a comparison of biochemical and morphological response. Cell. Mol. Biol. 41: 243-253, 1995.

Mertsch K., Haseloff, R.F. and Blasig, I.E. Investigation of radical scavengers using an *in vitro* model of blood- brain barrier. In: L.F.M. van Zutphen, M. Balls (Eds.), Dev. in Animal and Vet. Sci., Elsevier, Netherlands, 27: 881-887, 1997.

Milner R., Edwards G., Streuli C., French-Constant C. A role for alpha V beta 1 integrin expressed on oligodendrocyte precursors. J. Neurosci. 16: 7240-52, 1996.

Palluy O., Bonne C., Modat G. Hypoxia/reoxygenation alters endothelial prostacyclin synthesis-protection by superoxide dismutase. Free Rad. Biol. Med. 11/3: 269-275, 1991.

Pardridge WM, Triguero D, Yang J and Cancilla PA. Comparison of *in vitro* and *in vivo* models of drug transcytosis through the blood-brain barrier. J Pharm Exp Ther 253: 884-891, 1990.

Plateel M., Dehouk M.-P., Torpier G., Cecchelli R. and Teissier E. Hypoxia increases the susceptibility to oxidative stress and the permeability of the blood-brain barrier endothelial cell monolayer. J. of Neurochem. 65: 2138-2145, 1995.

Priestley T., Horne A.L., McKernan R.M., Kemp J.A. The effect of NMDA receptor glycine site antagonists on hypoxia-induced neurodegeneration of rat cortical cell cultures. Brain Res. 531: 183-8, 1990.

Roux F., Durieu-Trautmann O., Chaverot N., Claire M., Mailly P., Bourre I.-M., Strosberg A.D. and Couraud P.-O. Regulation of gamma-glutamyltranspeptidase and alkaline phosphatase activities in immortalized brain microvessel endothelial cells. J. Cell. Phys. 159: 101-113, 1994.

Shatos M.A., Doherty J.M., Stump D.C., Thomson D.H., Collen D. Oxygen radicals generated during anoxia followed by reoxygenation reduce the synthesis of tissue-type plasminogen activator and plasminogen activator-inhibitor-1 in human endothelial cells. J. Biol. Chem. 265: 20443-8, 1990.

Shukla A., Shukla R., Dikshit, M. and Skrimal R.C. Alterations in free radical scavenging mechanisms following blood-brain barrier disruption. Free Rad. Biol. Med. 15: 97-100, 1993.

Schurr A., Payne R.S., Rigor B.M. Protection by MK 801 against hypoxia-, excitotoxin-, and depolarization-induced neuronal damage *in vitro*. Neurochem. Int. 26: 519-525, 1995.

Siflinger-Birnboim A., Goligorski S.M., DelVecchio P.J. and Malik A.B. Activation of protein kinase C pathway contributes to hydrogen peroxide-induced increase in endothelial permeability. Lab. Invest. 67: 24-30, 1992.

Terada L.S. Hypoxia-reoxygenation increases O^{2-} efflux which injures endothelial cells by an extracellular mechanism. Am. J. Physiol. 270: H945-H950, 1996.

VonAsmuth E.J. and Buurman W.A. Endothelial cell associated platelet-activating factor (PAF), a costimulatory intermediate in TNF-alpha-induced H_2O_2 release by adherent neutrophil leucocytes. J. Immunol. 154: 1383-1390, 1995.

Voogd A., Sluiter W., vanEick H.G., Koster J.F. Low molecular weight iron and oxygen paradox in isolated rat hearts. J. Clin. Invest. 90: 2050-5, 1992.

Zöllner S., Haseloff R.F., Kirilyuk I.A., Blasig I.E., Rubanyi G.M. Nitroxides increase the detectable amount of nitric oxide released from endothelial cells. J. Biol. Chem. 272: 23076-23080, 1997.

Zweier J.L., Broderick R., Kuppusamy P., Thompson-Gorman S. and Lutty G.A. Determination of the mechanism of free radical generation in human aortic endothelial cells exposed to anoxia and reoxygenation. J. Biol. Chem. 269: 24156-24162, 1994.

RAT GLIA VULNERABILITY TO COMBINED HYPOXIA and HYPOGLYCEMIA INJURY *IN VITRO* and Selective Responses to Neuroprotective Agents.

Susan A. Lyons and Helmut Kettenmann

Department of Cellular Neurosciences

Max Delbrück Center for Molecular Medicine

Robert-Rössle-Str.10,

13122 Berlin-Buch

Tel. ++49 94 06 33 25

FAX: ++49 94 06 38 19

email: hketten@mdc-berlin.de

Summary

While the majority of research toward the understanding of ischemic damage (and protection from that damage) has been directed toward neurons, the remaining 85% of the brain's cell populations consist of glia. The major classes of glial cells, namely astrocytes, oligodendrocytes and microglial cells were compared in parallel for their susceptibility to damage after combined hypoxia and hypoglycemia or hypoxia alone. The three glial cell types were isolated from neonatal rat brains, separated, and incubated in N_2/CO_2-gassed buffer containing glucose or glucose substitutes, 2-deoxyglucose or mannitol, both non-metabolizable sugars. The damage to the cells after 6h exposure was determined at 0, 1, 3, 7 days based on lactate dehydrogenase (LDH) release and counting of ethidium bromide (EtBr) stained dead cells, double-stained with cell-type specific markers.

Depending on the length of exposure and the glucose substitution, each glia cell type exhibited selective vulnerability to either combined hypoxia and hypoglycemia or hypoxia alone. Primary cultures of rat oligodendrocytes were the most vulnerable to cell damage and death after exposure in all conditions tested. Purified astrocytes exhibited little cell death under all these conditions while microglia survival rates varied depending on the time and glucose substitute. The neuroprotective agent, U83836E, exacerbated the damage in glia after exposure to hypoxia and hypoglycemia at all concentrations used. The AMPA receptor antagonist, NBQX, decreased LDH release in both oligodendrocytes and astrocytes although it did not affect the overall survival rates. In conclusion, the results from these studies show that oligodendrocytes, then microglia are the most vulnerable glial cell types in response to hypoxic and/or hypoglycemic conditions while astrocytes from the same preparations survive and that glia responses to various neuroprotective agents are also selective.

Introduction

All brain cells absolutely require oxygen and glucose among many other crucial factors necessary for survival and to carry out normal functions. The pathologies created after oxygen and glucose deprivation in focal and global forms of ischemia, such as stroke, heart attack, hypoxia, etc., indicate that subsets of neurons are the most sensitive elements and are destroyed on the front line of injury. Later, other neurons undergo delayed neuronal cell death mediated by glia (Giulian and Vaca, 1993). Glial cells are thought to resist ischemic death, based mainly on the studies of cultured astrocytes (Kelleher et al., 1993; Swanson et al., 1993) and immunostaining studies of astrocytes and microglia after cerebral stroke (Endoh et al., 1994; Morioka et al., 1993; respectively). However, all brain cells are affected even if they survive the initial damage. The *in vivo* events initiated after ischemic episodes involve edema, breakdown of the blood brain barrier, invasion of leukocytes, depletion of ATP, production of nitric oxide (NO), formation of oxygen radicals and changes in ion concentrations affecting the buffering of potassium, calcium regulation and pH. In addition, there is release of cytokines, proteases, neurotransmitters and excitatory amino acids- primarily, glutamate. Astrocytes and microglia cells are activated and known to contribute in a myriad of these processes.

Astrocytes that bridge between the vascular system, neurons, and themselves detect perturbations in the microenvironment and undergo changes involving morphology, proliferation and pathology, such as gliosis (for review see Eddleston and Mucke, 1993). Endothelial cells at the blood brain barrier lose the integrity of tight junctions thus allowing blood-born cells to invade the brain tissue. The infiltrating blood-born macrophages, in concert with the resident microglia, undergo morphological and functional changes and migrate to the site of injury, which is described as 'activation'. In addition, these immuno-competent cells, including macrophages and microglia mount an inflammatory response (for review see; Kreutzberg, 1996). The response of the third major glial cell type, the oligodendrocyte, has not been clearly defined. However, their vulnerability seems likely since ischemia damages white matter, as well as gray matter.

The direct effects of oxygen and glucose deprivation on individual cell survival can be best tested *in vitro*. Indeed, it is nearly impossible to discern cell-type and specific factor contributions after injury without attempts to simplify the brain environment. Moreover, cultures of purified glial cell types of the mammalian brain have not been simultaneously or rigorously investigated. In the present study, we made use of protocols to isolate the three major glial cell types of the brain: oligodendrocytes, astrocytes and microglia. The cells were purified from the same material of neonatal rat brains and cultured as highly enriched populations. We employed cell-type specific markers to unequivocally identify the cells (see Methods). This approach allowed us to selectively test the individual glial cell types for vulnerability after exposure to combined hypoxia and hypoglycemia conditions and begin to test neuroprotective agents. We are aware that such an approach is far from the *in vivo* situation. Such studies provide essential information at the single cell level and may ultimately help to understand the complex interactions followed by ischemic damage *in vivo*.

Methods and Materials

Glial culture preparations. Cultures were prepared from whole brains of neonatal Wistar rats (Charles River Germany) in the manner of McCarthy and deVellis (1980). Briefly, meninges were removed and the dissociated brain was trypsinized (1.0% trypsin, 0.05% DNase (Worthington Biochem. Corp., Freehold, NJ, USA)) at room temperature in Hank's Balanced Salt Solution (HBSS) without Ca^{2+} and Mg^{2+}. The tissue was washed twice with HBSS, resuspended in Basal Medium Eagle's (BME) containing DNase (0.05% and 0.25% glucose) and triturated through Pasteur pipettes to yield single cells. The cell suspension was centrifuged at 800 rpm for 10 min at 4°C and washed twice with ice-cold HBSS. After resuspension in BME medium plus 10% heat-inactivated horse serum (Gibco, Gaithersburg, MD, USA), cells of approximately two brains were plated per poly-L-lysine coated (100µg/ml Sigma, Diesenhofen, Germany) culture flask (150 cm^2) and incubated at 37°C in 5% CO_2 atmosphere. One day later, cultures were washed twice with HBSS to remove cellular debris and maintained in same medium as before for 7-14 days. After reaching confluence, microglial cells, oligodendrocytes and their early precursor cells develop on top of a monolayer of astrocytes. Microglial cells were then dislodged by mild manual shaking, removed by washing the cultures with HBSS, spun down and plated in DMEM plus 10% fetal calf serum (Giulian and Baker, 1986). Oligodendrocytes were dislodged by strong manual shaking, spun down and resuspended in SATO (defined medium supplemented with 1% heat-inactivated horse serum, Bottenstein and Sato, 1979). This procedure was repeated every three to four days but not more than three times. Astrocytes were washed with HBSS, trypsinized, centrifuged, resuspended and maintained in BME containing 10% heat-inactivated horse serum. Cells were counted and plated onto poly-L-lysine-coated (20 µg/ml in phosphate-buffered saline) coverslips at densities of 3-5 x 10^4 cells/coverslip (15 mm diameter). Cells were maintained for 4-6 days in 4-well Nunc culture plates with the 500 µl of appropriate medium. Without additional growth factors, the majority of precursors develop into oligodendrocytes that begin to mature within a few days.

Hypoxia and hypoglycemia protocol. All experiments were performed with the following assay buffer containing (in mM): 124 NaCl, 4.9 KCl, 1.3 $MgSO_4$-7 H_2O, 2.0 $CaCl_2$-$2H_2O$, 1.2 KH_2PO_4, 25.6 $NaHCO_3$, 10 glucose at pH 7.4 and filter-sterilized. The hypoglycemic buffer was the same except the glucose was replaced by 10 mM 2-deoxyglucose or 10 mM mannitol.

Cells exposed to three different experimental conditions are schematized in Figure 1A. 1. *Combined Hypoxia and Hypoglycemia*: Glia deprived of both oxygen and glucose in the assay buffer represents the hypoxic/hypoglycemic state. Glucose was replaced by either 2-deoxyglucose or mannitol. 2. *Hypoxia*: Cells deprived only of oxygen in the presence of glucose, represent the hypoxic state. 3. *Hypoglycemia*: Cells exposed to normal atmosphere but glucose-deprived by the substitution of 2-deoxyglucose or mannitol in the buffer, represent the hypoglycemic state. 4. *Control*: Cells incubated with glucose and normoxic atmosphere represent the normal control state. Cultured glia exposed to hypoxia were placed in the gas-controlled hypoxia chamber (Fig. 1B) which, along with the cells under normoxic atmosphere, were placed in the incubator for 6 or 42 hours.

In each experiment, coverslips exposed to hypoxia and/or hypoglycemia were always compared to controls. Care was taken that the coverslips within one experiment

started out with a similar cell density and purity as judged by morphological criteria. After the experiment and at each time point, cells were stained with cell-type specific markers, described in Immunostaining Procedure section. Employing live and dead labeling techniques, we were able to selectively count the populations of live and dead astrocytes, oligodendrocytes and microglial cells. Additional experiments measuring lactose dehydrogenase (LDH) release yielded information about the stress the cells had encountered.

The easily constructed non-commercially available hypoxia chamber was used for all hypoxia experiments (Fig. 1B). This closed system chamber fit into a standard cell culture incubator. A constant flow of N_2/CO_2 and 37°C were maintained throughout all experiments.

Hypoxia and hypoglycemia were induced under sterile conditions on cells in 4-well plates that had been rinsed twice with buffer that had been gassed with 95% N_2/5% CO_2 for a minimum of one hour. One hour gassing was sufficient to remove 96-97% of the partial oxygen tension. Control buffer was gassed with 95% O_2/5% CO_2 for 1 hr. Under more stringent gassing for 4 hours or overnight, all but 0.3% oxygen tension could be removed as indicated by a pO_2 meter (Oxi 320/Set WFW, Weilheim, Germany). A chemical test using resazurine, an oxygen-sensitive dye that changes color depending on oxygen content, was used to further confirm the absence of oxygen in the buffer after 1 and 4h (Benndorf et al., 1991). Five to ten minutes was needed to change the medium to oxygen-free buffer, during which time the oxygen tension changed negligibly. The chamber was flushed with N_2/CO_2 before the cells were placed into the flow of the gas mixture. The open 4-well plates containing cells on coverslips were placed in a shallow volume of 350 µl buffer. This assured a large surface area for gas exchange close to the surface of the cells without danger of evaporation during the experiment. Once the cells were locked into the chamber and flushed again to remove oxygen, the closed chamber was placed into the 37°C incubator for 6h. Control coverslips were returned to the incubator at the same time.

At the end of the experiment, cells were removed from the chamber and 2 x 100 µl supernatant removed from each well for LDH ELISA analysis. The remaining assay buffer was aspirated off and replaced by defined SATO medium with glucose but without serum, as this interferes with the LDH determination (Boehringer Mannheim LDH Kit recommendation). The remaining unstained coverslips were returned to normal atmosphere in the incubator awaiting their time for live/dead determination.

For the hypoxia-alone experiments, glial cells were placed in the hypoxic chamber for 6h or 42h, removed for either immediate staining of live and dead cells or returned to the normoxic incubator to assess the long term effects of the hypoxia insult. Culture medium appropriate for each cell type containing glucose and serum was used for hypoxic experiments assessing cell survival, based on counting only. This ensured that any changes observed would be from the effects of hypoxia alone. In other experiments for hypoxia alone, the cells were in the buffer described above to determine the LDH release without serum.

Immunostaining procedures. The purity of the cultures and identification of the glia were confirmed by staining with cell-type specific markers. The O4 surface antigen (Boehringer Mannheim) was used to identify oligodendrocytes. This antigen recognizes

late precursor and mature oligodendrocytes of the oligodendrocyte lineage (for simplicity, we will refer to these cells as oligodendrocytes). After incubation with secondary antibodies, dichlorotriazinyl amino fluorescein (DTAF)- or Cy3-conjugated μ chain specific (both from Dianova, Hamburg, Germany), cells were fixed with 4% paraformaldehyde for 10 min prior to embedding in mowiol (Hoechst, Frankfurt, Germany). These oligodendrocyte cultures were 80-90% O4+.

Glial fibrillary acidic protein (GFAP from DAKO, Hamburg, Germany) was used to identify mature astrocytes. Cells were fixed with 4% paraformaldehyde for 10 min at room temperature. After rinsing, the primary polyclonal antibody against GFAP diluted in PBS containing 0.1% Triton, 1% BSA, and 1% normal goat serum was applied for 40 minutes. After washing, DTAF- or Cy3-conjugated secondary antibodies were applied for 40 min and mounted on coverslides. About 80% of cells in the enriched astrocyte cultures were GFAP+, the rest being immature GFAP- cells which were not counted.

Fluorescein isothiocynate (FITC)-conjugated isolectin B4 from *Griffonia simplicifonia* (Boehringer, Mannheim) was used to identify microglia by direct labeling. Isolectin was incubated with microglia cultures for 15 min, rinsed, fixed and mounted as described above. The typical microglia morphology was the rounded, ameboid and flat pancake-like shapes easily distinguished from the 1% and fewer of other cells present in culture.

Assessment of glia injury. A Live and Dead Kit (Molecular Probes, Leiden, Netherlands) was used to determine cell viability and cytotoxicity on glial cells after the hypoxia experiments in the presence of serum. Calcein AM was taken into live cells and remained as a marker for internal esterase activity and membrane integrity. At the same time, ethidium bromide homodimer-1 (EtBr), a nucleic acid stain, was taken into cells when the membrane was compromised. Each reagent was diluted together in the medium and applied to the cells immediately after exposure to hypoxia or specified time points for 5 min. The cells were fixed, mounted and counted later without loss of fluorescence. The staining was stable for the times investigated.

A LDH cytotoxicity kit (Boehringer Mannheim) was used to quantify cell cytotoxicity based on membrane permeability. Permeabilized cells release a stable cytoplasmic enzyme, lactate dehydrogenase, into the supernatant as an indicator of being damaged or lysed. One advantage of this assay was the quick determination of total cellular damage compared to time-intensive counting of individual cells. Another advantage was the ability to sample the medium during a one week time course from the same cells. Optimal cell density of each glial cell type was determined for detection of LDH under control conditions before plating the cells for the experiments. Aliquots of supernatant were removed from wells at specified times and frozen for LDH assay. The amount of LDH released was then compared with these controls for each of the experimental conditions, times and cell types. As there was a continual loss in cell numbers during the week, the typical normalization procedure was not practical for these experiments. To determine total LDH content, DMSO can be applied to lyse the remaining cells, but this was impractical as DMSO does not allow cells to be stained and counted at the end of the experiments.

Results

Oligodendrocytes are vulnerable to hypoxic damage in the presence of 2-deoxyglucose and mannitol

Oligodendrocytes were demonstratively damaged when exposed to 6h combined hypoxia and hypoglycemia when glucose was replaced with 2-deoxyglucose or mannitol. Immediately after the insult (t=0), nearly all cells (82 % +/- 5%, 390 of 476 for 2-DG and 90% +/- 3% (478 of 529) for mannitol) were EtBr+, indicating that they were dead. Dead O4+/EtBr+ oligodendrocytes are shown (open arrows, Fig. 2) except for one live O4+/EtBr- cell (solid arrow, Fig. 2). Even the few EtBr- cells underwent morphological changes: the extensive arborization of the processes, typical for healthy oligodendrocytes, had deteriorated. The remaining coverslips were maintained for 7d in the incubator in normoxic glucose-containing medium. At the end of 7d, few O4-labeled cells were present and of those, 90% +/- 4% (185 of 207 in 2-DG) and 95% +/- 1% (330 of 347 in mannitol) did not survive. Many oligodendrocytes survived in the control cultures at t =0 and 7d (not shown), although the total number of cells decreased with time in culture. Cell survival percentages based on all oligodendrocytes counted are shown in Figure 3. LDH release increased compared to the controls immediately after the insult. Monitoring the LDH release after 1, 3, 7 days revealed LDH levels below control levels (Fig. 3). This might reflect that only few cells survived on the coverslips as a potential source to release LDH. The results for oligodendrocyte survival and LDH release are similar under the mannitol conditions as well.

Astroglia recover after exposure to combined hypoxia and hypoglycemia in the presence of 2-deoxyglucose and mannitol

Astroglia survived, as expected, after combined hypoxia and hypoglycemia treatment while in the presence of 2-deoxyglucose or in mannitol (Fig. 4). After 6h exposure, GFAP+ cells (95% +/- 0.05%, 624 of 656 for 2-DG and 99% +/- 1%, 1381 of 1395 for mannitol) were EtBr- indicating the majority of cells were alive (solid arrow, open arrow indicates GFAP- cell). Seven days after the 6h insult, cell numbers had not changed. The total number of surviving astrocytes did not change over the one week period (Fig. 5). Surprisingly, the LDH release measured immediately after the insult strongly increased although the cells survived. The same was true for the mannitol experiments. Thus, the overall impact on the astrocytes and oligodendrocytes was not substantially changed in any of the tested parameters when comparing 2-deoxyglucose and mannitol substitution.

Microglial populations are more vulnerable under 2-deoxyglucose than in mannitol conditions of hypoxia and hypoglycemia

Microglia were susceptible to combined hypoxic and hypoglycemic damage in the presence of 2-deoxyglucose. The positive EtBr-staining right after the insult indicated that 88% +/- 6% (407 of 464) of the ILB4+ cells did not survive (all cells, first row Fig. 6). Seven days after the insult, the combined EtBr and ILB4-labeling indicated that more the percentage of dead cells increased (93% +/- 2%, 271 of 291 not shown). Control cultures exhibited lack of EtBr label at t = 0 and 7d (not shown). Microglia total survival and LDH release are shown in the graph (Fig. 7). LDH release right after the insult increased threefold and fell below control levels after 3 days.

However, the response of the microglia after the insult was quite different in the presence of mannitol. About half of the microglial population survived the 6h combined hypoxic and hypoglycemic treatment (49% +/- 15%, 1116 of 2282 cells, n = 5). This finding was based on the total number of ILB4+ cells that did not express EtBr staining

(solid arrows point to examples of live cells, second row Fig. 6). However, 7 days after the insult there were few surviving microglial cells (3% +/- 0.05%, 52 of 1745, all EtBr+). In the majority of the dead cells, the nucleus appeared condensed, emphasized by the intensity of the EtBr staining (about 20 of 30 cells). Control cultures of microglia conversely exhibited only a few EtBr+ cells (not shown). Total cell survival is shown, as well as the LDH release for both t = 0 and 7d (Fig. 7).

Purified oligodendrocytes are vulnerable to damage by hypoxia exposure

Oligodendrocytes were shown to be more susceptible to damage from hypoxia than both microglia and astroglia as evidenced by decreased cell survival after 6h exposure time (middle column), when compared to the controls (first column, Fig. 8A). Immediately following 6h exposure to hypoxia alone, only 24% of O4+ cells (85 of 353) survived. Seven days after the insult, the total cell number had decreased to about half of the original numbers and of these, 54% (92 of 171) cells survived. We found a similar overall decline in cell number of the controls within 7 days. Under hypoxia-alone conditions, the LDH release for oligodendrocytes was only slightly less than combined hypoxia and hypoglycemia at all time points (data not shown). A 42h exposure of oligodendrocytes to hypoxic conditions resulted in severe damage in every experiment. Only thirteen percent (40 of 306) of the cells were alive (third column Fig. 8A). Astrocytes and microglia, in contrast, were not similarly effected after 42h exposure to hypoxia when compared to controls (Fig. 8B and 8C).

Microglia survival was not as affected after 6h hypoxia when compared to the controls (Fig. 8B). The percentage of surviving cells at this first time point after 6h hypoxia was 95% (485 of 508). Although microglia appear to be resistant to hypoxia death in culture, the total number of cells decreased over one week in culture whether or not they were exposed to hypoxia for 6h. The LDH release for microglia was significantly less at all time points compared to combined hypoxia and hypoglycemia (data not shown).

Similarly, astrocytes appeared to be resistant to 6h hypoxia in culture as seen in Fig. 8C as the percent of cell death after 6h exposure to hypoxia was low and comparable to the control. The percentage of surviving cells immediately after 6h hypoxia was 89% (417 of 470). Although the total number of cells varied at each time point, all increased in total cell number at 7d. Under conditions of 6h hypoxia alone, in parallel with the combined hypoxia and hypoglycemia experiments, the LDH release for astroglia was also significantly less at all time points (data not shown).

Hypoglycemic conditions alone did not affect the survival of glial cell types

Glial cells were maintained in buffers for 6h at normoxic atmosphere where glucose was either replaced by mannitol or 2-deoxyglucose. Neither oligodendrocytes, astrocytes, nor microglial cells showed different survival patterns from controls. In all cases, the LDH release was the same as control levels (not shown). The cell survival was followed for 7 days to analyze possible delayed, long-term damage which was not observed. We conclude that all brain glial cell types can survive 6h glucose-free conditions in culture.

Neuroprotective agents produce selective effects in glia

The lazaroid, U83836E, was tested on purified glia cultures during their exposure to combined hypoxia and hypoglycemia to examine whether the oxygen scavenging properties were useful in protecting glia. Under the concentrations tested (300nM, 3uM

30uM), the lazaroid increased the release of LDH and decreased the survival of all glia. In parallel experiments, Vitamin E (of which U83836E is an analog) was tested in microglia under the same conditions and was found to be protective- both in lowering the LDH levels and in the number of surviving cells.

The AMPA receptor antagonist, NBQX (10uM), was applied to glia cultures just before their exposure to 6h combined hypoxia and hypoglycemia. While there was no significant difference in the survival rates of astrocytes or oligodendrocytes, there was a consistent decrease in the release of LDH when compared to the non-treated cells.

Discussion

Glial cells are thought to be much more resistant to hypoxic and hypoglycemic stress as compared to neurons. Typically, reports of glial survival or injury to damage during or after ischemic injury refers primarily to astrocytes (Goldberg and Choi, 1993; Nedergaard et al., 1991). Here we confirm that astrocytes are more resistant to *in vitro* ischemic damage than other glia under these experimental conditions. Astrocytes with their glycogen stores have a beneficial effect on neuronal survival under glucose deprivation in culture (Swanson and Choi, 1993) and for themselves as well. Thus, the plastic and surviving astrocytes may serve as important entities necessary for the survival of the other brain cells. Our comparative approach in assaying the survival of microglia and oligodendrocytes, however, revealed that these populations are more susceptible to such insults. Thus, there is no common glial survival rate, but a rather distinct one for astrocytes, oligodendrocytes and microglia, respectively. In general, the most damage to glial cells occurred immediately after combined hypoxia and hypoglycemia rather than at later time points. Whether this cell death is apoptotic or necrotic is currently being investigated.

LDH release is not a reliable assay for measuring glia-toxicity

Typically, the release of LDH has been used as a standard method to analyze the survival rate of neurons and other cell types after different types of insults. In many studies, the rate of released LDH correlates well with the loss of neurons (Goldberg and Choi, 1993). Our data indicate that this assay can not be used to study comparative glial survival. While astrocytes exhibit a dramatic release in LDH after the ischemic/hypoxic insult, their survival is not affected. Astrocytes were stressed at first but this did not affect the overall surviving numbers of astroglia nor the long-term basal release of LDH. If we relied solely on LDH release data, we would conclude that astrocytes were the most susceptible to injury by combined hypoxia and hypoglycemia when compared to microglia and oligodendrocytes, when, in fact, the opposite is true. The LDH release did not correlate with number of dead cells counted after the insult. We, therefore, had to base our studies on counting cells after live/dead staining or EtBr-uptake into dead cells. This serves as a word of caution to others when considering LDH release assays to measure cytotoxicity.

While the LDH assay seems inappropriate to monitor glial death, it contains valuable information. Measuring LDH release is a technique indicating the time course of stress of a total population of cells, including those that die and lift off into the medium, which would never be counted by a staining technique. LDH release was very high initially after the insult in all cells. After the initial determination and a 30 minute reperfusion with glucose and at later time points, the LDH level returned towards control. This corresponds with LDH determination after the hypoxia insults, when the greatest damage occurs to cells after ischemia during the reperfusion period when radicals and proteases are released (Mertsch et al., 1995). In the case of the oligodendrocytes and microglia, LDH release fell even below the control levels. This may indicate that the injury to the glial cells occurs primarily at the initial time point and/or the level of LDH in the surviving cells is below the sensitivity of the assay.

Oligodendrocytes are the most vulnerable glial cell type

Oligodendrocytes appear to be nearly as sensitive as neurons to perturbations of oxygen and glucose in comparison to microglia and astrocytes under the conditions implemented in our experiments. Neurons in culture demonstrate similar responses to damage by hypoxia and/or hypoglycemia as shown by Goldberg and Choi, 1993. Husain and Juurlink (1995) and Qi and Dawson (1993) analyzed the effect of hypoxia on

oligodendrocytes and described extreme vulnerability with or without coculturing with astrocytes. It was expected that the removal of glucose (substituted by 2-deoxyglucose or mannitol) under the hypoxic conditions would exacerbate the damage to oligodendrocytes, which indeed, was the case. Although mannitol confers protection in some cell types under various stresses (Gillbe et al., 1996), cultured oligodendrocytes did not show an increase in survival after hypoxia and hypoglycemia in the presence of mannitol.

Oligodendrocyte susceptibility to damage in culture by hypoxia and combined hypoxia and hypoglycemia is not surprising as they are difficult to culture and to maintain under normal conditions. Oligodendroglia exhibit sensitivity to various kinds of damage in culture as demonstrated by others. Nitric oxide (NO), released from endothelia, astrocytes and microglia after being triggered by stimuli such as ischemia, causes lipid peroxidation in oligodendrocytes, as well as necrotic cell death (Merrill et al., 1993). *In situ* demonstration of oligodendroglial paranodal loops detaching from rat optic nerve axons after 1h anoxia indicates selective vulnerability (Waxman et al., 1994). Under extreme conditions, white matter may be damaged immediately after a focal stroke but usually the breakdown of white fiber tracts is found at later stages of ischemia. Models of white matter tract ischemia show destruction in the white matter, implicating the involvement of oligodendrocytes (Ferrer et al., 1994). Unfortunately, there are few data available on the survival of oligodendrocytes *in vivo* after such an insult. Juurlink (1997) suggests in a review that oligodendrocytes may be more susceptible to oxidative stress after ischemia due to their low glutathione contents- important in reactive oxygen scavenging, and their higher iron contents- contributing to increased radical formation. Mandai and coworkers (1997) recently demonstrated, in a mouse model of MCAO, oligodendrocyte degeneration within 12-24 hours. This was followed by subsequent proliferation from oligodendrocytes 5 days after damage near the ischemic core.

Microglia survive partially in the presence of mannitol

Microglia are strongly damaged after experiencing an ischemic insult in culture, nearly as much as oligodendrocytes or neurons. The presence of mannitol, however, partially protected microglial cells but not oligodendrocytes. Microglia exhibited about 50% survival under hypoxia with mannitol present in comparison to less than 10% survival after hypoxic exposure in the presence of 2-deoxyglucose. It seems most likely that mannitol serves as a free radical scavenger and thus protects microglia from their own products. Indeed, stimulation of microglia with LPS leads to an oxidative burst (Banati et al. 1991). It has not yet been investigated whether the combined hypoxia and hypoglycemia insult results in a similar response, but if so, microglial cells would damage each other and themselves. This would explain the lack of mannitol effect on oligodendrocyte survival since these cells are not known to generate oxidative bursts.

We were unable to find any reports regarding microglia death in vivo or in situ. It would require elegant work with double markers such as shown for dying and proliferating oligodendrocytes in mouse brain mentioned above by Mandai et al., 1997. Susceptibility of microglia in culture would conceivably be greater and more easily detected than in vivo. Cultures of microglia after combined hypoxia and hypoglycemia may create an environment of increased nitric acid accumulation, as well as cytokines, proteases, etc. that would increase self-toxicity. The authors are aware of ongoing discussions concerning the fate of microglia in pathological states as yet unsupported by convincing data.

CONCLUSION

It is apparent from these studies that the initial events are the most important to characterize. Long term survival of glia in culture after exposure to hypoxia and /or hypoglycemia depends on the number of cells surviving the immediate damage. Evidently, there appears to be no massive delayed cell death for glia in culture as is known for neurons *in vivo,* particularly in the CA1 region of the hippocampus. Of course, glial cells grown in cell culture differ in important ways from their *in vivo* counterparts. Further investigations are required to understand the interactions between glia and neurons within the complex cascade of events in ischemia. Nonetheless, the use of this simpler model system can be utilized to ask questions about neuronal/glia signaling systems that change in response to injury. Later, the answers to these questions may be tested at the next biological levels of complexity, such as cocultures and brain slices.

REFERENCES

.Banati RB. Rothe G. Valet G. Kreutzberg GW (1991) Respiratory burst activity in brain macrophages: a flow cytometric study on cultured rat microglia. *Neuropathol-Appl-Neurobiol* 17(3): 223-30

.Benndorf K. Bollmann G. Friedrich M. Hirche H (1992) Anoxia induces time-independent K^+ current through K_{ATP} channels in isolated heart cells of the guinea-pig. *J Phys* 454:339-357

.Bottenstein JE. Sato GH (1979) Growth of a rat neuroblastoma cell line in serum-free supplemented medium. *Proc Natl Acad Sci U S A* 76:514-517

.Eddleston M. Mucke L (1993) Molecular profile of reactive astrocytes- implications for their role in neurologic disease. *Neuroscience* 54:15-36

.Endoh M. Maiese K. Wagner J (1994) Expression of the inducible form of nitric oxide synthase by reactive astrocytes after transient global ischemia. *Brain Res* 651:92-100

.Ferrer I. Tortosa A. Macaya A. Sierra A. Moreno D. Munell F. Blanco R. Squier W. (1994) Evidence of nuclear DNA fragmentation following hypoxia-ischemia in the infant rat brain and transient forebrain ischemia in the adult gerbil. *Brain Pathol* 4:115-122

.Gillbe CE. Sage FJ. Gutteridge JM (1996) Commentary: mannitol: molecule magnifique or a case of radical misinterpretation. *Free Radic Res* 24:1-7

.Giulian D. Baker TJ (1986) Characterization of ameboid microglia isolated from developing mammalian brain. *J Neurosci* 6:2163-2178

.Giulian D. Vaca K (1993) Inflammatory glia mediate delayed neuronal damage after ischemia in the central nervous system. *Stroke* 24:I 84-I 90

.Goldberg MP. and Choi DW (1993) Combined oxygen and glucose deprivation in cortical cell culture: calcium-dependent and calcium-independent mechanisms of neuronal injury. *J. Neurosci* 13:3510-3524

.Husain J. Juurlink BH (1995) Oligodendroglial precursor cell susceptibility to hypoxia is related to poor ability to cope with reactive oxygen species. *Brain Res* 698:86-94

.Kelleher JA. Chan PH. Chan TYY. Gregory GA (1993) Modification of hypoxia-induced injury in cultured rat astrocytes by high levels of glucose. *Stroke* 24:855-863

.Kreutzberg GW (1996) Microglia: a sensor for pathological events in the CNS. *Trends Neurosci* 19:312-318

.Mandai K. Matsumoto M. Kitagawa K. Matsushita K. Ohtsuki T. Mabuchi T. Colman DR. Kamada T. Yanagihara T. (1997) Ischemic damage and subsequent proliferation of oligodendrocytes in focal cerebral ischemia. *Neurosci* 77:849-861

.McCarthy KD. deVellis J (1980) Preparation of separate astroglial and oligodendroglial cell cultures from rat cerebral tissue. *J Cell Biol* 85:890-902

.Merrill JE. Ignarro LJ. Sherman MP. Melinek J. Lane TE (1993) Microglial cell cytotoxicity of oligodendrocytes is mediated through nitric oxide. *J Immunology* 151:2132-2141

.Mertsch K. Grune T. Siems WG. Ladhoff A. Saupe N. Blasig IE (1995) Hypoxia and regeneration of brain endothelial cells *in vitro*: a comparison of biochemical and morphological response. *Cellular and Molecular Biol* 41:243-253

.Morioka T. Kalehua AN. Streit WJ (1993) Characterization of microglial reaction after middle cerebral artery occlusion in rat brain. *J Comp Neurology* 327:123-132

.Nedergaard M. Goldman SA. Desai S. Pulsinelli WA (1991) Acid-induced death in neurons and glia. *Neurosci* 11: 2489-2497

.Qi Y. Dawson G (1993) Effects of hypoxia on oligodendrocyte signal transduction. *J Neurochem* 61:1097-1104

.Swanson RA. Choi DW (1993) Glial glycogen stores affect neuronal survival during glucose deprivation *in vitro*. *J Cerebral Blood Flow and Metab* 13:162-169

.Waxman SG. Black JA. Ransom BR. Stys PK (1994) Anoxic injury of rat optic nerve: ultrastructural evidence for coupling between Na+ influx and Ca2+-mediated injury in myelinated CNS axons. *Brain Res* 644:197-204

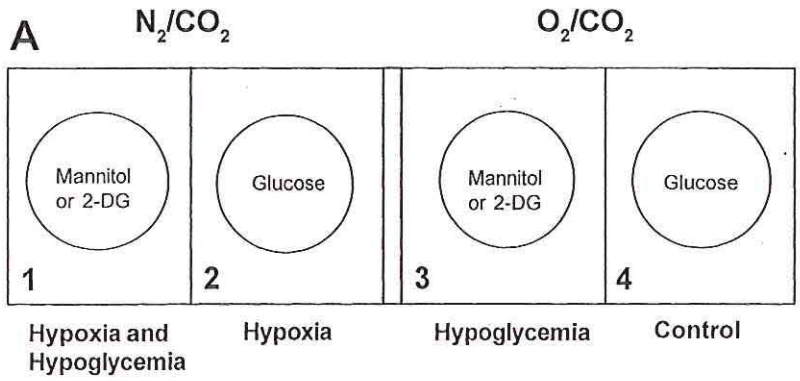

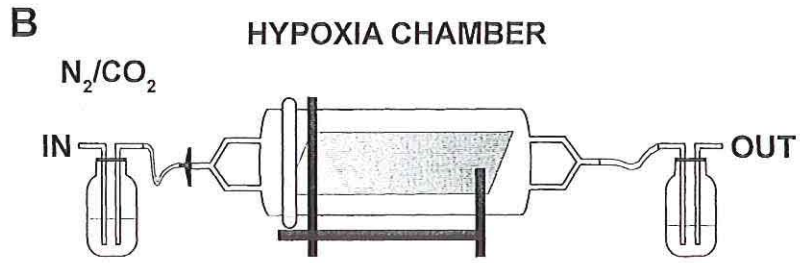

FIGURE 1. Experimental Paradigm. Equal numbers of coverslips from each of oligodendroglia, microglia and astrocytes were cultured from the same rat brain preparation. Cultures of these glia were chosen for matching density and exposed to combined hypoxia and hypoglycemia (A1) or hypoxia-alone (A2). These cells were minimally covered in N2/CO2-gassed buffer for 6h or 42h and kept in the gas-controlled chamber (see scheme in B). Glia exposed to normoxic atmosphere were kept either in glucose-substituted buffer (A3) or in glucose-containing buffer gassed with O2/CO2 (A4). B schematically depicts the small closed system chamber that was flushed with N2/CO2 during the experiments.

Oligodenrocytes after 6h Combined Hypoxia and Hypoglycemia

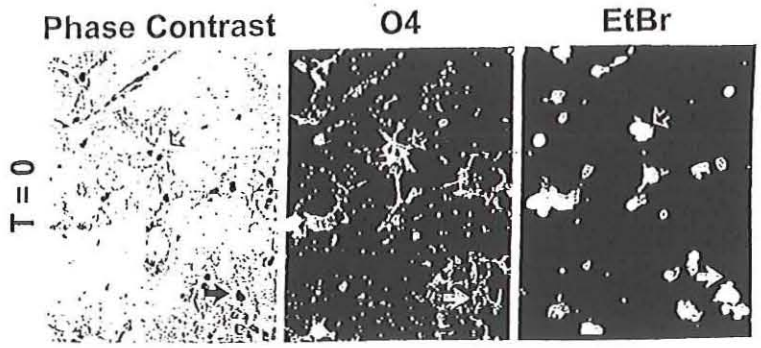

FIGURE 2. Oligodendrocytes are shown after 6h exposure to combined hypoxia and hypoglycemia in 2-DG. The phase contrast, O4 immunoreactivity and EtBr staining are shown of the same field at T = 0. Cells at the solid arrows are alive and those at open arrows are dead. All photomirographs are at equal magnification. Scale bar = 60mm.

Astrocytes after 6h Combined Hypoxia and Hypoglycemia

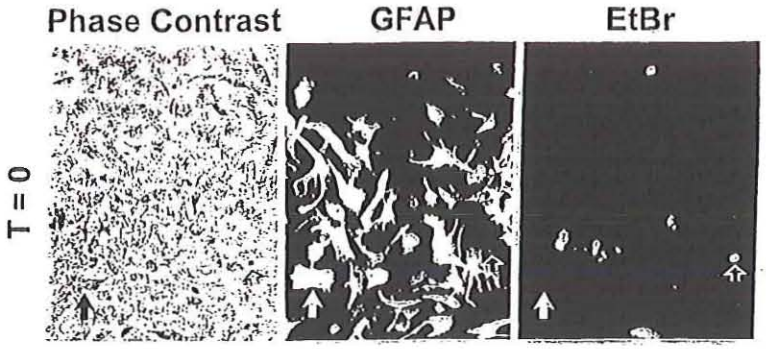

FIGURE 4. Astrocytes are shown after 6h exposure to combined hypoxia and hypoglycemia in 2-DG. The phase contrast, GFAP immunoreactivity and EtBr staining are shown of the same field at T = 0. All photomicrographs are at equal magnification. Scale bar = 60mm.

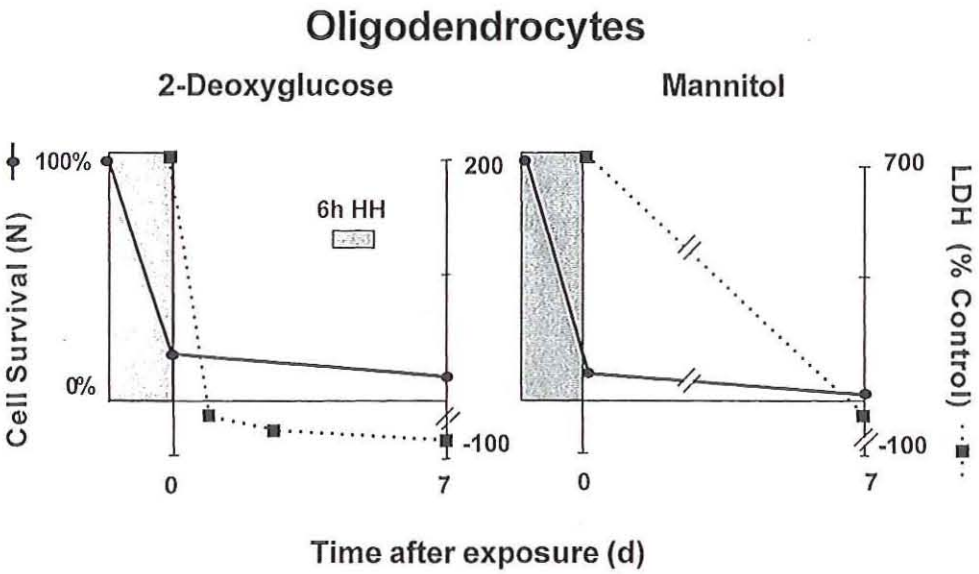

FIGURE 3. Oligodendrocyte survival after 6h combined hypoxia and hypoglycemia with 2-deoxyglucose and mannitol substituted for glucose. The left graph illustrates the survival of oligodendrocytes (solid line) based on the counted cells and the concomitant release of LDH (dotted line) after the 6h of combined hypoxia and hypoglycemia (HH, shaded box). LDH levels were measured at 0, 1, 3 and 7 d, after combined hypoxia and hypoglycemia (n = 3) and normalized to the percent of control LDH values. The right graph illustrates the oligodendrocytes in mannitol containing buffer.

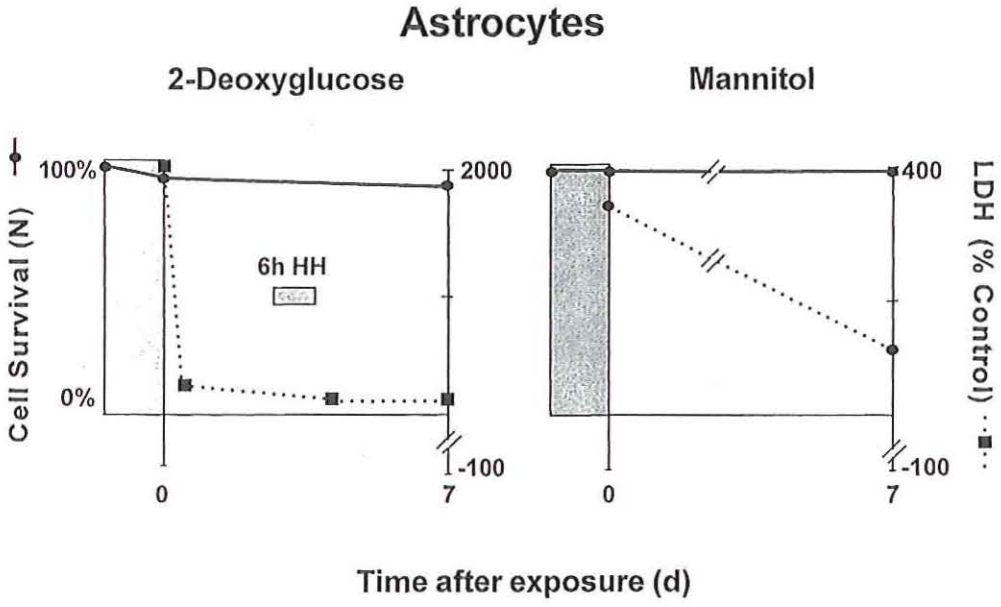

FIGURE 5. Astrocyte survival after 6h combined hypoxia and hypoglycemia with 2-deoxyglucose and mannitol substituted for glucose. The left graph illustrates the survival (solid line) of cells based on the number of cells counted and the concomitant release of LDH (dotted line) after the 6h exposure to combined hypoxia and hypoglycemia (HH, shaded box). The levels of LDH were measured at 0 and 7 d, after combined hypoxia and hypoglycemia (n = 3) and normalized to control LDH values. The right graph in illustrates the survival in the presence of mannitol.

Microglia after 6h Combined Hypoxia and Hypoglycemia

2-Deoxyglucose

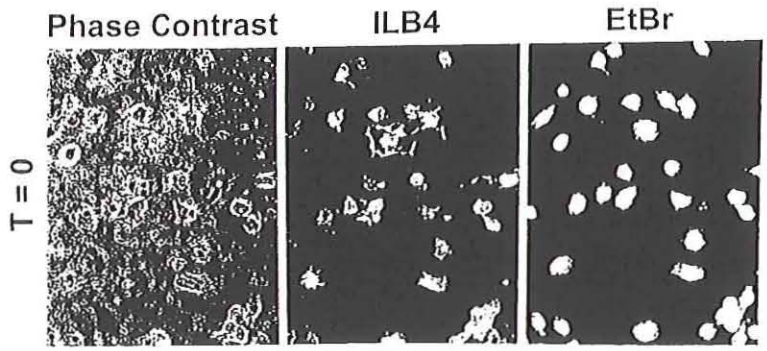

Mannitol

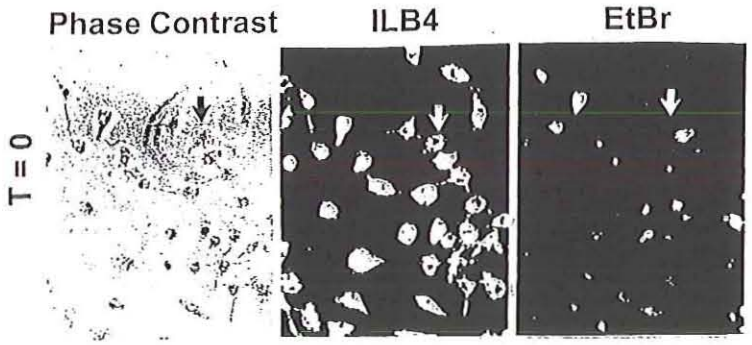

FIGURE 6. Cultured microglia exhibit low survival after 6h exposure to combined hypoxia and hypoglycemia with 2-deoxyglucose present (top row). The phase contrast, ILB4-staining of microglia and EtBr-staining of dead cells from the same experiment are shown in the photomicrographs immediately after 6h exposure. Cultures microglia exhibit about 50% survivial after 6h exposureto combined hypoxia and hypoglycemia with mannitol present in the buffer (second row, examples of live cells are indicated with solid arrows). All photomicrographs are at equal magnification. Scale bar = 60mm.

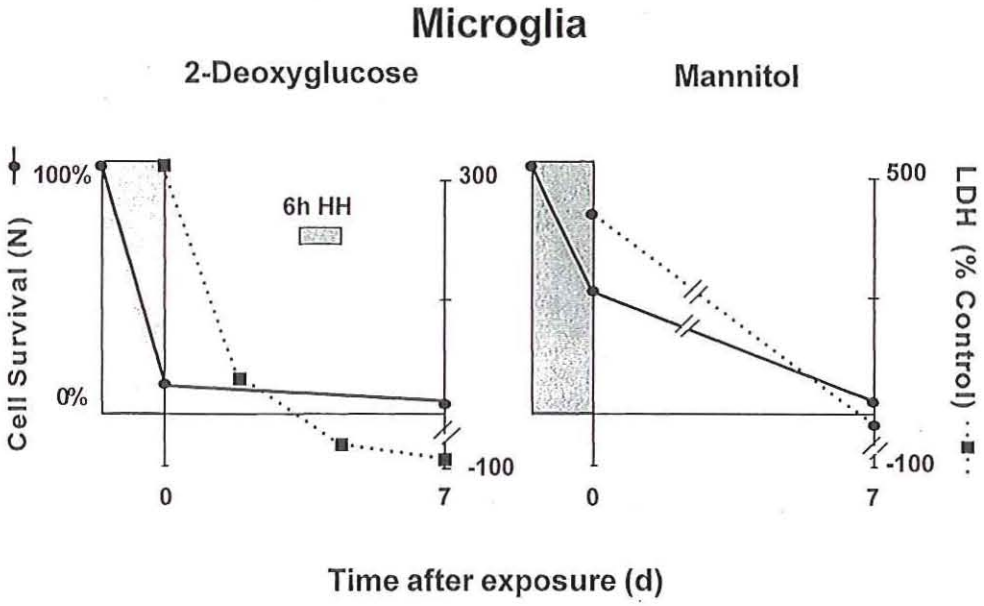

FIGURE 7. Microglia survival after 6h combined hypoxia and hypoglycemia with 2-deoxyglucose and mannitol substituted for glucose. The left graph illustrates the survival (solid line) of cells based on the number of cells counted and the concomitant release of LDH (dotted line) after the 6h exposure to combined hypoxia and hypoglycemia (HH, shaded box). The levels of LDH were measured at 0 and 7 d, after combined hypoxia and hypoglycemia (n = 3) and normalized to control LDH values. The right graph in illustrates the survival in the presence of mannitol.

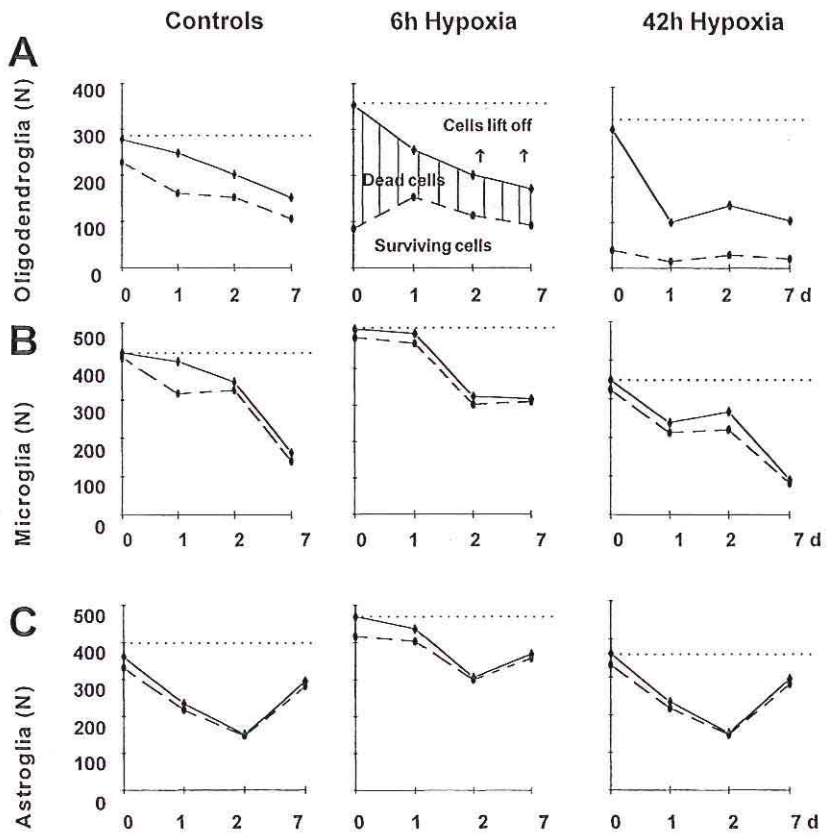

FIGURE 8. Cultured oligodendrocytes (A), microglia (B) and astrocytes (C) were exposed to 6h and 42h of hypoxia-alone in the presence of the normal medium containing glucose and serum (n = 3). Cells were stained with EtBr and calcein green for the counting of dead and live cells, respectively. Each row shows graphs for Control, 6h and 42h hypoxia experiments. Solid lines represent the total numbers of specific glia counted at the light microscope level. The dashed lines represent the total numbers of surviving glia (calcein green). The area between the solid and dotted lines represents the number of EtBr+ dead cells (see hatched section in A for 6h Hypoxia exposure). The area above the solid line represents the number of cells that lifted up-given that approximately the same numbers of cells were present on each coverslip at the beginning of the experiments (represented by the dotted line). The area under the dashed line represents surviving cells.

Schriften des Forschungszentrums Jülich.
Reihe Lebenswissenschaften/Life Sciences:

1. **Toxizitätsprüfungen in Zellkulturen für eine Vorhersage der akuten Toxizität (LD50) zur Einsparung von Tierversuchen**
   von W. Halle (1998), 92 Seiten
   ISBN 3-89336-221-5

2. **Die Rolle der Reaktionstechnik in der mikrobiellen Verfahrensentwicklung**
   von D. Weuster-Botz (1999), II, 320 Seiten
   ISBN 3-89336-245-2

3. **Cell Culture Models as Alternatives to Animal Experimentation for the Testing of Neuroprotective Compounds in Stroke Research**
   Practical Handbook of Methods
   edited by A. J. Carter, H. Kettenmann (1999), 144 Seiten
   ISBN 3-89336-250-9

Forschungszentrum Jülich

Band/Volume 3
ISBN 3-89336-250-9

Lebenswissenschaften
Life Sciences